

**B cell biology:
The role of Nbs1, KRC and $\lambda 5$**

INAUGURALDISSERTATION

zur

**Erlangung der Würde eines Doktors der Philosophie
vorgelegt der
Philosophisch-Naturwissenschaftlichen Fakultät der
Universität Basel**

von

**Eva Harfst
aus Mainz, Deutschland**

Basel, 2004

Genehmigt von der Philosophisch-Naturwissenschaftlichen Fakultät auf Antrag von
Professor Antonius Rolink und Professor Ed Palmer.

Basel, den 28 September 2004

Prof. Dr. Hans-Jakob Wirz

Dekan

Contents

1	General Introduction.....	1
1.1	V(D)J recombination	1
1.1.1	Organization of the BCR complex and its genomic locus.....	1
1.1.2	Organization of the TCR complex and its genomic locus.....	2
1.1.3	V(D)J recombination	4
1.1.4	Regulation of V(D)J recombination	6
1.2	B cell development	9
1.2.1	B cell development in the bone marrow	9
1.2.2	B cell development in the spleen.....	12
1.2.3	Factors influencing formation of mature B cell populations.....	13
1.3	Thesis objectives	17
1.4	References	19
2	Normal V(D)J recombination in cells from patients with Nijmegen breakage syndrome.....	27
2.1	Addendum.....	44
2.1.1	The hairpin opening activity.....	44
2.1.2	The role of Nbs1.....	45
2.1.3	References	48
3	Targeting of the <i>KRC</i> locus	51
3.1	Introduction	51
3.2	Results	54
3.2.1	Cloning of the targeting construct.....	54
3.2.2	Targeting of the <i>KRC</i> locus.....	55
3.2.3	Characterization of the Integration Event.....	56
3.2.4	Developmental consequences of the targeted <i>KRC</i> locus.....	58
3.2.5	Characterization of heterozygous mice.....	59
3.3	Discussion	63
3.4	References	66
4	Analysis of the mature B cell compartments in $\lambda 5$ deficient mice .	69
4.1	Introduction	69
4.2	Results	72
4.2.1	Characterization of B cell populations in $\lambda 5$ deficient mice.....	72
4.2.2	Turnover of mature peripheral B cells in $\lambda 5$ deficient mice	76

4.2.3	Humoral primary and secondary immune responses in $\lambda 5$ deficient mice	78
4.2.4	Wild type and $\lambda 5^{-/-}$ mixed bone marrow chimeras	83
4.3	Discussion	88
4.4	References	93
5	Summary	97
5.1	References	99
6	Abbreviations.....	101
7	Materials and Methods	103
7.1	General buffers and solutions	103
7.2	Bacterial media and supplements	104
7.3	Cell culture media and supplements.....	105
7.4	Vectors.....	106
7.5	Primers	107
7.6	Antibodies.....	110
7.6.1	Antibodies for FACS Analysis	110
7.6.2	Antibodies for ELISA.....	110
7.6.3	Antibodies for Histology.....	110
7.7	Molecular biology methods	111
7.7.1	Agarose gel electrophoresis of DNA fragments.....	111
7.7.2	Preparation of electro-competent <i>E. coli</i>	111
7.7.3	Transformation of electro-competent <i>E. coli</i>	111
7.7.4	Preparation of plasmid DNA from <i>E. coli</i> cultures	111
7.7.5	Restriction enzyme digestion of DNA	111
7.7.6	Purification of DNA from agarose gels.....	112
7.7.7	Phosphatase treatment of DNA.....	112
7.7.8	Ligation of DNA fragments into vectors.....	112
7.7.9	DNA Ethanol Precipitation	112
7.7.10	DNA phenol-choloroform Extraction	112
7.7.11	Polymerase chain reaction.....	113
7.7.12	Sequencing of plasmid DNA.....	113
7.7.13	Quantitative Real-Time PCR Assay.....	114
7.7.13.1	<i>PCR reaction setup for quantitative real-time PCR assay.....</i>	<i>114</i>
7.7.13.2	<i>Primers and probes for real-time quantitative PCR.....</i>	<i>114</i>
7.7.13.3	<i>Interpretation of real-time PCR data.....</i>	<i>114</i>
7.7.13.4	<i>Relative quantitation with the comparative method</i>	<i>115</i>
7.7.14	Preparation of genomic DNA of mouse tails.....	115
7.7.15	Extraction of ES cell genomic DNA	115
7.7.16	Southern blot analysis	116
7.7.16.1	<i>Digestion and gel electrophoresis of genomic DNA.....</i>	<i>116</i>

7.7.16.2	<i>Alkaline Blotting</i>	116
7.7.16.3	<i>Labeling of a southern blot probe</i>	116
7.7.16.4	<i>Hybridization and washing of the blot</i>	116
7.7.16.5	<i>Stripping of blots</i>	117
7.7.17	Typing of single blastocysts	117
7.7.18	Identifying genomic integration sites by Inverse PCR	117
7.7.19	ELISA	118
7.8	Cellular techniques	119
7.8.1	Lysis of red blood cells	119
7.8.2	Surface staining of cells for FACS analysis	119
7.8.3	Intracellular anti-BrdU staining	119
7.8.4	Staining of sections for fluorescence microscopy	120
7.9	Mouse work	120
7.9.1	Thymus dependent and independent Immunization	120
7.9.2	BrdU labeling	120
7.9.3	Mixed bone marrow chimeras	120
7.10	Cell culture methods	121
7.10.1	Determination of cell numbers	121
7.10.2	Freezing and thawing of cells	121
7.10.3	ES cell culture, transfection and selection	121
7.11	Computational methods	123
7.11.1	<i>In silico</i> genome walking.....	123
7.12	References	123
8	Curriculum Vitae	125
9	Acknowledgements	127

1 General Introduction

Vertebrates are constantly exposed to a variety of potentially pathogenic microorganisms, like bacteria, viruses or fungi, against which they have to defend themselves. In millions of years an effective and protective mechanism, the immune system, evolved. This potent defense machinery consists of two separated but interacting parts. One, termed innate immunity, is more unspecific relying on a number of barriers that are effective against a wide variety of pathogens. The other is the adaptive immunity being specific for particular microorganisms or molecules. Key players of the adaptive immunity are the B lymphocytes (B cells) and T lymphocytes (T cells). Together, they are able to respond to virtually any kind of pathogen or molecule based on the great diversity of their antigen specific receptors, the B cell receptor (BCR) of B cells and the T cell receptor (TCR) of T cells.

1.1 V(D)J recombination

1.1.1 Organization of the BCR complex and its genomic locus

The BCR is a protein complex composed of two identical heavy and light chains. Each of the two light chains is covalently linked by a disulfide bond to one of the two heavy chains, which in turn are also covalently linked by disulfide bonds (see figure 1.1 A). The amino-terminal region of a light and heavy chain vary greatly among antibodies of different specificity. These domains of highly variable sequence are called V regions and constitute the antigen-binding site. Variability in the V regions is not uniformly distributed, but is very pronounced in three segments, termed complementarity-determining regions (CDRs), forming most of the antigen-binding site. The regions with relatively constant sequence, beyond the variable regions, are called C regions. Heavy and light chain comprise several protein domains, forming antiparallel β pleated sheets which are folded into globular domains, hence they are also called immunoglobulins (Igs). Immunoglobulins can be expressed either membrane bound, as BCR, or secreted as soluble antibody, depending on alternative splicing of the primary mRNA in- or excluding the trans-membrane region encoding exons (Early et al., 1980; Rogers et al., 1980). BCR cell surface deposition also requires the expression of two accessory membrane proteins called Ig- α (*mb-1*) and

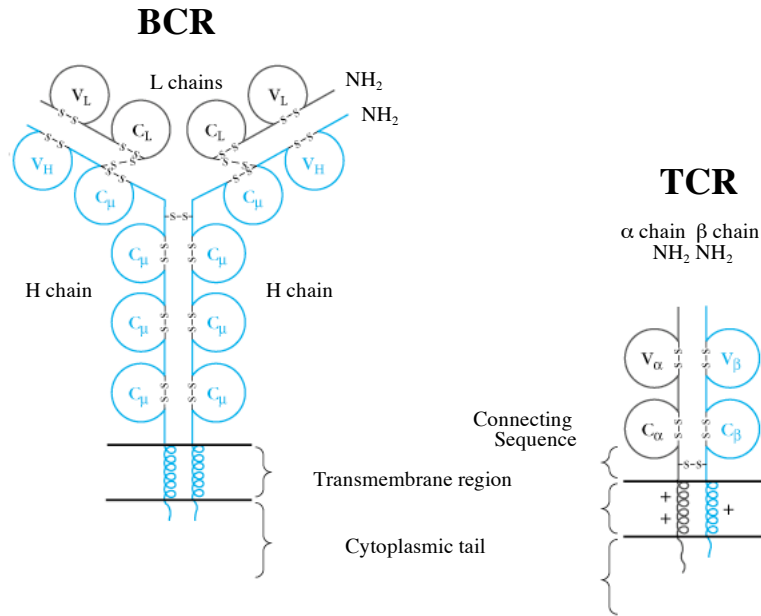
Ig- β (B29) forming a heterodimer (Hombach et al., 1990). Both proteins contain two immunoreceptor tyrosine based activation motifs (ITAMs) and are responsible for the signal transduction upon BCR engagement.

Immunoglobulin genes are located in three different genomic loci (see figure 1.1 B). The Ig heavy (IgH) chain locus is found on chromosome 12 in the mouse. The locus spans over 2 Mb and comprises regions coding for over 100 variable (V_{1-500}), 13 diversity (D_{1-12}), 4 joining (J_{1-4}) and 8 constant (C_{μ} , δ , γ_3 , γ_1 , γ_2b , γ_2a , ϵ , α) gene segments. The V_H gene segments are grouped into 15 families based on their coding sequence homology. Chromosome 6 harbours the κ light chain locus, comprising nearly 100 functional variable, 4 functional joining and 1 constant gene segment. The λ light chain locus is located on chromosome 16 consisting only of 3 variable, 3 joining and 3 constant gene segments. In contrast to the IgH locus, the Ig light (IgL) chain gene loci include no diversity gene segments.

1.1.2 Organization of the TCR complex and its genomic locus

Depending on the expression of their T cell receptor genes, T cells are subgrouped into $\alpha\beta$ and $\gamma\delta$ T cells. $\alpha\beta$ T cells express disulfide linked heterodimers of a TCR α chain together with a TCR β chain (see figure 1.1 A). Within a given species the C-terminal regions of the TCR α , β , γ or δ chains are non-variable, while the highly variable N-terminal regions, like in the Ig molecules, form the antigen binding site. Expression and signaling depends, like for the BCR, on the presence of accessory proteins, in this case the CD3 complex (Samelson et al., 1985). This complex consists of five invariant proteins, forming three different dimers: a heterodimer of γ and ϵ chains, a heterodimer of δ and ϵ chains and a homodimer of two ζ chains or a heterodimer of ζ and η chains. All chains are characterized by the presence of at least one ITAM, essential for signal transduction. Unlike Igs, the TCR is only found as a membrane bound complex. Classical $\alpha\beta$ T cells do additionally express either the CD4 or CD8 coreceptor and are accordingly grouped into CD4⁺ or CD8⁺ T cells. Depending on the expression of the coreceptor, they are restricted to recognize presented peptide antigens either in the context of major histocompatibility complex class I (MHC cII) (CD8⁺ T cells) or class II (MHC cl II) (CD4⁺ T cells). Non-classical $\alpha\beta$ T cells and $\gamma\delta$ T cells can also recognize non-peptide and unprocessed peptide

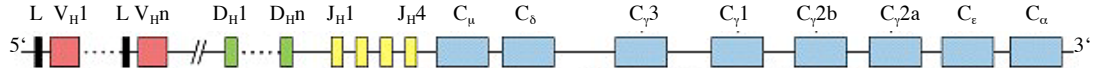
A



B

Immunoglobulin genomic loci

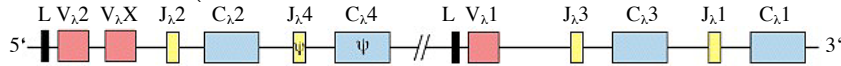
Heavy chain DNA $n \approx 134$



κ -chain DNA $n \approx 96$



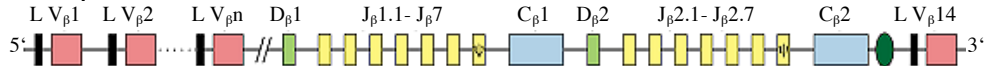
λ -chain DNA (chromosome)



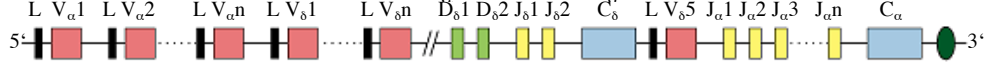
1.1

TCR genomic loci

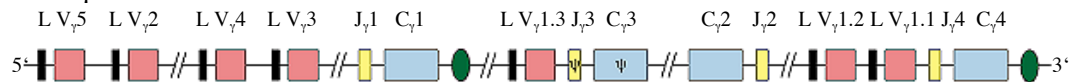
TCR β chain DNA $n \approx 20-30$



TCR α chain and δ chain DNA $V_{\alpha} n \approx 100$ $V_{\delta} n \approx 10$



TCR γ chain DNA



● = Enhancer ψ = pseudogene

Figure 1.1: Schematic representation of the BCR and TCR (A) and the Ig genomic locus (B) and TCR genomic locus (C) in the mouse. Adapted from (Kuby, 2001).

antigens, presented either by classical or non-classical antigen presenting molecules. The genes encoding the TCR chains are similarly organized like the Ig genes (see figure 1.1 C). The β chain locus in the mouse, located on chromosome 6, and the δ chain locus, found on chromosome 14, comprise several V (β : $n=25$, δ : $n=10$), D (β : $n=2$, δ : $n=2$), and J (β : $n=12$, δ : $n=2$), gene segments. The α (chromosome 14) and γ (chromosome 13) chain loci only contain V (α : $n=100$, γ : $n=7$), and J (α : $n=50$, γ : $n=3$) gene segments. Interestingly, the α chain locus is located on the same chromosome as the δ chain locus. In fact, the latter is embedded in the α chain locus. As a consequence, upon rearrangement of the α chain locus the δ chain locus is deleted, committing a T cell irreversibly to the $\alpha\beta$ lineage.

1.1.3 V(D)J recombination

Diversity of the antigen receptors of B and T cells is generated by a somatic gene rearrangement process. During this process single variable (V), sometimes diversity (D) and joining (J) gene segments are recombined together by a mechanism termed accordingly V(D)J recombination (Tonegawa, 1983). Rearrangement is a stepwise process, first rearranging a D to a J gene segment and subsequently a V to the prearranged DJ, in case of the IgH or the TCR β locus. The V and J elements of the IgL and TCR α/γ loci are directly joined. Gene segments are flanked by so called recombination signal sequences (RSS), which consist of a conserved palindromic heptamer and an AT-rich nonamer separated by a nonconserved spacer of either 12 or 23 base pairs. Recombination takes place only between two segments which are neighboured by RSS with different spacer length, referred to as the 12/23 rule (Schatz et al., 1992). Rearrangement is initiated by the binding of the recombination activating gene (RAG) proteins 1 and 2 to a pair of RSS (McBlane et al., 1995; van Gent et al., 1995). Eventually, a precleavage complex is formed where the RSS, together with the adjacent coding regions, are brought into close proximity. A single strand nick is introduced by the RAG proteins right at the border between the coding sequence and the RSS. The liberated 3'-OH group of the coding gene segment then attacks, catalyzed by the RAG proteins, in a direct transesterification reaction the phosphodiester bond on the opposite DNA strand. Thereby a hairpinned coding end

and a blunt ended signal end are created, the latter still retaining the RSSs (van Gent et al., 1996).

The DNA ends are held in a stable postcleavage synaptic complex (Hiom and Gellert, 1997) to which then general DNA repair factors of the non homologous end joining (NHEJ) DNA repair pathway are recruited to perform processing and ligation of the DNA ends. Ku86 and Ku70 form a DNA binding heterodimer (Ku) which recruits another NHEJ factor, the DNA-PK-catalytic subunit (DNA-PK_{-cs}), forming together the DNA-PK holoenzyme (Gottlieb and Jackson, 1993). This complex recruits and activates XRCC4 which in turn forms an DNA end-ligation complex together with DNA ligase IV, which is responsible for joining of the DNA ends (Grawunder et al., 1997; Li et al., 1995). Artemis, an additional NHEJ factor, is also recruited into the complex and activated (Moshous et al., 2001). Deficiency in any of the six NHEJ factors results in severe combined immunodeficiency (SCID), lacking B and T cells, due to the inability to process and join RAG cleaved coding ends and form complete antigen receptor genes. Ligation of signal ends, in contrast, still occurs in the absence of DNA-PK_{-cs} or Artemis, reflecting the differential needs for further processing of signal and respectively coding ends.

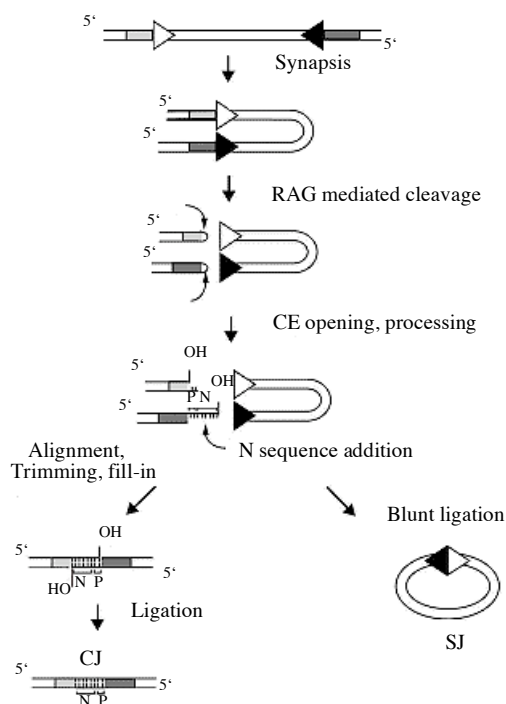


Fig. 1.2. Schematic representation of V(D)J recombination. CE = coding end, P = palindromic nucleotide, N = nontemplated nucleotide, CJ = coding joint, SJ = signal joint. Adapted from (Grawunder and Harfst, 2001).

Signal ends can be ligated without any further processing, generating a signal joint retaining both RSSs. *In vivo* they are formed with over 95% fidelity and can be detected as extrachromosomal excision circles in case of a deletional recombination event. In contrast, hairpinned coding ends have to be opened before the XRCC4/DNA ligase IV complex can form a coding joint. Hairpin nicking can occur at the tip or off-center, the latter generating either a 3' or 5' overhang. 3' extensions have, normally, to be resected before ligation can take place, unless both coding ends have compatible regions, leading to the deletion of a few nucleotides in the joining. A 5' overhang, in contrast, can directly be filled in, generating thereby short palindromic regions, termed P nucleotides. The terminal deoxynucleotidyl transferase (TdT) a lymphocyte specific protein, not belonging to the NHEJ repair pathway, is also involved in the processing of the coding ends, adding occasionally nontemplated nucleotides (N nucleotides) to the coding ends (Gilfillan et al., 1993). Combinatorial association of V, D and J gene segments, coupled with imprecise processing of the coding ends and N-nucleotide addition, produce together an enormous repertoire of primary B cell and T cell receptors.

1.1.4 Regulation of V(D)J recombination

The V(D)J recombination machinery is responsible for assembling gene segments of the immunoglobulin as well as the TCR locus. Thus, V(D)J recombination has to be tightly regulated in a stage and tissue specific way. To account for the different levels of regulation, an accessibility model has been proposed, whereby germline RSS sites, which are inaccessible for the recombination machinery due to chromatin structure or modification, must be actively „opened“ before recombination takes place.

Transcriptional enhancers embedded within antigen receptor loci have been extensively documented to play a role in tissue- and stage-specific assembly of endogenous antigen receptor gene segments (Krangel, 2003). Correspondingly, deletion of enhancer elements from endogenous mouse Ig and TCR loci blocks or significantly impairs V(D)J recombination of the corresponding loci, concomitant with impaired germline transcription (Bouvier et al., 1996; Mathieu et al., 2000). Numerous studies over the years have further shown that transcription is strongly correlated with, but not necessarily sufficient for rearrangement of adjacent antigen receptor gene segments (Senoo et al., 2001; Sikes et al., 1999). It is also not clear, if

germline transcription might not constitute a by-product arising from an accessible locus.

Generally, the role of enhancers is to open the locus to facilitate assembly of the basal transcription machinery on promoters via mechanisms that involve general chromatin opening associated with histone acetylation, CpG demethylation, recruitment of transcriptional coactivators and repositioning of promoter bound nucleosomes. These processes are likely interdependent as, for example, transcriptional coactivators often contain histone acetylase activities. Many of these events also have been implicated in regulation of V(D)J recombination. For example, CpG demethylation was recognized as an attribute of V(D)J accessible loci (Inlay and Xu, 2003; Mostoslavsky et al., 1998), although by itself it is not sufficient and/or required for VDJ recombination (Cherry et al., 2000; Gauss et al., 1998). Additionally, it was shown that CpG methylation can inhibit binding of RAG1/2 to the RSS and that direct methylation of the RSS hampers V(D)J cleavage. Enhancers, additionally, direct stage-specific acetylation of histones in chromatin of the antigen receptor genes in a pattern that strongly correlates with V(D)J accessibility (Mathieu et al., 2000; McMurry and Krangel, 2000), but histone acetylation may also not be sufficient to generate full accessibility (Senoo et al., 2001). Histone methylation has also been shown to negatively regulate V(D)J recombination (Osipovich et al., 2004). Nucleosomal RSS packaging *in vitro* inhibits V(D)J recombination and in some instances can be alleviated via histone acetylation and/or the actions of nucleosome-remodeling complexes (Golding et al., 1999; Kwon et al., 1998; Kwon et al., 2000). However it remains uncertain whether nucleosomes inhibit RAG access *in vivo*, since full-length RAG2 itself has been hypothesized to possess chromatin remodeling activity (Kirch et al., 1998; Liang et al., 2002). Early replication (Mostoslavsky et al., 2001) and central subnuclear positioning (Kosak et al., 2002) are also potentially important in regulating VDJ recombinational accessibility. As with transcription, it is not clear whether any or all of these correlates act/s as causes or are only effects of an open locus.

Mechanisms directing and stabilizing synapsis of V and (D)J RSS located over large (1-2 Mb) chromosomal distances also remain to be determined. Probably, an active coupling of RAG accessible V and D RSS takes place, as random collision between RAG bound RSS seems inefficient. In this respect, recent experimental data are interesting implicating the transcription factor Pax5 in the contraction of the IgH

chain locus, facilitating thereby rearrangement of distal V_H - DJ_H gene segments (Fuxa et al., 2004). By what mechanism this contraction is achieved remains to be explored. Finally, controlled and coordinate expression of the *RAG* genes is another mechanism to regulate V(D)J recombination. Several genetic elements are involved in the lymphocyte and stage specific expression of *RAG1/2* (Hsu et al., 2003; Monroe et al., 1999; Yu et al., 1999). In both B and T cells, levels of RAG2 are controlled by RAG2 protein degradation during transition from G1 to S phase, limiting RAG2 presence to the G0/G1 phase of the cell cycle (Lin and Desiderio, 1995). A recent report described an E3 ubiquitin ligase activity for RAG1, raising the possibility that this activity may be involved in degrading proteins, possibly also the RAG proteins themselves (Mizuta et al., 2002), to regulate V(D)J recombination (Yurchenko et al., 2003). This tight control of RAG protein expression seems to be important especially in the context of generation of DNA double strand breaks (DSB), which are always a potential danger for the integrity of the genome.

1.2 B cell development

1.2.1 B cell development in the bone marrow

B cell development takes place in the bone marrow, a primary lymphoid organ in mammals. B cells derive from hematopoietic stem cells (HSC). Analysis of the developmental potential of different stem cell and progenitor populations shows that HSC can develop into different directions entering either the megakaryocyte-platelet pathway or developing into the myeloid/lymphoid lineage (Katsura, 2002). The question if development then proceeds through a „pure“ lymphoid progenitor, a so called common lymphoid progenitor (CLP), or rather through separated B and T progenitors retaining myeloid potential is still a matter of debate.

Several nomenclatures are used in different laboratories characterizing the stages of B cell development according to their cell surface phenotype and the rearrangement status of their immunoglobulin loci. Table 1 cross-references the different nomenclatures. In this work, the nomenclature according to Rolink and Melchers will be employed.

The earliest types of characterized B cell progenitors are the pre/proB cells (see figure 1.3 A). Pre/proB cells are positive for the pan B cell marker B220 and additionally they express the interleukin 7 receptor α -chain (IL7-R, CD127) as well as the receptor for stem cell factor CD117 (*c-kit*). The following stage, proB cells, are phenotypically very similar but have gained CD19 expression. CD19 forms part of the B cell receptor (BCR) complex. The CD19 gene is a direct target of the transcription factor PAX5, thought to be responsible for B cell lineage commitment (Nutt et al., 1999). ProB cells start rearranging their IgH chain loci and eventually become preB-I cells. PreB-I cells have DJ rearrangements on both IgH alleles. Their surface phenotype resembles that of proB cells, with CD19, c-kit and IL7-R expression.

Rolink and Melchers	Pro-B	PreB-I	Large preB-II	Small preB-II	Immature B	Mature B
Osmond	Early pro-B	Intermediate pro-B	Late preB/ large preB-II	Small pre-B	Immature B	Mature B
Nishikawa Hardy	B-Pro I PA6 only A	B-Pro I PA6-IL7 B C C'	CFU-IL-7 only	D	Immature B	Mature B
		Pre/pro-B Pro-B Pro-B				

Table 1: Nomenclatures for B-lineage cells used by different laboratories.

PreB-I cells start to rearrange the prearranged DJ_H segments to a V heavy (V_H) chain gene segment, thereby producing a μ H chain. The synthesized μ H chain is then tested for pairing with the surrogate light chain (SL), consisting of a VpreB and a λ 5 protein, which associated resemble a λ light chain. The complex of a SL together with a μ H can be expressed on the cell surface, as a so called preB cell receptor (preBCR). First, only one allele is rearranged and in the case of a productive rearrangement, the cell proceeds to the following developmental stage. Only if no preBCR is expressed, will the second allele be rearranged. This sequential type of rearrangement ensures that a B cell will express only one μ H on the cell surface, thereby avoiding cells with two different specificities, a mechanism called allelic exclusion (Nussenzweig et al., 1987).

After successful rearrangement RAG-1/2 and TdT are downregulated and the cells become cycling large preB-II cells (Grawunder et al., 1995). These cells lose c-kit expression, gain CD25 expression and are positive for cytoplasmic μ H. Initially they still show CD43 and also preBCR expression, which they eventually lose. Upon preBCR expression large preB-II cells undergo 2-5 rounds of division and become afterwards resting small preB-II cells (Rolink et al., 2000). The recombination machinery, except TdT, is upregulated again and the cells start to rearrange their IgL chain loci. Rearrangement is initiated more often at the κ L chain locus than at the λ L chain locus, resulting in a ratio of 10:1 κ L chain to λ L chain expressing B cells (ten Boekel et al., 1995). Upon a successful rearrangement the cells become surface IgM (sIgM) positive immature B cells, expressing intermediate levels of B220 and low to high levels of sIgM. Immature B cells expressing a BCR with auto-reactivity are negatively selected in the bone marrow, exposure to antigen results in downregulation of sIgM and B220 expression (Hartley et al., 1993). Since these cells still express RAG-1 and RAG-2 they can undergo secondary L chain rearrangements, a rescue mechanism termed receptor editing (Gay et al., 1993). Thereby they possibly can still escape negative selection. Also cells with L chains not at all or only insufficiently pairing with the μ H chain can undergo secondary L chain rearrangement, thus improving the quality of their BCR. Only sIgM^{high} immature B cells leave the bone marrow to enter the spleen (Rolink et al., 2004). Nonetheless, of the ca. 2×10^7 B cells that develop daily in the bone marrow, only about 10-20% will enter the spleen (ten Boekel et al., 1998).

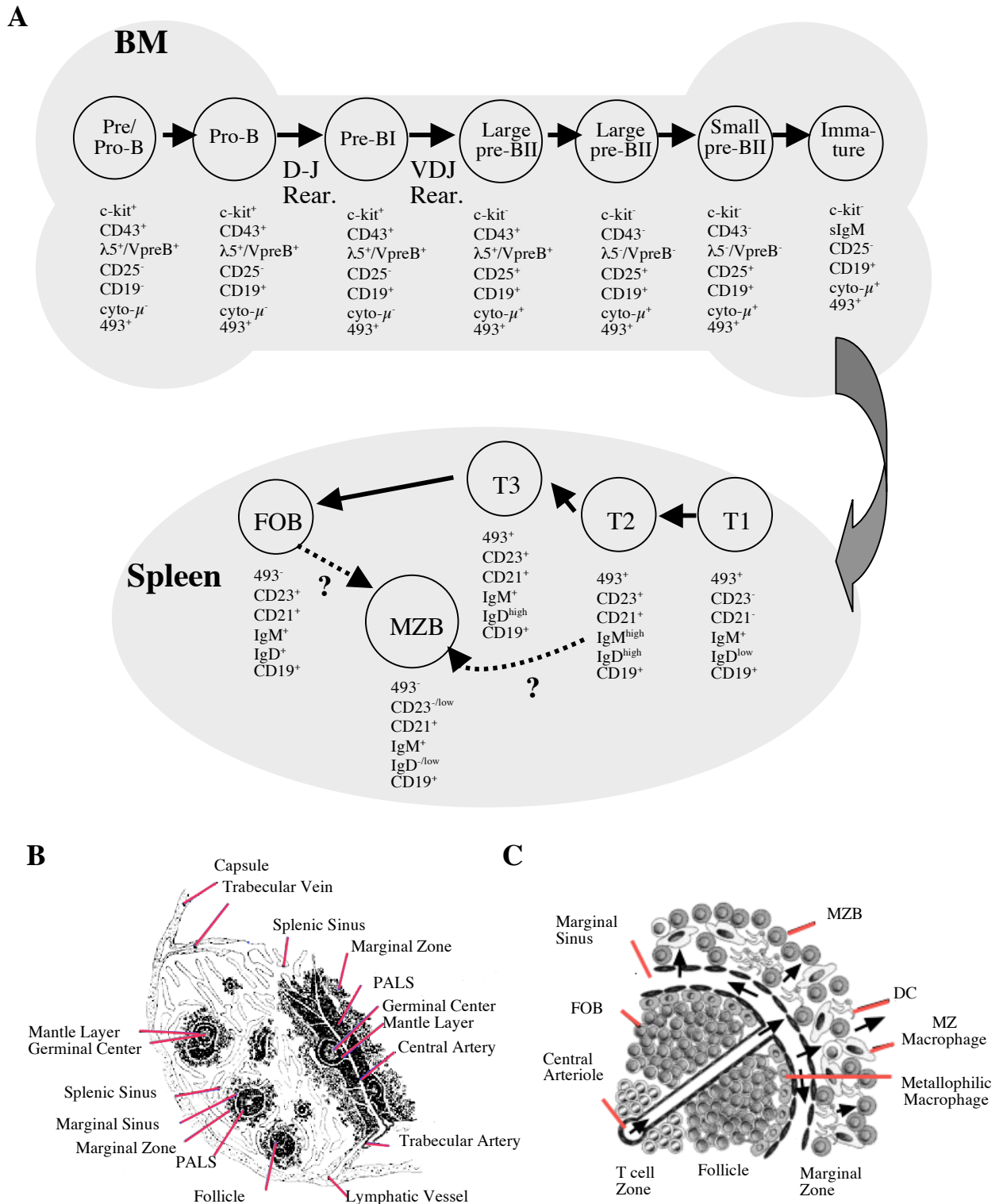


Figure 1.3: Schematic representation of B cell development in the bone marrow and spleen (A) and of the structure of the spleen (B/C). A) BM = bone marrow, T = transitional type B cell, FOB= follicular B cell, MZB = marginal zone B cell. B) PALS = periarteriolar lymphoid sheath. Adapted from (Paul, 1998). C) Arrows indicate flow of blood. DC = dendritic cell, MZ = marginal zone, FOB = follicular B cell, MZB = marginal zone B cell. Adapted from (Tanigaki et al., 2003).

1.2.2 B cell development in the spleen

Immature B cells transit via the blood to the spleen (see figure 1.3 B/C). They first enter via the terminal branches of the central arterioles the marginal sinuses, to reach the outer zone of the periarteriolar lymphoid sheath (PALS) (Liu, 1997). In the spleen, immature B cells pass through further developmental stages, until about 50% enters the pool of mature long-lived B cells (Rolink et al., 2004). Three sequential, short lived transitional B cell stages have been distinguished, transitional type 1 cells (T1), T2 and T3 cells (see figure 1.3 A). All cells of the transitional compartment are characterized by the expression of the C1q-like receptor C1qRp (CD93) recognized by the 493 antibody (as well as by the AA4.1 antibody). T1 cells are $IgM^{high}/IgD^{low}/CD19^{+}/B220^{+}$ but still $CD21^{-}/CD23^{-}$. They appear to be localized at the outer limits of the PALS whereas T2 migrate to the B cell follicles (Liu, 1997; Loder et al., 1999). T2 transitional cells become CD21 and CD23 positive and gain a higher level of IgD expression. T3 show the same cell surface phenotype as T2 cells, except that they express lower levels of sIgM. During development through the transitional stages, the cells respond differently to BCR engagement. Whereas T1 cells, like immature B cells, still undergo apoptosis upon stimulation of the BCR, later stages seem to be resistant to apoptosis and acquire the ability to proliferate (Chung et al., 2003). There is some disagreement in the literature if this change in responsiveness is already acquired at the T2 stage or rather in the mature stages.

Mature B cell stages are all 493⁺. Most prominent in the spleen are the follicular B cells (FOB). They are characterized by $CD23/CD21/IgM/IgD/CD19/B220$ expression, located inside the follicles (see figure 1.3 B/C) and participate mainly in the thymus dependent (TD) immune responses including the germinal center formation. The other main mature B cell subset of the spleen, though much less abundant, are the marginal zone B cells (MZB). The cells are $CD21^{+}/IgM^{high}/CD19^{+}/B220^{+}$ but in contrast to FOB $CD23^{-/low}/IgD^{-/low}$. Topographically, they are located at the outer rim of the follicles, neighbouring the marginal sinus in close interaction with the marginal zone macrophages and dendritic cells (see figure 1.3 B/C). The origin of MZB cells is still a matter of debate. Some authors suggest that they are directly derived from T2 cells (Saito et al., 2003) whereas other experimental data indicate that MZBs originate from FOB or even memory B cells (Vinuesa et al., 2003). MZB are thought to constitute a first line of defense against blood-borne antigens based on their optimal topographical

position right beside the marginal sinuses, where the post-arterial blood flow circulates. They mainly participate in thymus independent (TI) responses. MZB easily generate IgM secreting plasma cells and can become potent antigen presenting cells (Martin et al., 2001; Oliver et al., 1997; Oliver et al., 1999). The strategical localization together with their functional properties make them predestined to react to blood borne pathogens, thereby helping to bridge the time interval between the immediate innate immune response and the delayed TD adaptive immune response.

Another mature B cell population, B1 B cells, participates in this early response. B1 B cells are mostly involved in TI responses and are the major source of natural IgM (innate, IgM secreted without apparent antigenic presence) in the serum. Natural antibodies are important in the early immune response since they can have a protective role, delaying pathogenicity of infecting agents until antigen-induced high affinity Igs of all isotypes are produced (Baumgarth et al., 2000). B1 B cells are not very numerous in the spleen but constitute the main B cell population in the peritoneal and pleural cavities. They develop prior to weaning and further persist as a self-replenishing population.

1.2.3 Factors influencing formation of mature B cell populations

The mechanisms influencing selection of B cells into one compartment or the other are not yet fully resolved. Different naturally occurring and experimentally induced mutations affecting B cell development have helped our understanding of factors that are involved B cell lineage decision.

Enrichment of certain antigen specificities in the B1 and MZB compartment suggest that the selection into one population or the other is influenced by the presence of antigen, either self or foreign. Additionally, transgenic mice expressing certain self-reactive heavy chains show an enrichment of cells in the MZB compartment (Martin and Kearney, 2000). Also mutations affecting BCR signaling influence the lineage decision. CD19 and CD21 function together as coreceptor of the BCR to lower the threshold of BCR signaling, but CD19 can also have CD21 independent negative regulatory effects on BCR signaling. CD19^{-/-} mice lack B1 cells as well as MZB (Martin and Kearney, 2000; Rickert et al., 1995) whereas CD21 deficient mice show an enlarged MZB compartment (Cariappa et al., 2001). Deficiency in CD22, a negative regulator of BCR signaling, leads to reduced MZB cell numbers; in contrast

B1 B cells are present in normal numbers (Samardzic et al., 2002). Several other mutations affecting BCR signaling, including intracellular components of the signaling machinery, have been analyzed in respect of their effect on B lineage decision. Nonetheless, a conclusive picture of how BCR signaling and its strength are involved could not yet be drawn.

Mutations and manipulations of integrins and factors involved in migration and adhesion also affect B cell subpopulations and their localization differently. Combined inhibition of the integrins LFA-1 and $\alpha 4\beta 1$ for example causes a rapid and selective release of B cells from the MZ (Lu and Cyster, 2002). Deficiency in Pyk2, a tyrosine kinase essential for migration and adhesion in response to chemokine and integrin signals, leads to a defect in MZB cells (Guinamard et al., 2000).

Also Notch signaling is involved in the lineage decision. Initially, it was found that mice deficient for RBP-J, a transcription factor downstream of Notch, lack MZB cells (Tanigaki et al., 2002). Later on, it could be shown that Notch2 is involved in MZB generation. Mice lacking Notch2 have no MZB cells (Tanigaki et al., 2002). Already Notch2 haploinsufficiency leads to a reduction of MZB cells as well as of B1 B cells (Witt et al., 2003). The corresponding Notch ligand was found to be Delta-like 1 (Hozumi et al., 2004).

Mutations affecting the rate of B cell generation also influence the B cell lineage decision. Mice deficient in the B cell survival and differentiation factor BAFF or BAFF receptor lack FOB and MZB cells, but have a normal B1 B cell compartment. Conversely, mice transgenic for BAFF show an enlarged T2 compartment and increased numbers of mature B cells, especially MZB (Rolink and Melchers, 2002). In contrast, increased bone marrow B cell generation in IL-7 over-expressing mice leads to a massive expansion of FOB cells, but MZB cell numbers slightly decrease (Ceredig et al., 2003). IL-7 deficient mice have a block in early B cell development. Nonetheless, the mice have a normal B1 B cell compartment and most of the generated peripheral B2 B cells resemble MZB cells (Carvalho et al., 2001). Also in genetically manipulated mice in which B cells are only formed in the perinatal period, B1 B cells are present and most of the persisting B2 B cells belong to the MZB compartment (Hao and Rajewsky, 2001). Thus, it seems that in a B lymphopenic situation there is a tendency of B cells to develop into the more „innate“ compartments.

The question of how lineage decisions are made in B cells and what factors influence them, is therefore not yet solved. Different mechanisms have been implicated like for e.g. strength of the BCR signaling or antigenic selection. But, it still remains to be seen what holds true and if not a combination of several mechanisms is involved in the decision of a B cell which way to go.

1.3 Thesis objectives

V(D)J recombination is the mechanism generating the enormous diversity of antigen receptors of B and T cells. Many factors directly involved in the mechanism or in the regulation of it have been discovered like for example RAG1/2, proteins essential for the rearrangement to take place. But still, certain aspects of the mechanism have not yet been elucidated completely, and in fact, it has not been possible until now to reconstitute V(D)J recombination biochemically with purified proteins.

One step, which at the beginning of thesis had not been resolved unequivocally, is the opening of the hairpinned coding ends. Several proteins have been implicated in this process, including the RAG proteins themselves (Besmer et al., 1998; Shockett and Schatz, 1999), which were shown to open coding ends *in vitro*.

The Nbs1/Mre11/Rad50 complex has also been hypothesized to be responsible for the nicking of the coding ends. This DNA repair complex was shown to open hairpinned coding ends *in vitro* (Paull and Gellert, 1999). Additionally, its homologues in yeast participate, amongst others, in the NHEJ DNA repair mechanism. Until now all factors of the NHEJ DNA repair pathway also have been shown to participate in V(D)J recombination, therefore it would be conceivable that the Nbs1/Mre11/Rad50 complex is also involved in V(D)J recombination and that, in fact, it constitutes the hairpin opening activity. A detailed analysis of V(D)J recombination in cells of patients with a mutation in the *Nbs1* gene, suffering from the genetic instability disorder Nijmegen breakage syndrome (Varon et al., 1998), should help to test this hypothesis.

Another factor, identified based on its RSS binding ability (Wu et al., 1993), the kappa B and RSS recognition component (KRC) has also been hypothesized to be a yet unidentified protein participating in the regulation or directly in the mechanism of V(D)J recombination. The expression pattern of KRC, being mainly lymphoid apart from neuronal (Wu et al., 1996), together with the affinity to the RSS, additionally shown to be regulated (Wu et al., 2001), would correspond to it. Targeting of the *KRC* locus in the mouse and subsequent analysis of the effects of KRC deficiency on lymphoid development, especially on V(D)J recombination, should help to clarify the role of KRC.

The first completely assembled protein product of V(D)J recombination during B cell development is the μ H chain. In preB-II cells the μ H chain is „quality-tested“ by co-expression with the SL chain for pairing and surface expression. Successful deposition of the preBCR complex on the cell surface allows the cells to expand and develop further. Deficiency in one of the components of the SL, the λ 5 protein, leads to a block in early B cell development (Kitamura et al., 1992). However, the block is not complete allowing the generation of some mature B cells. Since in other experimental systems it has been shown, that the rate of B cell generation influences the shaping of mature B cell populations, the question is how λ 5 deficiency and the concomitant reduction in B cell generation affect proportioning of the mature B cell populations in the λ 5^{-/-} mice. A detailed analysis of the different peripheral B cell compartments, their turnover and repopulation ability should help to address this question.

1.4 References

- Baumgarth, N., Herman, O. C., Jager, G. C., Brown, L. E., Herzenberg, L. A., and Chen, J. (2000). B-1 and B-2 cell-derived immunoglobulin M antibodies are nonredundant components of the protective response to influenza virus infection. *J Exp Med* *192*, 271-280.
- Besmer, E., Mansilla-Soto, J., Cassard, S., Sawchuk, D. J., Brown, G., Sadofsky, M., Lewis, S. M., Nussenzweig, M. C., and Cortes, P. (1998). Hairpin coding end opening is mediated by RAG1 and RAG2 proteins. *Mol Cell* *2*, 817-828.
- Bouvier, G., Watrin, F., Naspetti, M., Verthuy, C., Naquet, P., and Ferrier, P. (1996). Deletion of the mouse T-cell receptor beta gene enhancer blocks alphabeta T-cell development. *Proc Natl Acad Sci U S A* *93*, 7877-7881.
- Cariappa, A., Tang, M., Parnig, C., Nebelitskiy, E., Carroll, M., Georgopoulos, K., and Pillai, S. (2001). The follicular versus marginal zone B lymphocyte cell fate decision is regulated by Aiolos, Btk, and CD21. *Immunity* *14*, 603-615.
- Carvalho, T. L., Mota-Santos, T., Cumano, A., Demengeot, J., and Vieira, P. (2001). Arrested B lymphopoiesis and persistence of activated B cells in adult interleukin 7(-/-) mice. *J Exp Med* *194*, 1141-1150.
- Ceredig, R., Bosco, N., Maye, P. N., Andersson, J., and Rolink, A. (2003). In interleukin-7-transgenic mice, increasing B lymphopoiesis increases follicular but not marginal zone B cell numbers. *Eur J Immunol* *33*, 2567-2576.
- Cherry, S. R., Beard, C., Jaenisch, R., and Baltimore, D. (2000). V(D)J recombination is not activated by demethylation of the kappa locus. *Proc Natl Acad Sci U S A* *97*, 8467-8472.
- Chung, J. B., Silverman, M., and Monroe, J. G. (2003). Transitional B cells: step by step towards immune competence. *Trends Immunol* *24*, 343-349.
- Early, P., Rogers, J., Davis, M., Calame, K., Bond, M., Wall, R., and Hood, L. (1980). Two mRNAs can be produced from a single immunoglobulin mu gene by alternative RNA processing pathways. *Cell* *20*, 313-319.
- Fuxa, M., Skok, J., Souabni, A., Salvagiotto, G., Roldan, E., and Busslinger, M. (2004). Pax5 induces V-to-DJ rearrangements and locus contraction of the immunoglobulin heavy-chain gene. *Genes Dev* *18*, 411-422.
- Gauss, G. H., Domain, I., Hsieh, C. L., and Lieber, M. R. (1998). V(D)J recombination activity in human hematopoietic cells: correlation with developmental stage and genome stability. *Eur J Immunol* *28*, 351-358.
- Gay, D., Saunders, T., Camper, S., and Weigert, M. (1993). Receptor editing: an approach by autoreactive B cells to escape tolerance. *J Exp Med* *177*, 999-1008.

- Gilfillan, S., Dierich, A., Lemeur, M., Benoist, C., and Mathis, D. (1993). Mice lacking TdT: mature animals with an immature lymphocyte repertoire. *Science* *261*, 1175-1178.
- Golding, A., Chandler, S., Ballestar, E., Wolffe, A. P., and Schlissel, M. S. (1999). Nucleosome structure completely inhibits in vitro cleavage by the V(D)J recombinase. *Embo J* *18*, 3712-3723.
- Gottlieb, T. M., and Jackson, S. P. (1993). The DNA-dependent protein kinase: requirement for DNA ends and association with Ku antigen. *Cell* *72*, 131-142.
- Grawunder, U., and Harfst, E. (2001). How to make ends meet in V(D)J recombination. *Curr Opin Immunol* *13*, 186-194.
- Grawunder, U., Leu, T. M., Schatz, D. G., Werner, A., Rolink, A. G., Melchers, F., and Winkler, T. H. (1995). Down-regulation of RAG1 and RAG2 gene expression in preB cells after functional immunoglobulin heavy chain rearrangement. *Immunity* *3*, 601-608.
- Grawunder, U., Wilm, M., Wu, X., Kulesza, P., Wilson, T. E., Mann, M., and Lieber, M. R. (1997). Activity of DNA ligase IV stimulated by complex formation with XRCC4 protein in mammalian cells. *Nature* *388*, 492-495.
- Guinamard, R., Okigaki, M., Schlessinger, J., and Ravetch, J. V. (2000). Absence of marginal zone B cells in Pyk-2-deficient mice defines their role in the humoral response. *Nat Immunol* *1*, 31-36.
- Hao, Z., and Rajewsky, K. (2001). Homeostasis of peripheral B cells in the absence of B cell influx from the bone marrow. *J Exp Med* *194*, 1151-1164.
- Hartley, S. B., Cooke, M. P., Fulcher, D. A., Harris, A. W., Cory, S., Basten, A., and Goodnow, C. C. (1993). Elimination of self-reactive B lymphocytes proceeds in two stages: arrested development and cell death. *Cell* *72*, 325-335.
- Hiom, K., and Gellert, M. (1997). A stable RAG1-RAG2-DNA complex that is active in V(D)J cleavage. *Cell* *88*, 65-72.
- Hombach, J., Tsubata, T., Leclercq, L., Stappert, H., and Reth, M. (1990). Molecular components of the B-cell antigen receptor complex of the IgM class. *Nature* *343*, 760-762.
- Hozumi, K., Negishi, N., Suzuki, D., Abe, N., Sotomaru, Y., Tamaoki, N., Mailhos, C., Ish-Horowicz, D., Habu, S., and Owen, M. J. (2004). Delta-like 1 is necessary for the generation of marginal zone B cells but not T cells in vivo. *Nat Immunol* *5*, 638-644.
- Hsu, L. Y., Lauring, J., Liang, H. E., Greenbaum, S., Cado, D., Zhuang, Y., and Schlissel, M. S. (2003). A conserved transcriptional enhancer regulates RAG gene expression in developing B cells. *Immunity* *19*, 105-117.
- Inlay, M., and Xu, Y. (2003). Epigenetic regulation of antigen receptor rearrangement. *Clin Immunol* *109*, 29-36.

- Katsura, Y. (2002). Redefinition of lymphoid progenitors. *Nat Rev Immunol* 2, 127-132.
- Kirch, S. A., Rathbun, G. A., and Oettinger, M. A. (1998). Dual role of RAG2 in V(D)J recombination: catalysis and regulation of ordered Ig gene assembly. *Embo J* 17, 4881-4886.
- Kitamura, D., Kudo, A., Schaal, S., Muller, W., Melchers, F., and Rajewsky, K. (1992). A critical role of lambda 5 protein in B cell development. *Cell* 69, 823-831.
- Kosak, S. T., Skok, J. A., Medina, K. L., Riblet, R., Le Beau, M. M., Fisher, A. G., and Singh, H. (2002). Subnuclear compartmentalization of immunoglobulin loci during lymphocyte development. *Science* 296, 158-162.
- Krangel, M. S. (2003). Gene segment selection in V(D)J recombination: accessibility and beyond. *Nat Immunol* 4, 624-630.
- Kuby, J. (2001). *Immunology*, Fourth Edition edn).
- Kwon, J., Imbalzano, A. N., Matthews, A., and Oettinger, M. A. (1998). Accessibility of nucleosomal DNA to V(D)J cleavage is modulated by RSS positioning and HMG1. *Mol Cell* 2, 829-839.
- Kwon, J., Morshead, K. B., Guyon, J. R., Kingston, R. E., and Oettinger, M. A. (2000). Histone acetylation and hSWI/SNF remodeling act in concert to stimulate V(D)J cleavage of nucleosomal DNA. *Mol Cell* 6, 1037-1048.
- Li, Z., Otevrel, T., Gao, Y., Cheng, H. L., Seed, B., Stamato, T. D., Taccioli, G. E., and Alt, F. W. (1995). The XRCC4 gene encodes a novel protein involved in DNA double-strand break repair and V(D)J recombination. *Cell* 83, 1079-1089.
- Liang, H. E., Hsu, L. Y., Cado, D., Cowell, L. G., Kelsoe, G., and Schlissel, M. S. (2002). The "dispensable" portion of RAG2 is necessary for efficient V-to-DJ rearrangement during B and T cell development. *Immunity* 17, 639-651.
- Lin, W. C., and Desiderio, S. (1995). V(D)J recombination and the cell cycle. *Immunol Today* 16, 279-289.
- Liu, Y. J. (1997). Sites of B lymphocyte selection, activation, and tolerance in spleen. *J Exp Med* 186, 625-629.
- Loder, F., Mutschler, B., Ray, R. J., Paige, C. J., Sideras, P., Torres, R., Lamers, M. C., and Carsetti, R. (1999). B cell development in the spleen takes place in discrete steps and is determined by the quality of B cell receptor-derived signals. *J Exp Med* 190, 75-89.
- Lu, T. T., and Cyster, J. G. (2002). Integrin-mediated long-term B cell retention in the splenic marginal zone. *Science* 297, 409-412.
- Martin, F., and Kearney, J. F. (2000). Positive selection from newly formed to marginal zone B cells depends on the rate of clonal production, CD19, and btk. *Immunity* 12, 39-49.

- Martin, F., Oliver, A. M., and Kearney, J. F. (2001). Marginal zone and B1 B cells unite in the early response against T-independent blood-borne particulate antigens. *Immunity* 14, 617-629.
- Mathieu, N., Hempel, W. M., Spicuglia, S., Verthuy, C., and Ferrier, P. (2000). Chromatin remodeling by the T cell receptor (TCR)-beta gene enhancer during early T cell development: Implications for the control of TCR-beta locus recombination. *J Exp Med* 192, 625-636.
- McBlane, J. F., van Gent, D. C., Ramsden, D. A., Romeo, C., Cuomo, C. A., Gellert, M., and Oettinger, M. A. (1995). Cleavage at a V(D)J recombination signal requires only RAG1 and RAG2 proteins and occurs in two steps. *Cell* 83, 387-395.
- McMurry, M. T., and Krangel, M. S. (2000). A role for histone acetylation in the developmental regulation of VDJ recombination. *Science* 287, 495-498.
- Mizuta, R., Mizuta, M., Araki, S., and Kitamura, D. (2002). RAG2 is down-regulated by cytoplasmic sequestration and ubiquitin-dependent degradation. *J Biol Chem* 277, 41423-41427.
- Monroe, R. J., Chen, F., Ferrini, R., Davidson, L., and Alt, F. W. (1999). RAG2 is regulated differentially in B and T cells by elements 5' of the promoter. *Proc Natl Acad Sci U S A* 96, 12713-12718.
- Moshous, D., Callebaut, I., de Chasseval, R., Corneo, B., Cavazzana-Calvo, M., Le Deist, F., Tezcan, I., Sanal, O., Bertrand, Y., Philippe, N., *et al.* (2001). Artemis, a novel DNA double-strand break repair/V(D)J recombination protein, is mutated in human severe combined immune deficiency. *Cell* 105, 177-186.
- Mostoslavsky, R., Singh, N., Kirillov, A., Pelanda, R., Cedar, H., Chess, A., and Bergman, Y. (1998). Kappa chain monoallelic demethylation and the establishment of allelic exclusion. *Genes Dev* 12, 1801-1811.
- Mostoslavsky, R., Singh, N., Tenzen, T., Goldmit, M., Gabay, C., Elizur, S., Qi, P., Reubinoff, B. E., Chess, A., Cedar, H., and Bergman, Y. (2001). Asynchronous replication and allelic exclusion in the immune system. *Nature* 414, 221-225.
- Nussenzweig, M. C., Shaw, A. C., Sinn, E., Danner, D. B., Holmes, K. L., Morse, H. C., 3rd, and Leder, P. (1987). Allelic exclusion in transgenic mice that express the membrane form of immunoglobulin mu. *Science* 236, 816-819.
- Nutt, S. L., Heavey, B., Rolink, A. G., and Busslinger, M. (1999). Commitment to the B-lymphoid lineage depends on the transcription factor Pax5. *Nature* 401, 556-562.
- Oliver, A. M., Martin, F., Gartland, G. L., Carter, R. H., and Kearney, J. F. (1997). Marginal zone B cells exhibit unique activation, proliferative and immunoglobulin secretory responses. *Eur J Immunol* 27, 2366-2374.
- Oliver, A. M., Martin, F., and Kearney, J. F. (1999). IgM^{high}CD21^{high} lymphocytes enriched in the splenic marginal zone generate effector cells more rapidly than the bulk of follicular B cells. *J Immunol* 162, 7198-7207.

- Osipovich, O., Milley, R., Meade, A., Tachibana, M., Shinkai, Y., Krangel, M. S., and Oltz, E. M. (2004). Targeted inhibition of V(D)J recombination by a histone methyltransferase. *Nat Immunol* 5, 309-316.
- Paul, W. E. (1998). *Fundamental Immunology*, Fourth edn).
- Paull, T. T., and Gellert, M. (1999). Nbs1 potentiates ATP-driven DNA unwinding and endonuclease cleavage by the Mre11/Rad50 complex. *Genes Dev* 13, 1276-1288.
- Rickert, R. C., Rajewsky, K., and Roes, J. (1995). Impairment of T-cell-dependent B-cell responses and B-1 cell development in CD19-deficient mice. *Nature* 376, 352-355.
- Rogers, J., Early, P., Carter, C., Calame, K., Bond, M., Hood, L., and Wall, R. (1980). Two mRNAs with different 3' ends encode membrane-bound and secreted forms of immunoglobulin mu chain. *Cell* 20, 303-312.
- Rolink, A. G., Andersson, J., and Melchers, F. (2004). Molecular mechanisms guiding late stages of B-cell development. *Immunol Rev* 197, 41-50.
- Rolink, A. G., and Melchers, F. (2002). BAFFled B cells survive and thrive: roles of BAFF in B-cell development. *Curr Opin Immunol* 14, 266-275.
- Rolink, A. G., Winkler, T., Melchers, F., and Andersson, J. (2000). Precursor B cell receptor-dependent B cell proliferation and differentiation does not require the bone marrow or fetal liver environment. *J Exp Med* 191, 23-32.
- Saito, T., Chiba, S., Ichikawa, M., Kunisato, A., Asai, T., Shimizu, K., Yamaguchi, T., Yamamoto, G., Seo, S., Kumano, K., *et al.* (2003). Notch2 is preferentially expressed in mature B cells and indispensable for marginal zone B lineage development. *Immunity* 18, 675-685.
- Samardzic, T., Marinkovic, D., Danzer, C. P., Gerlach, J., Nitschke, L., and Wirth, T. (2002). Reduction of marginal zone B cells in CD22-deficient mice. *Eur J Immunol* 32, 561-567.
- Samelson, L. E., Harford, J. B., and Klausner, R. D. (1985). Identification of the components of the murine T cell antigen receptor complex. *Cell* 43, 223-231.
- Schatz, D. G., Oettinger, M. A., and Schlissel, M. S. (1992). V(D)J recombination: molecular biology and regulation. *Annu Rev Immunol* 10, 359-383.
- Senoo, M., Mochida, N., Wang, L., Matsumura, Y., Suzuki, D., Takeda, N., Shinkai, Y., and Habu, S. (2001). Limited effect of chromatin remodeling on D(beta)-to-J(beta) recombination in CD4+CD8+ thymocyte: implications for a new aspect in the regulation of TCR beta gene recombination. *Int Immunol* 13, 1405-1414.
- Shockett, P. E., and Schatz, D. G. (1999). DNA hairpin opening mediated by the RAG1 and RAG2 proteins. *Mol Cell Biol* 19, 4159-4166.
- Sikes, M. L., Suarez, C. C., and Oltz, E. M. (1999). Regulation of V(D)J recombination by transcriptional promoters. *Mol Cell Biol* 19, 2773-2781.

Tanigaki, K., Han, H., Yamamoto, N., Tashiro, K., Ikegawa, M., Kuroda, K., Suzuki, A., Nakano, T., and Honjo, T. (2002). Notch-RBP-J signaling is involved in cell fate determination of marginal zone B cells. *Nat Immunol* 3, 443-450.

Tanigaki, K., Kuroda, K., Han, H., and Honjo, T. (2003). Regulation of B cell development by Notch/RBP-J signaling. *Semin Immunol* 15, 113-119.

ten Boekel, E., Melchers, F., and Rolink, A. (1995). The status of Ig loci rearrangements in single cells from different stages of B cell development. *Int Immunol* 7, 1013-1019.

ten Boekel, E., Melchers, F., and Rolink, A. G. (1998). Precursor B cells showing H chain allelic inclusion display allelic exclusion at the level of pre-B cell receptor surface expression. *Immunity* 8, 199-207.

Tonegawa, S. (1983). Somatic generation of antibody diversity. *Nature* 302, 575-581.

van Gent, D. C., McBlane, J. F., Ramsden, D. A., Sadofsky, M. J., Hesse, J. E., and Gellert, M. (1995). Initiation of V(D)J recombination in a cell-free system. *Cell* 81, 925-934.

van Gent, D. C., Mizuuchi, K., and Gellert, M. (1996). Similarities between initiation of V(D)J recombination and retroviral integration. *Science* 271, 1592-1594.

Varon, R., Vissinga, C., Platzer, M., Cerosaletti, K. M., Chrzanowska, K. H., Saar, K., Beckmann, G., Seemanova, E., Cooper, P. R., Nowak, N. J., *et al.* (1998). Nibrin, a novel DNA double-strand break repair protein, is mutated in Nijmegen breakage syndrome. *Cell* 93, 467-476.

Vinuesa, C. G., Sze, D. M., Cook, M. C., Toellner, K. M., Klaus, G. G., Ball, J., and MacLennan, I. C. (2003). Recirculating and germinal center B cells differentiate into cells responsive to polysaccharide antigens. *Eur J Immunol* 33, 297-305.

Witt, C. M., Won, W. J., Hurez, V., and Klug, C. A. (2003). Notch2 haploinsufficiency results in diminished B1 B cells and a severe reduction in marginal zone B cells. *J Immunol* 171, 2783-2788.

Wu, L. C., Hicar, M. D., Hong, J., and Allen, C. E. (2001). The DNA-binding ability of HIVEP3/KRC decreases upon activation of V(D)J recombination. *Immunogenetics* 53, 564-571.

Wu, L. C., Liu, Y., Strandtmann, J., Mak, C. H., Lee, B., Li, Z., and Yu, C. Y. (1996). The mouse DNA binding protein Rc for the kappa B motif of transcription and for the V(D)J recombination signal sequences contains composite DNA-protein interaction domains and belongs to a new family of large transcriptional proteins. *Genomics* 35, 415-424.

Wu, L. C., Mak, C. H., Dear, N., Boehm, T., Foroni, L., and Rabbitts, T. H. (1993). Molecular cloning of a zinc finger protein which binds to the heptamer of the signal sequence for V(D)J recombination. *Nucleic Acids Res* 21, 5067-5073.

Yu, W., Misulovin, Z., Suh, H., Hardy, R. R., Jankovic, M., Yannoutsos, N., and Nussenzweig, M. C. (1999). Coordinate regulation of RAG1 and RAG2 by cell type-specific DNA elements 5' of RAG2. *Science* 285, 1080-1084.

Yurchenko, V., Xue, Z., and Sadofsky, M. (2003). The RAG1 N-terminal domain is an E3 ubiquitin ligase. *Genes Dev* 17, 581-585.

2 Normal V(D)J recombination in cells from patients with Nijmegen breakage syndrome

Eva Harfst, Suzanne Cooper, Susann Neubauer, Luitpold Distel, Ulf Grawunder

Molecular Immunology, 37 (2000) 915-929



PERGAMON

Molecular Immunology 37 (2000) 915–929

**Molecular
Immunology**

www.elsevier.com/locate/molimm

Normal V(D)J recombination in cells from patients with Nijmegen breakage syndrome

Eva Harfst^{a,1}, Suzanne Cooper^a, Susann Neubauer^b, Luitpold Distel^b,
Ulf Grawunder^{a,*}

^a Basel Institute for Immunology, Grenzacherstr. 487, CH-4005 Basel, Switzerland

^b Klinik und Poliklinik für Strahlentherapie, Friedrich-Alexander-Universität Erlangen-Nürnberg, Universitätsstr. 27, D-91054 Erlangen, Germany

Received 10 October 2000; accepted 29 December 2000

Abstract

The majority of antigen receptor diversity in mammals is generated by V(D)J recombination. During this process DNA double strand breaks are introduced at recombination signals by lymphoid specific RAG1/2 proteins generating blunt ended signal ends and hairpinned coding ends. Rejoining of all DNA ends requires ubiquitously expressed DNA repair proteins, such as Ku70/86 and DNA ligase IV/XRCC4. In addition, the formation of coding joints depends on the function of the *scid* gene encoding the catalytic subunit of DNA-dependent protein kinase, DNA-PK_{CS}, that is somehow required for processing of coding end hairpins. Recently, it was shown that purified RAG1/2 proteins can cleave DNA hairpins *in vitro*, but the same activity was also described for a protein complex of the DNA repair proteins Nbs1/Mre11/Rad50. This leaves the possibility that either protein complex might be involved in coding end processing in V(D)J recombination. We have therefore analyzed V(D)J recombination in cells from patients with Nijmegen breakage syndrome, carrying a mutation in the *nbs1* gene. We find that V(D)J recombination frequencies and the quality of signal and coding joining are comparable to wild-type controls, as analyzed by a cellular V(D)J recombination assay. In addition, we did not detect significant differences in CDR3 sequences of endogenous Ig λL and κL chain gene loci cloned from peripheral blood lymphocytes of an NBS patient and of healthy individuals. These findings suggest that the Nbs1/Mre11/Rad50 complex is not involved in coding end processing of V(D)J recombination. © 2001 Elsevier Science Ltd. All rights reserved.

Keywords: DNA repair; Nijmegen breakage syndrome; V(D)J recombination

Abbreviations: AT, Ataxia telangiectasia; CDR, complementary determining region; CJ, coding joint; DNA-PK_{CS}, DNA dependent protein kinase (catalytic subunit); DSB, DNA double strand break; DSB_R, DNA double strand break repair; EBV, Epstein–Barr virus; FCS, fetal calf serum; IRIF, irradiation induced nuclear foci; NBS, Nijmegen breakage syndrome; NHEJ, non-homologous DNA end joining; PBL peripheral blood lymphocyte; RAG, recombination activating gene; RSS, recombination signal sequence; SJ, signal joint; WT, wild-type.

* Corresponding author. Tel.: +49-731-50023373; fax: +49-731-50023367.

E-mail address: ulf.grawunder@medizin.uni-ulm.de (U. Grawunder).

¹ Present address: Universität Ulm, Universitätsklinikum, Abteilung Immunologie, Albert-Einstein-Allee 11, D-89081 Ulm, Germany

1. Introduction

Immunoglobulin and T cell receptor diversity is mainly generated by V(D)J recombination, a somatic DNA recombination process occurring during early B and T lymphopoiesis. The antigen receptor gene loci are organized in clusters of V (variable), sometimes D (diversity) and J (joining) gene segments (Tonegawa, 1983) from which each one segment can be randomly selected and site-specifically recombined. Each lymphocyte, thereby, creates a novel V(D)J region encoding a unique variable domain of an antigen receptor molecule. The site-specificity of V(D)J recombination is mediated by conserved recombination signal sequences (RSS) flanking all functional V-, D- and J-coding regions. The RSS are recognized by the lymphocyte specific RAG-1 and RAG-2 proteins, which cleave DNA

at the border of the signals and coding regions (McBlane et al., 1995). This reaction generates blunt signal and covalently sealed hairpinned coding ends (van Gent et al., 1995), which are held together in a postcleavage complex (Agrawal and Schatz, 1997). Ubiquitously expressed DNA repair factors are targeted to this complex including the DNA end binding proteins Ku70 and Ku86 and the catalytic subunit of DNA-dependent protein kinase (DNA-PK_{CS}). Eventually, coding and signal joints are formed by the DNA ligase IV/XRCC4 complex (Critchlow et al., 1997; Grawunder et al., 1997). Mutations in genes for any of the above mentioned components interfere with the completion of V(D)J recombination and lead to severe combined immunodeficiencies in animals (Frank et al., 1998; Gao et al., 1998a,b; Grawunder et al., 1998; Gu et al., 1997; Nussenzweig et al., 1996; Taccioli et al., 1998; Zhu et al., 1996).

Signal ends are usually religated without major modifications, whereas coding ends undergo extensive processing resulting in increased junctional diversity at coding joints (CJs). This processing includes the addition of N-nucleotides by the template independent DNA polymerase terminal deoxynucleotidyl transferase (Gilfillan et al., 1993; Komori et al., 1993). Furthermore, CJs sometimes contain P-nucleotides, which are the result of an off-center cleavage of hairpinned coding end intermediates, followed by DNA polymerase fill-in (Roth et al., 1992). Finally, coding end sequences are often found to be shortened by exonucleolytic nibbling catalyzed by yet unidentified DNA nucleases.

DNA-PK_{CS}, which is only essential for CJ formation, has been implicated in the processing of DNA hairpins, because hairpinned coding end intermediates accumulate in *scid* lymphocytes (Roth et al., 1992). Based on the biochemical activity of purified RAG-1/2 proteins in vitro, it was recently suggested that the RAG-1/2 proteins themselves contain the hairpin nicking activity (Besmer et al., 1998; Shockett and Schatz, 1999). However, a ternary protein complex of Nbs1/Mre11/Rad50 has also been shown to be capable of catalyzing this reaction in vitro (Paull and Gellert, 1999), leaving open which activity is involved in CJ processing in vivo.

Nbs1, Mre11 and Rad50 are involved in the repair of DNA DSBs in mammalian cells, and mutations in any of these genes lead to genetic instability and increased sensitivity to ionizing radiation (Carney et al., 1998; Luo et al., 1999; Stewart et al., 1999; Varon et al., 1998). The Nbs1/Mre11/Rad50 protein complex appears to localize to sites of DNA damage, as evidenced by the formation of irradiation induced nuclear foci (IRIF) that can be visualized after challenging cells with ionizing radiation (Maser et al., 1997). Mutations in either Nbs1 or Mre11 prevent IRIF formation (Carney et al., 1998; Stewart et al., 1999). In the case of Mre11 it was further shown that the protein localizes,

within 30 min, to subnuclear volumes that had been exposed to ionizing radiation (Nelms et al., 1998). These findings suggest a direct association of the Nbs1/Mre11/Rad50 complex with DSBs. Despite these findings, the precise function of the mammalian Nbs1/Mre11/Rad50 complex remains unknown.

In particular, it remains unclear to what extent Nbs1/Mre11/Rad50 participate in either homologous DNA repair or non-homologous DNA end joining (NHEJ). NBS cells, like AT cells, are characterized by an impaired p53 response upon induction of DSBs leading to defective G₁/S cell cycle checkpoint control (Antocchia et al., 1999; Jongmans et al., 1997). It has, therefore, been suggested that the Nbs1/Mre11/Rad50 complex might be required to sense and to signal the presence of DSBs. Interestingly, mammalian cells with a complete null mutation of either *mre11* or *rad50* appear not to be viable, suggesting indispensable cellular functions of Mre11 and Rad50 (Luo et al., 1999; Xiao and Weaver, 1997; Yamaguchi-Iwai et al., 1999). In contrast, mutations of the yeast homologues *sc-xrs2*, *sc-mre11*, and *sc-rad50* result in viable yeast strains. The yeast homologues are part of the *rad52* epistasis group, whose members are essential for homologous DNA repair and meiotic recombination. In addition, *sc-xrs2*, *sc-mre11*, and *sc-rad50*, form a sub-epistasis group that is also required for repairing DSBs by NHEJ (Boulton and Jackson, 1998; Moore and Haber, 1996).

In humans, mutations in the *nbs1* gene lead to the rare genetic instability disorder Nijmegen breakage syndrome (NBS) (Carney et al., 1998; Matsuura et al., 1998; Varon et al., 1998). Cells from NBS patients are characterized by chromosomal instability, defects in cell cycle checkpoints, and sensitivity to ionizing radiation. Hallmarks of the disease are microcephaly, growth retardation, immunodeficiency, and an increased predisposition to cancer, in particular lymphomas [for a concise review, see (Digweed et al., 1999)]. The clinical phenotype of NBS patients is similar to patients suffering from *Ataxia telangiectasia* (AT), a disease caused by mutations in the *atm* gene encoding the ATM protein belonging to the phosphatidylinositol-3-phosphate (PI3) kinase family (Savitsky et al., 1995).

Because of the capability of a purified Nbs1/Mre11/Rad50 complex to open hairpinned DNA substrates in vitro, and the possibility that these proteins might be involved in NHEJ in mammalian cells, we analyzed V(D)J recombination in NBS cells in vivo. This was done (1) by measuring V(D)J recombination on extra-chromosomal V(D)J recombination substrates (2) by the sequencing of CDR3 regions from endogenous Ig λ and Igk light chain gene loci from PBLs of an NBS patient. We found that the frequency and the quality of signal and coding joint formation in NBS cells is normal when compared to wild-type and AT controls. Furthermore, we could not detect significant differences

in CDR3 regions between NBS patients and normal individuals. These findings suggest that Nbs1 does not play a role in V(D)J recombination *in vivo*.

2. Materials and methods

2.1. Patients and cell lines

Peripheral blood samples from healthy donors and patients diagnosed with AT, and in one case with NBS, were analyzed after informed consent. From some patients lymphoblastoid cell lines (LCLs) were established by Epstein–Barr virus (EBV) transformation according to standard protocols (Neizel, 1986). Cell line NBS-P122 was derived from an NBS patient diagnosed with NBS and carrying a homozygous 5 bp deletion at position 657 of exon 6 of the *nbs1* gene. Cell line AT-P104 was derived from an AT patient. Two additional EBV transformed NBS cell lines, MS1 and MS2 were kindly provided by Dr Markus Stumm, University of Magdeburg, Germany. Control cell lines from healthy donors included the EBV transformed LCLs MC8866 and MC221, that were kindly provided by Dr Marina Cella (The Basel Institute for Immunology, Basel, Switzerland). For V(D)J recombination assays, the human preB-ALL cell line Nalm-6 and a DNA ligase IV deficient cell line derived from it (Grawunder et al., 1998) were used as additional positive and negative controls, respectively. All cells were grown in RPMI 1640 medium, supplemented with 10% FCS, 50 μ M 2-mercaptoethanol, 2 mM L-glutamine, 100 U penicillin, and 100 μ g/ml streptomycin, in a humidified incubator at 37°C and 5% CO₂.

2.2. Analysis of DNA repair

2.2.1. Cytogenetic analyses

For the analysis of radiosensitivity, EBV transformed LCLs were analyzed alongside peripheral T cells from patients as controls. To generate peripheral T cells, PBLs were stimulated with 2.5 mg/ml phytohemagglutinin for 48 h. Cells were exposed to final doses of 0.7 and 2.0 Gy γ -irradiation generated by a 6 MeV linear accelerator (Mevatron) with a dose-rate of 2.2 Gy/min. After irradiation cells were cultured for 48 h. For the analysis of metaphase karyotypes, cells were treated with 0.1 μ g/ml colcemid for 90 min in order to block mitosis and metaphase spreads were prepared according to standard protocols. The metaphase spreads were subjected to a three color fluorescence *in situ* hybridization (FISH) using DNA libraries of human chromosomes 1, 2 and 4 as previously published (Neubauer et al., 1996). Metaphases were visualized by means of a fluorescence microscope equipped with appropriate filter combinations.

Metaphases were only taken into account if all six painted chromosomes could be detected. Chromosomal aberrations were scored from 200 (2.0 Gy), 400 (0.7 Gy) and 1000 (unirradiated) metaphases according to classical cytogenetic criteria (Savage, 1975). Chromosomal damage was expressed as number of breakpoints per mitosis.

2.2.2. Analysis of DNA DSB kinetics

For determining the efficiency of DNA repair, LCLs were γ -irradiated on ice using a 120 kV irradiator at a dose of 12 Gy/min. Cells that were not allowed to repair their DNA damage were directly irradiated in agarose plugs, otherwise they were irradiated in suspension and incubated afterwards for different lengths of time at 37°C. To terminate DNA repair, cell suspensions were mixed 1:1 with a 1.0% agarose solution at 65°C and left to solidify at 4°C. Agarose plugs containing 4×10^4 cells were excised and incubated in lysis buffer (10 mM Tris, 50 mM NaCl, 100 mM EDTA, 2% lauroylsarcosyl, 1 μ g/ml proteinase K) for 2 h at 4°C and 20 h at 50°C. Plugs were inserted into a 0.5% agarose gel and covered with a top layer of agarose solution. Electrophoresis was carried out in $0.5 \times$ TBE at room temperature for 16 h at a constant field strength of 0.85 V/cm. The gel was stained with ethidium bromide and fluorescence was captured using a CCD camera. Quantitative analysis was performed with Optimas 6.5 image analysis software (Media Cybernetics, Silver Spring, MD). The fraction of DNA released into the gel was calculated. By means of a calibration curve displaying DNA damage as a function of irradiation dose, the measurements of the kinetics were converted into Gy equivalents. The experiments were performed at least twice with four quantifications from two independent samples.

2.3. Western blot analysis for Nbs1, Mre11 and Rad50

Western blot analysis were performed as previously described (Grawunder et al., 1996). In brief, total cell lysates were prepared from cells in RIPA buffer, such that an equivalent of 5×10^5 cells could be loaded per lane and separated on a 10% SDS–polyacrylamide gel. Western blot detection of endogenous Nbs1, Mre11 and Rad50 proteins was performed using a polyclonal rabbit IgG anti-Nbs1 antibody (Novus Biologicals, Littleton, CO), monoclonal mouse IgG1 anti-Mre11 antibody 12D7 (GeneTex, San Antonio, TX), and monoclonal mouse IgG1 anti-Rad50 antibody 13B3 (GeneTex), and either horseradishperoxidase (HRP) labeled polyclonal goat-anti rabbit IgG or HRP labeled polyclonal goat-anti mouse IgG as secondary reagents, that were detected using an ECL kit (Amersham).

2.4. Cloning of a *nbs1* cDNA expression vector

The human *nbs1* cDNA was cloned from the cDNA of the human preB ALL cell line Nalm-6. The PCR cloning was performed with primers UG530 (5'-CGGGATCCATGTGGAAACTGCTGCCCGC-CGCGGG-3') and UG531 (5'-GCGACGCGTGTTATCTTCTCCTTTTAAATAAGG-3') and the RT-PCR fragment was cloned as a BamHI/MluI digested PCR product into a pCDNA3.1 hygro (Invitrogen) expression vector with modified multiple cloning site, in order to generate the wild-type NBS1 expression vector pUG125. The cDNA insert was entirely sequenced and determined to be free of PCR mutations. However, in contrast to the published sequence (Genbank accession no. NM_002485) we found a G > A point mutation in the wobble position of codon 672 of the *nbs1* cDNA resulting in a silent mutation. This silent mutation was found in several different cDNA clones, even when they were derived from different PCR amplifications. We therefore believe that this mutation represent an allelic variation of the *nbs1* gene that is already present in the genome of the Nalm6 cell line.

2.5. Analysis of V(D)J recombination in cell lines

V(D)J recombination was analyzed by a cellular V(D)J recombination assay relying on the transient transfection of extrachromosomal V(D)J recombination substrates (Hesse et al., 1987). Different substrate plasmids were used either retaining a signal (pGG49) or a coding joint (pGG51), as previously described (Gauss and Lieber, 1993). In brief, 3×10^6 cells resuspended in RPMI 1640 containing 10 $\mu\text{g/ml}$ DEAE dextran were transfected by electroporation with 1 μg of substrate plasmid and (if necessary) with 3 μg of each RAG1 and RAG2 expression vectors pMS119c and pMS201 (Sadofsky et al., 1993, 1994), respectively. In one set of experiments with the NBS cell line, 3 μg of the expression vector pUG125 for wild-type NBS1 was cotransfected as well. Plasmids were recovered 2 days post transfection, digested with DpnI and NheI (in order to remove unreplicated, and potentially untransfected substrate plasmids, as well as cotransfected expression vectors), deproteinized, transformed into DH10B *Escherichia coli* and plated in parallel on LB plates containing ampicillin (amp) alone and ampicillin/chloramphenicol (amp/cam). The ratio of amp/cam double resistant colonies versus amp single resistant colonies corresponds to the frequency of V(D)J recombination. Individual amp/cam colonies were randomly selected, and miniprep DNA was prepared and analyzed by restriction enzyme digestion and/or automated DNA sequencing. From the NBS-P122 cell line 150 CJ products were sequenced (3×40 , 1×30 minipreps from

four independent V(D)J assays), from the wild-type MC8866 cell line 100 CJ products (2×30 , 2×20 minipreps from four different V(D)J assays), and from the AT-P104 cell line 50 CJ products (2×15 , and 2×10 minipreps from four independent V(D)J assays).

Statistical evaluation of the sequencing data was assessed by the Fisher's exact probability test run on the public domain ExactSignificance (EXTSIG) v1.3 Software package from the University of Texas, M.D. Anderson Cancer Center, Department of Biomathematics, Houston, Texas. All *P*-values represent two-tailed mid-*P* values.

2.6. PCR cloning and DNA sequencing of endogenous IgL CDR3 regions

Genomic DNA samples of peripheral blood lymphocytes (PBLs) from one NBS patient and the two heterozygous, healthy individuals (the parents of the patient) were used as templates for the amplification of CDR3 regions from endogenous $V_{\lambda}J_{\lambda}$ and $V_{\kappa}J_{\kappa}$ rearrangements. These samples were kindly provided by Dr. Zenker, University of Erlangen, Germany. Sequences of the primers binding in the various V gene segments of different V_{κ}/J_{κ} families and the different J_{λ}/J_{κ} gene segments are listed at the end of this section and cited from Farner et al., 1999 and Foster et al., 1997. All external V_{κ}/J_{κ} primers bind in the leader sequences, whereas all internal V_{κ}/J_{κ} primers bind in the 5' region of FR1. Individual rearrangements, including CDR3 regions, were amplified by a nested PCR approach. For the initial PCR, 200–800 ng of the genomic DNA was used for amplification with 25 cycles at annealing temperatures of 56 and 50°C for $V_{\kappa}J_{\kappa}$ and $V_{\lambda}J_{\lambda}$ PCRs, respectively. The nested PCR was performed with internal primers at 65°C ($V_{\kappa}J_{\kappa}$) and 62°C ($V_{\lambda}J_{\lambda}$) annealing temperatures, again with 25 PCR cycles. PCR reactions were fractionated by agarose gel electrophoresis, bands of correct sizes were isolated and purified using a QIAquick Gel Extraction Kit (QIAGEN) and directly ligated into the pCR4-TOPO vector. Cloned CDR3 regions were sequenced using a BigDye-Termination Cycle Sequencing Kit and appropriate M13 forward/reverse sequencing primers binding in the vector backbone. Automated DNA sequencing was performed on an ABI Prism 310 Genetic Analyzer. The sequences were analyzed using the IgBLAST program (www.ncbi.nlm.nih.gov/igblast/) and the Genebank and EMBL databases. Primers:

External V_{κ}/J_{κ} primers

V κ I/II-E	5'-GCTCAGCTCCTGGGGCT-3'
V κ III-E	5'-GGAA(AG)CCCCAGC(AGT)CAGC-3'
J κ 2-E	5'-ACGTTTGATCTCCAGCTTG-3'
J κ 5-E	5'-CTTACGTTTAATCTCCAGTC-3'

Internal V_k/J_k primers

VκI-I	5'-CATCCAG(AT)TGACCCAGTCTCC-3'
VκII-I	5'-TCCAGTGGGGATATTGTGATGAC-3'
VκIII-I	5'-GTCT(GT)TGTCTCCAGGGGAAAGAG-3'
Jκ2-I	5'-CAGCTTGGTCCCCTGGCCAAA-3'
Jκ5-I	5'-CCAGTCGTGTCCCTGGCCG-3'

External V_λ/J_λ primers

Vλ1-E	5'-CCTGGGCCAGTCTGTG-3'
Vλ2-E	5'-CTCCTCA(GC)(TC)CTCCTCACT-3'
Vλ3-E	5'-TC(CT)TATG(TA)GCTGAC(TA)CAG-3'
Vλ5/9-E	5'-CCCTCTC(CG)CAG(CG)CTGTG-3'
Vλ7/8-E	5'-ATTC(CT)CAG(GA)CTGTGGTGAC-3'
Jλ-E	5'-AGGACGGT(CG)A(CG)CT(GT)GGT-3'

Internal V_λ/J_λ primers

Vλ1-I	5'-CCAGTCTGTG(CT)TGAC(GT)CAGCC-3'
Vλ2-I	5'-CAGTCTGCCCTGACTCAGCC-3'
Vλ3-Ia	5'-TGACTCAGGACCCTGCTGTGTC-3'
Vλ3-Ib	5'-TGAC(TA)CAGCCAC(CT)CTC(AG)GTGTC-3'
Vλ5/9-I	5'-CAG(CG)CTGTGCTGACTCAGCC-3'
Vλ7/8-I	5'-CTGTGGTGAC(CT)CAGGAGCC-3'
Jλ1-I	5'-GGT(CG)ACCTTGGT(CG)CCA(CG)T(GT)CC-3'
Jλ2/3-I	5'-GGTCAGCT(GT)GGT(CG)CCTCC(GT)CC-3'

The CDR3 sequences displayed in Fig. 5 and Fig. 6 can be retrieved from the Genbank/EMBL database with accession numbers AJ408396 through AJ408595.

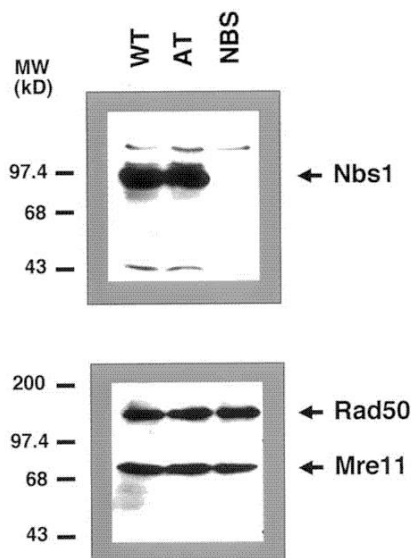


Fig. 1. Western blot analysis of Nbs1, Mre11, and Rad50 proteins in EBV transformed LCLs from cell lines NBS-P122 (NBS), AT-P104 (AT) and MC8866 (WT = wild-type). Total cell lysates equivalent to 5×10^5 cells are analyzed per lane.

3. Results

3.1. Growth, transfectability and Western blot analysis of EBV transformed LCLs

In order to test a possible role of Nbs1 in V(D)J recombination, three different EBV transformed lymphoblastoid cell lines (LCLs), MS1, MS2 and NBS-P122, were obtained from patients diagnosed with NBS. All patients carried a homozygous 5 bp deletion at position 657 of exon 6 of the *nbs1* gene (data not shown), which is the most commonly occurring mutation in patients with NBS (Varon et al., 1998). Control EBV transformed LCLs MC8866 and MC221 from normal individuals were kindly provided by Dr Marina Cella (Basel Institute for Immunology, Basel, Switzerland). As an additional control, one EBV transformed LCL was generated from an AT patient (designated AT-P104), because it had previously been reported that AT cell lines display a wild-type phenotype for V(D)J recombination (Hsieh et al., 1993). Comparable growth kinetics were found for cell lines NBS-P122 and AT-P104, with doubling times of approximately 32–36 h, whereas MS1 and MS2 proliferated significantly slower (data not shown). In contrast, wildtype EBV transformed LCLs MC8866 and MC221, displayed faster doubling times of approximately 24–26 h (data not shown). It was assessed whether the slower growth rates of AT and NBS cells were the result of increased spontaneous apoptosis, which was determined by a TUNEL assay. The frequency of spontaneous apoptosis for NBS, AT and control cell lines were not found to be significantly different and were determined to be in the range of 5.8–6.7% for all different cell lines analyzed (L.D. et al., manuscript in preparation). This would indicate that the slower growth rates of NBS and AT cells are the result of slower cell cycle progression. Transient cellular V(D)J recombination assays repeatedly performed with all of the above mentioned cell lines revealed that only cell lines NBS-P122, AT-P104 and MC8866 could be transfected at high enough levels, which is the reason why we decided to restrict our analysis to these three cell lines.

Western blot analysis for the expression of Nbs1, Mre11 and Rad50 in these three cell lines showed that Nbs1 protein was undetectable in the NBS-P122 cell line, whereas Mre11 and Rad50 expression levels remained unaffected and remained comparable to expression levels found in the wild-type MC8866 and AT-104 control cell lines (Fig. 1). These findings are in line with previously published data (Carney et al., 1998).

3.2. Analysis of DNA repair in NBS and AT cells

In order to characterize the NBS-P122 and AT-P104 cell lines further, we analyzed the radiosensitivity of

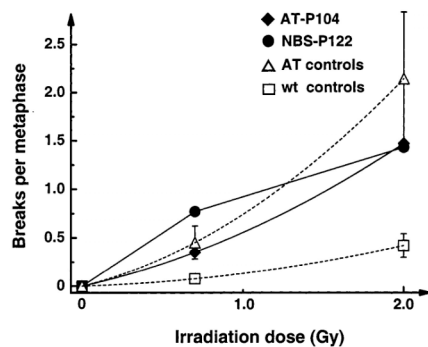


Fig. 2. Cytogenetic analysis of chromosomal aberrations. Chromosomal translocations in chromosomes 1, 2 and 4 were quantitated by three color FISH analysis in metaphase spreads of cells 48h after irradiation with 0.7 and 2.0 Gy as indicated. Unirradiated cells were used as controls. Lymphoblastoid cell lines NBS-P122 (filled circle) and AT-P104 (filled diamond) were compared to combined data of lymphocytes examined from ten healthy donors (open squares) and 11 AT patients (open triangles). Chromosomal aberrations were scored from 200 (2.0 Gy), 400 (0.7 Gy) and 1000 (unirradiated) metaphases and are represented as chromosomal breaks per metaphase. Standard deviations are included for data from the ten healthy controls and 11 AT patient samples.

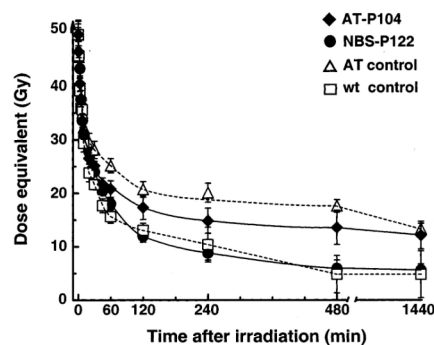


Fig. 3. Kinetics of DSB repair in lymphoblastoid cell lines. DSB repair was analyzed after irradiation with 50 Gy and determined by constant field gel electrophoresis at different time points post irradiation. DNA damage is expressed as dose-equivalent, which is calculated from a standard curve of unrepaired DNA damage in cells plotted as a function of X-ray dose. Cell lines analyzed are wild-type control cells (open squares), NBS-P122 (filled circles) and AT-P104 cell line (filled diamond), as well as another control AT lymphoblastoid cell line (open triangle). Each data point represents the mean value of four measurements from two independent experiments including standard deviation.

these cells by a cytogenetic approach. We scored for chromosomal aberrations and chromosomal breaks induced with 0.7 and 2.0 Gy 6 MeV photons by means of a three color FISH technique (Fig. 2). Peripheral T cells stimulated by phytohemagglutinin from a total of 11 AT patients and ten normal donors were used as controls. Both lines, NBS-P122 and AT-P104, exhibited an increased frequency of chromosomal aberrations similar to that found in previously characterized AT cells

(Fig. 2). This result demonstrates that the EBV transformed LCLs maintain a genetic instability that is characteristic for primary cells carrying mutations in either *nbs1* or *atm* genes. Similar elevated frequencies of chromosomal aberrations were found in the NBS cell line also on other chromosomes, when analyzed by a 24 multicolor-FISH analysis (data not shown).

The ability of these cells to repair DSBs was further assessed by a DSBR kinetics (Fig. 3). For this, a constant field gel electrophoresis assay was performed on DNA from cells that had been irradiated and subsequently cultured for different periods of time. The kinetics of DSB repair demonstrates biphasic kinetics of DNA repair with a rapid repair of the majority of DSBs within the first 30–60 min, followed by a slower repair of DSBs reaching a plateau indicative of residual unrepaired DNA damage after roughly 6 h (Fig. 3). The initial rapid decrease of DNA damage within 30–60 min was almost identical in AT, NBS and wild-type control cells. However, after long-term DNA repair, i.e. 24 h post irradiation, AT-P104 cells and a previously characterized AT control cell line, but not the NBS-P122 cell line, retained increased residual DNA damage, as compared to a wild-type control line (Fig. 3). These observations are in agreement with previously published studies (Blocher et al., 1991; Foray et al., 1997; Kraakman-van der Zwet et al., 1999) and illustrates again an important difference between the DNA repair phenotypes of NBS and AT cells. This analysis further demonstrates that the NBS-P122 and AT-P104 cells lines share important characteristics of previously characterized NBS and AT cell lines.

3.3. Quantitative analysis of V(D)J recombination in NBS and AT cells

We next tested the EBV transformed NBS-P122, AT-P104 and the MC8866 wild-type cell lines for V(D)J recombination using an established cellular V(D)J recombination assay based on the transient transfection of extrachromosomal V(D)J plasmid substrates containing two bacterial resistance markers (Hesse et al., 1987). The ampicillin marker is constitutively expressed, whereas the chloramphenicol marker can only be expressed after V(D)J recombination, because a bacterial transcriptional terminator flanked by recombination signals is located between the promoter and the open reading frame of the chloramphenicol gene. Rescue of transiently transfected substrates from mammalian cells and transformation into *E. coli* allows the determination of V(D)J recombination frequencies, by analyzing amp/cam double resistant versus amp single resistant *E. coli* colonies. Two independent V(D)J recombination substrates were used that either retain a CJ or a SJ after V(D)J recombination, depending on the orientation of the recombination signals flanking the bacterial transcriptional terminator (Gauss et al., 1998).

V(D)J recombination frequencies for all EBV transformed LCLs were performed in quadruplicate experiments. Comparison of V(D)J recombination frequencies revealed that mean values for CJ and SJ formation in the NBS-P122 and the AT-P104 cell lines are almost identical and lie within a factor of two (CJ: 0.031% for NBS, 0.021% for AT; SJ: 0.055% for NBS, 0.027% for AT). In contrast, CJ and SJ frequencies in the wild-type MC8866 cell line are slightly (roughly fivefold) increased with mean values of 0.17% for CJ formation and 0.13% for SJ (Table 1). This might indicate that V(D)J recombination on extrachromosomal plasmid substrates is slightly more efficient in wild-type cells than in AT or NBS cells. The slightly lower V(D)J recombination frequencies in NBS cells could not be compensated by cotransfection of the wild-type Nbs-1 expression vector pUG125 in our transient V(D)J recombination assays (data not shown, please refer to Section 2.4 for cloning of pUG125), suggesting that the lower frequency is not a direct consequence of the lack of Nbs1 expression. In any case, up to fivefold differences in V(D)J recombination frequencies can be considered more or less insignificant, because it is known that different wild-type human cell lines vary in their capability to mediate V(D)J

recombination on extrachromosomal V(D)J substrates by up to three orders of magnitude (Gauss et al., 1998). It has been reported that V(D)J recombination in AT cells is normal (Hsieh et al., 1993), and our values for CJ formation (0.021 vs 0.13% published) and SJ formation (0.027 vs 0.093% published) support the published data. From our results, we conclude that DNA end joining in V(D)J recombination is not quantitatively and significantly affected in cells carrying a mutation in the *nbs-1* gene. The small difference in SJ and CJ formation frequencies in AT and NBS cells compared to the wildtype LCL control could be the result of the genetic instability and reduced proliferative capacity of the AT and NBS cell lines (see Section 3.1), but such a claim would have to be substantiated by analyzing significantly larger numbers of cell lines.

V(D)J recombination in EBV transformed LCLs without transient cotransfection of RAG-1 and RAG-2 expression vectors was, as expected, practically undetectable (Table 1). As additional positive and negative controls for the assay, duplicate experiments were performed with the wild-type human preB-ALL line Nalm-6 and its DNA ligase IV deficient mutant, which is deficient for V(D)J recombination (Grawunder et al., 1998). V(D)J recombination frequencies for SJ and CJ

Table 1
V(D)J recombination in different human cell lines

Cell line	RAG vectors ^a	SJ			CJ		
		DAC ^b	DA ^c	%rec ^d	DAC ^b	DA ^c	%rec ^d
Nalm-6	–	3000	76 000	3.95	3040	188 8000	1.62
	–	1960	47 500	4.13	1670	100 0000	1.67
LIG4–/–	–	2	120 000	0.0017	1	70 000	0.0014
	–	1	76 000	0.0013	1	85 000	0.0012
MC8866 (WT)	–	0	195 000	<0.00051	1	243 000	0.00043
	+	554	312 000	0.18	480	312 000	0.15
	+	840	468 000	0.19	552	390 000	0.14
	+	424	292 500	0.14	236	195 000	0.12
	+	880	585 000	0.15	184	156 000	0.12
	–	0	97 000	<0.00093	0	160 000	<0.00062
AT-P104	+	26	115 000	0.023	27	100 000	0.027
	+	14	80 000	0.018	38	216 000	0.018
	+	15	78 000	0.019	13	47 000	0.028
	+	14	58 000	0.024	32	96 000	0.033
	–	0	165 000	<0.00061	1	200 000	0.00050
NBS-P122	+	228	766 000	0.030	238	440 000	0.054
	+	146	500 000	0.029	480	800 000	0.060
	+	68	220 000	0.031	94	250 000	0.038
	+	66	192 000	0.034	154	225 000	0.068

^a Cells not expressing endogenous RAG proteins were either not transfected with RAG expression vectors as a negative control (–), or co-transfected with 3 µg of each RAG-1 and RAG-2 expression vectors PMS127B and pMS216, respectively (+).

^b DAC numbers reflect re-extracted V(D)J recombination substrate plasmids that were digested with DpnI restriction enzyme, in order to remove unreplicated and potentially untransfected plasmids. *E. coli* transformed with these plasmids were plated on ampicillin/chloramphenicol containing LB-plates thereby scoring for V(D)J recombination events.

^c DA numbers reflect substrates treated like under ^b, but plated on LB-plates containing ampicillin, allowing measurement of the total transfected substrate plasmids.

^d %rec is calculated by dividing DAC/DA numbers, expressed as percentage.

formation in Nalm-6 cells were found to be significantly higher compared to LCLs, with roughly 4.0 and 1.6%. In contrast, the DNA ligase IV deficient cell line displayed roughly a $1-2 \times 10^3$ -fold reduced activity, confirming previously published data (Grawunder et al., 1998) (Table 1). The comparatively high levels of V(D)J recombination in the Nalm-6 cell line are probably the result of endogenous RAG-1 and RAG-2 protein expression in Nalm-6 cells that allows V(D)J recombination events in every transfected cell, whereas in EBV transformed LCLs the cotransfection of substrate plasmids with RAG-1 and RAG-2 expression vectors might be limiting. These differences might also indicate that expression of RAG proteins from the expression vectors in the EBV transformed LCLs might not be comparable to endogenous RAG expression levels.

3.4. Quality of SJ and CJ formation on extrachromosomal substrates

In order to examine the quality of signal and coding joint formation in the various genetic backgrounds, individual SJ and CJ plasmids were rescued from the V(D)J experiments with the NBS-P122 and the AT-P104 and MC8866 control cell lines. Precise signal joint formation on these substrates can easily be determined, because the exact head to head ligation of two recombination signals creates a novel ApaLI restriction site. Therefore, 30 SJ products from the transient cellular V(D)J recombination assays with LCLs from each genetic background were isolated and analyzed by a diagnostic ApaLI restriction digest (Fig. 4a). In each genetic background, all 30 SJ products showed the characteristic ApaLI restriction fragment pattern, indicative of precise signal joining (Fig. 4b). Together with the normal frequencies in SJ formation, these data suggest that a mutation in *nbs-1* has no effect on the rejoining of signal ends in V(D)J recombination.

ApaLI digestion of CJ products does not reveal precise sequence information. However, it will liberate a diagnostic restriction fragment from the CJ substrate that, due to V(D)J recombination, is 273 base pairs (bp) shorter than a fragment from an unrearranged substrate (as a result of the loss of the RSS flanked bacterial transcriptional terminator). We detected normal sized ApaLI fragments, indicative of regular CJ formation in 150 CJ plasmids from NBS-P122, and 150 CJ plasmids from AT-P104 (50) and MC8866 (100) control cells. The only exception were six plasmids isolated from a single V(D)J experiment in NBS-P122 cells, which contained shorter deletions. DNA sequencing revealed that these plasmids contained a 80 or 81 bp non-V(D)J related deletion in a central region of the transcriptional terminator (data not shown) that we could not reproduce in any of the other NBS-P122 V(D)J experiments. We therefore have to consider this

unusual deletion as an artifact, whose origin we cannot explain.

DNA sequence analysis of 150 CJs from the NBS-P122 and 150 CJs from the wild-type MC8866 and AT-P104 cell lines shows that there are no significant differences in the quality of coding joint formation (Fig. 5). If the Nbs1 protein was involved in opening or processing of coding end hairpins *in vivo*, one would expect an effect on the frequency or presence of P-nucleotides in CJ sequences from NBS cells. However, we find P nucleotides in CJs rescued from all genetic backgrounds at similar frequencies: NBS-P122 cells: 9.3% (14/150), MC8866 cells: 9.0% (9/100), and AT-P104 cells: 20.0% (10/50); or if CJs from wildtype and AT cells are combined: 12.7% (19/150) (Table 2). With the given sample numbers these differences are not statistically significant, as evidenced by the two-tailed mid *P* values of *P* = 1.0, if the frequency of P nucleotides is compared between the 150 NBS sequences and the 100 sequences from wildtype MC8866 cells. If the frequency of P-nucleotides in NBS cells is compared to the combined 150 CJ sequences from the MC8866 and AT cell lines (which according to (Hsieh et al., 1993), can be considered wild-type for V(D)J recombination) the difference in frequencies is also not significant (*P* = 0.46).

Furthermore, comparing the mean nucleotide loss per coding end, we do not find significant differences, as these values range from 2.70 for NBS-P122 cells, 2.49 for the wild-type MC8866 cell line, and 2.68 for the AT-P104 cell line and therefore differ less than 8% (Table 2). We also find comparable frequencies in the usage of one or two bp microhomologies in coding joints from all genetic backgrounds, although the value for NBS-P122 of 47.3% (71/150) is slightly reduced to the values of the MC8866 63.0% (63/100) and AT-P104 60.0% (30/50) cell lines. Statistical evaluation of these values reveals a two tailed *P*-value of 0.015 when comparing 150 NBS CJs with 150 CJs from WT and AT cells, which is close to being statistically significant. However, the most frequent CJ formed contains a TC two-bp microhomology that is the predominant CJ in all genetic backgrounds. This indicates that there is not a major influence on microhomology usage in NBS cells.

Taken together we conclude that, like in the case of SJ formation, coding joining is not qualitatively different in NBS-P122 cells, as compared to the wild-type MV8866 and/or AT-P104 cell lines.

3.5. CDR3 sequences of endogenous *IgλL* and *IgκL* chain gene loci

Since the analysis presented so far was restricted to a limited number of cell lines, we extended our study to the analysis of endogenous *Igκ* and *λ* light chain gene

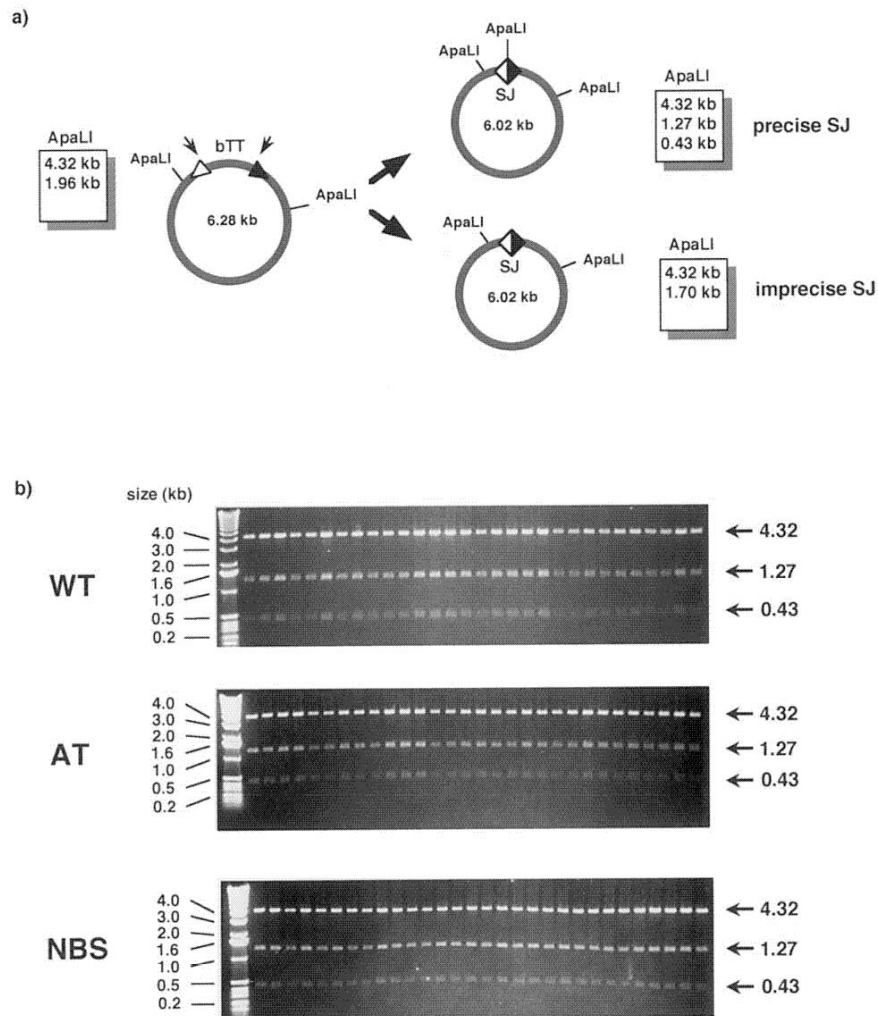


Fig. 4. Analysis of V(D)J signal joints on substrates recovered from NBS, AT and wild-type cells. (a) Schematic drawing indicating the position of a novel diagnostic ApaLI site in extrachromosomal V(D)J recombination substrates that results from the head-to-head ligation of signal sequences during V(D)J recombination. The positions of additional ApaLI sites in the substrate backbone relative to recombination signals and the bacterial transcriptional terminator (bTT) are indicated with the expected sizes of restriction fragments. (b) Ethidium bromide stained agarose gels of diagnostic ApaLI digests performed on 30 individual SJ products recovered from V(D)J recombination experiments with cell lines NBS-P122, AT-P104 and wild-type (WT) line MC8866.

rearrangements from one NBS patient and two healthy individuals (the heterozygous parents of the patient). We concentrated our analysis on the IgL chain gene loci, because the rearrangements in these loci only involve V_L and J_L gene segments and the CDR3 regions are less complex due to the absence of D elements. Furthermore, it is known that a certain fraction of IgL chain gene rearrangements are devoid of N-region sequences, which should facilitate the identification of P-nucleotide sequences. We cloned and determined 100 CDR3 sequences from the IgkL and IglL chain gene loci of one NBS patient (Fig. 6a) and compared them to 100 CDR3 sequences from the two healthy parents (Fig. 6b).

We found non-germline encoded P- and/or N-nucleotide sequences at altogether 65% of the L chain CJs in the NBS patient (32/50 in $V_{\kappa}J_{\kappa}$ rearrangements, and 33/50 in $V_{\lambda}J_{\lambda}$ rearrangements), which is almost identical to the value of 68% of the CJs from the healthy individuals (33/50 in $V_{\kappa}J_{\kappa}$ rearrangements, and 35/50 in $V_{\lambda}J_{\lambda}$ rearrangements) (Table 3). This is similar to a value of 54% found for IgL sequences published in the literature (Table 3). Of the 65 CJs from the NBS patient containing non-germline sequences, 29 (44.6%) CJs contained P nucleotides as opposed to 39 (57.4%) of 68 CJs from the healthy individuals. According to the Fisher's exact probability test this is not statistically significant (two-tailed P -value: 0.17). In addition, the

value for published sequences (34%) lies right in the middle of these measurements (Table 3). From this we conclude that P nucleotides are generated in NBS cells practically with the same efficiency as in wild-type cells.

CDR3 regions from IgL chain gene loci from NBS cells show a mean loss of 2.58 nucleotides per coding end, as compared to an average of 3.38 nucleotides in the two healthy individuals and 2.01 nucleotides in published sequences (Table 3). Thus, the loss of nucleotides per coding end in CDR3 regions of the NBS patient lies within the values for wild-type cells measured in this study and reported in the literature. In the CDR3 regions from normal individuals 2.98 N/P nucleotides are added per CJ (2.50 N/P nucleotides per CJ

reported in the literature) compared to 2.18 nucleotides per CJ in NBS lymphocytes. We believe that these differences are not significant as the most important features of CDR3 regions, P- and N-nucleotides are present at almost identical frequencies. Overall, we also detect a similarly diverse repertoire of CDR3 regions of NBS cells, as compared to CDR3 regions from PBLs of healthy individuals.

4. Discussion

Our analysis of V(D)J recombination in cells from patients with NBS does not provide evidence that the

NBS coding joints		WT coding joints		AT coding joints	
ATCCCCGGGGATCC	GTCGACCTGCAGCC	ATCCCCGGGGATCC	GTCGACCTGCAGCC	ATCCCCGGGGATCC	GTCGACCTGCAGCC
ATCCCCGGGGATC-	---GACCTGCAGCC 23x	ATCCCCGGGGATC-	---GACCTGCAGCC 24x	ATCCCCGGGGATC-	---GACCTGCAGCC 8x
ATCCCCGGGG---	--CGACCTGCAGCC 16x	ATCCCCGGGGATCC	---GACCTGCAGCC 13x	ATCCCCGGGGA---	-----CCTGCAGCC 6x
ATCCCCGGGGATCC	-----TGAGCC 16x	ATCCCCGGGGA---	-----CCTGCAGCC 8x	ATCCCCGGGGATCC	-----TGAGCC 4x
ATCCCCGGGGATC-	----ACCTGCAGCC 10x	ATCCCCGGGGATCC	GTCGACCTGCAGCC 6x	ATCCCCGGGGA---	<u>G</u> GTCGACCTGCAGCC 4x
ATCCCCGGGGA---	----CCTGCAGCC 10x	ATCCCCGGGGA---	<u>G</u> GTCGACCTGCAGCC 6x	ATCCCCGGGGATC-	GTCGACCTGCAGCC 3x
ATCCCCGGGGA---	<u>G</u> GTCGACCTGCAGCC 8x	ATCCCCGGGGATCC	-----CCTGCAGCC 4x	ATCCCCGGGGATCC	---GACCTGCAGCC 3x
ATCCCCGGGGATCC	GTCGACCTGCAGCC 7x	ATCCCCGGGGATC-	-----TGAGCC 4x	ATCCCCGGGGATC-	---ACCTGCAGCC 2x
ATCCCCGGGGATCC	---GACCTGCAGCC 6x	ATCCCCGGGGATC-	----ACCTGCAGCC 4x	ATCCCCGGGGATCC	ATCCCCGGGGATCC 2x
ATCCCCGGGGAT--	----ACCTGCAGCC 5x	ATCCCCGGGG---	GTCGACCTGCAGCC 3x	ATCCCCG---	---ACCTGCAGCC 2x
ATCCCCGGGGATC-	GTCGACCTGCAGCC 5x	ATCCCCGGGG---	--CGACCTGCAGCC 3x	ATCCCCGGGGATCC	GTCGACCTGCAGCC 2x
ATCCCCGGGGATCC	-----CTGCAGCC 5x	ATCCCCGGGG---	-TCGACCTGCAGCC 3x	ATCCCCGGGGATC-	<u>G</u> GTCGACCTGCAGCC 1x
ATCCCCGGGG---	-TCGACCTGCAGCC 4x	ATCCCCGGGGATCC	-----TGAGCC 2x	ATCCCCGGGG---	ATCCCCGGGG---
ATCCCCGGGGATC-	-----TGAGCC 3x	ATCCCCG---	----ACCTGCAGCC 2x	ATCCCCGGGGAT--	-----GAGCC 1x
ATCCCCGGGGATCC	----ACCTGCAGCC 3x	ATCCCCGGGGATCC	--CGACCTGCAGCC 2x	ATCCCC---	<u>GG</u> --CGACCTGCAGCC 1x
ATCCCCGGGG---	ATCCCCGGGG 3x	ATCCCCGGGG---	---GACCTGCAGCC 2x	ATCCCCGGGG---	ATCCCCGGGG---
ATCCCCGGGGATC-	-----GAGCC 2x	ATCCCCGGGGATCC	GTCGACCTGCAGCC 1x	ATCCCCGGGGATCC	<u>GG</u> -----CCTGCAGCC 1x
ATCCCCGGGGATCC	<u>GG</u> -----CCTGCAGCC 2x	ATCCCCGGGGATC-	---GACCTGCAGCC 1x	ATCCCCGGGGATCC	<u>G</u> ---GACCTGCAGCC 1x
ATCCCCGGGGA---	--CGACCTGCAGCC 2x	ATCCCCGGGGATCC	<u>GG</u> -----CCTGCAGCC 1x	ATCCCC---	<u>AC</u> GTCGACCTGCAGCC 1x
ATCCCC---	---ACCTGCAGCC 1x	ATCCCCGGGGATCC	ATCCCCGGGGATC-	ATCCCCGGGGATC-	ATCCCCGGGGATC-
ATCCCCGGGGATCC	<u>G</u> ---GACCTGCAGCC 1x	ATCCCCGGGGAT--	---ACCTGCAGCC 1x	ATCCCCGGGG---	<u>GAC</u> GTCGACCTGCAGCC 1x
ATCCCCGGGGATC-	-----(-18) 1x	ATCCCCGGGGAT--	---GACCTGCAGCC 1x	ATCCCCGGGGATCC	-----(-14) 1x
ATCCCCGGGGATC-	-----GCC 1x	ATCCCCGGGG---	-----CCTGCAGCC 1x	ATCCCCGGGGA---	GTCGACCTGCAGCC 1x
ATCCCCGGGGATC-	<u>G</u> -----CCTGCAGCC 1x	ATCCCCGGGGAT--	-----(-14) 1x	ATCCCCGGGGATC-	-----TGAGCC 1x
ATCCCCGGGG---	-----TGAGCC 1x	ATCCCCGGGGATCC	-----GCC 1x	ATC-----	---GACCTGCAGCC 1x
ATCCCCGGGGATCC	-----CAGCC 1x	ATCCCCGGGGATC-	---CGACCTGCAGCC 1x		50
ATCCCCGGGGAT--	GTCGACCTGCAGCC 1x	ATCCCCGGGGATC-	-----(-15) 1x		
ATCCCCGGGGATCC	<u>G</u> -----CCTGCAGCC 1x	ATCCCCGGGGA---	--CGACCTGCAGCC 1x		
ATCCCC---	-----CCTGCAGCC 1x	ATCC-----	---GACCTGCAGCC 1x		
ATCCCCGGGGATCC	-TCGACCTGCAGCC 1x	ATCCCCGGGGAT--	GTCGACCTGCAGCC 1x		
ATCCCCGGGGATCC	--CGACCTGCAGCC 1x		100		
ATCCCCGGGGAT--	<u>G</u> ---GACCTGCAGCC 1x				
ATCCCCG---	<u>G</u> GTCGACCTGCAGCC 1x				
ATCCCCGGGGATCC	-----AGCC 1x				
ATCC-----	---GACCTGCAGCC 1x				
ATCCCCGGG---	----ACCTGCAGCC 1x				
ATCCCCGGGGA---	---GACCTGCAGCC 1x				
ATCCCCGGGGATCC	-----CCTGCAGCC 1x				
ATCCCCG---	-----CAGCC 1x				
	150				

Fig. 5. Sequence analysis of V(D)J coding joints from NBS, AT and wildtype cell lines. DNA sequences were determined for 150 CJ products of cell line NBS-P122, 100 CJ products of wild-type cell line MC8866, and 50 CJ products of AT-P104 cell line. Full-length coding end sequences are indicated on top of each column in boldface type. Deleted nucleotides from coding ends are indicated by dashes, P-nucleotides are underlined, and nucleotides at coding ends that could have resulted from microhomology joining are given in boldface print. The fold representation of each coding joint in a given set of sequences is given at the right of each sequence.

Table 2 Characteristics of CJ recovered from LCLS

Cell line	NBS-P122	MC8866 (WT ^a)	AT-P104	AT + WT ^a
Number of sequences	150	100	50	150
P nucleotides	9.3% (14/150)	9.0% (9/100)	20.0% (10/50)	12.7% (19/150)
Nucleotide loss/end	2.70 nt ^b	2.49 nt ^b	2.68 nt ^b	2.55 nt ^b
Microhomology CJs	47.3% (71/150)	63.0% (63/100)	60.0% (30/50)	62.0% (93/150)

^a WT = wild-type.
^b nt = nucleotide.

a)				b)			
NBS patient: V _K J _K rearrangements				NBS patient: V _λ J _L rearrangements			
A27	GCAGTATGGTAGCTCACC---		-GTACACCTTTGGCCA JK2	V1-2	TGTGCAGGCAGCAACAATTT-		---GGGTGTTCCG Jλ3
A27	ACAGTACGGTAGCTCACC---		TGTACACTTTTGGCCA JK2	V1-2	TATGCAGGCAGCAACAATTT-	GGA	---GTGTTCGG Jλ3/7
A27	GCAGTATGGTAGCTCACC---	GTCC	---ACGTTTCGGCCA JK1	V1-3	TATACAGCAGC-----	TGCCTCTAA	---GGGTGTTCCG Jλ3
A27	GCAGTATGGTA-----	CCTC	GTGGACGTTTCGGCCA JK1	V1-3	TATGCAGGCAGCTACACTTT-		---GGTATTCCG Jλ2
A27	GCAGTATGGTAGCTCACCCT-		---GGACGTTTCGGCCA JK1	V1-3	TATGCAGGCAGTACACTTT-		---GGGTGTTCCG Jλ3
A27	GCAGTATGGTAGCTCACC---	C	---ATCACCTTCGGCCA JK5	V1-3	TATGCAGGCAGCTACAC---	CTA	TGTGGTATTCCG Jλ2
A30	ACAGCATAAATAGTTACCCCT-		---TGGACGTTTCGGCCA JK1	V1-4	TATACAGCAGCAGCAGCACT-		---GGTATTCCG Jλ2
A30	ACAGCATAAATAGTTACCCCT-	CG	---ACACTTTTGGCCA JK2	V1-4	TATACAACCAGCAGCAGCT---	TG	---GGTATTCCG Jλ2
A30	ACAGCATAAATAGTTACCCCT-	C	---GGACGTTTCGGCCA JK1	V1-5	TATACAAGCAGCAGCACT---	GTGA	---TATTCCG Jλ2
L1	ACAGTATAAATAGTTACCC---	CC	---TCACCTTCGGCCA JK5	V1-7	TATGCAGCTAGT-----	GGCTC	---ATTCCG Jλ2
L12	ACAGTATAAATAGTTA-----	CCT	---CITTTGGCCA JK2	V1-7	TATGCAGGTAGTAGCACTTT-		---GGTATTCCG Jλ2
L12	ACAGTATAAATAGTTATTCTCC		---GTACACTTTTGGCCA JK2	V1-7	TATGCAGGTAGTAGT-----	TACTCCC	---GTGTATTCCG Jλ2
L12	ACAGTATAAATA-----	ATCTCCCCC	---GTACACTTTTGGCCA JK2	V1-7	TATGCAGGTAGTAGCACTTT-		---GGGTGTTCCG Jλ3
L12	ACAGTATAAATAGTTAT-----	CC	GTGGACGTTTCGGCCA JK1	V1-7	TATGCAGGTAGTAGT-----	TACTCCCC	---GGTATTCCG Jλ2
L12	ACAGTATAAATAGTTATTCT-		---CACTTTTGGCCA JK2	V1-7	TATGCAGGTAGTAGCACTTT-	GAA	---GTGTTCGG Jλ3/7
L14	ACTGCGTAATACTTACCCT-	TGATGCACCTC	---TTGGCCA JK2	V1-7	TATGCAGGTAGTAGCGCT---	CCC	---GTGTATTCCG Jλ2
L18	ACAGTTAATAATACCCTC---	TT	TGTACACTTTTGGCCA JK2	V1-7	TATGCAGGTAGTAGCACTTT-	AA	---GGTATTCCG Jλ2
L23	ACAGTATTATAGTACC---	T	---ACCTTCGGCCA JK5	V1-7	TATGCAGGTAGTAGCACTTT-		---GGGTGTTCCG Jλ3
L25	GCAGGATTATAAAGTTAC---	ACCC	TGTACACTTTTGGCCA JK2	V1-7	TATGCAGGTAGTAGCACTTT-		---GGTATTCCG Jλ2
L25	GCAGGATTATAAAGTTAC---	GG	---ACTTTTGGCCA JK2	V1-7	TATGCAGGTAGT-----	CTACGG	---GGTATTCCG Jλ3
L25	GCAGGATTATAAAGTTACCTC-		---TTGGCCA JK2	V1-7	TATGCAGGTAGT-----	GGCCCC	TTGGGTGTTCCG Jλ3
L4/18a	ACAGTTAATAAGTTA-----	TCC	GTGGACGTTTCGGCCA JK1	V1-7	TATGCAGGTAGTAGCACTTT-	TGA	---TATTCCG Jλ2
L5	ACAGGCTAACAGTTTCCCT-		---GTACACTTTTGGCCA JK2	V1-7	TATGCAGGTAGTAGCACT---	CCCC	---GTGTATTCCG Jλ2
L6	GCAGCGTAGCAACTGGCCCTC		---CACTTTTGGCCA JK2	V1-11	CGATGACAGCCTGAGTGGT-		---GGTATTCCG Jλ2
L8	ACAGCTTAATAGTTACCTT-		---TGGACGTTTCGGCCA JK1	V1-13	TGACAGCAGCCTGAGTGGTTC		---GGTATTCCG Jλ2
L8	ACAGCTTAATAGTTAC---	TC	---GATCACCTTCGGCCA JK5	V1-16	GGATGACAGCCTGAAATG---	AC	---ATTCCG Jλ2
L8	ACAGCTTAATAGTTACCC---		---GATCACCTTCGGCCA JK5	V1-16	GGATGACAGCCTGAAATGCTC-	CC	---GGTATTCCG Jλ3
L8	ACAGCTTAATAGTTACCCCTC	GA	---ACACTTTTGGCCA JK2	V1-16	GGATGACAGCCTGAAATGCT-	GA	---GGTATTCCG Jλ3/7
L8	ACAGCTTAATAGTTACCCCTC		---GTACACTTTTGGCCA JK2	V1-16	GGATGACAGCCTGAAATGCT-		---GTGTATTCCG Jλ2
012/02	ACAGAGTTACAGTACCCTC---		---GTACACTTTTGGCCA JK2	V1-16	GGATGACAGCCTGAAATGCT-	TCT	---GTGTTCGG Jλ3
012/02	ACAGAGTTACAGTACCCTC-	AG	---GTACACTTTTGGCCA JK2	V1-17	GGATGACAGCCTGAGTGGTCC	GG	---GTGTTCGG Jλ2/3/7
012/02	ACAGACTTGCAGTACCCTC---		---GTACACTTTTGGCCA JK2	V1-17	GGATGACAGCCTGAGTGGTCC	GG	---GGGTGTTCCG Jλ3
012/02	ACAGAGTTACAGTACCCTC---	TCTGG	---GTACACTTTTGGCCA JK2	V1-17	GGATGACAGCCTGAGTGGTCC		---GTGTATTCCG Jλ2
012/02	ACAGAGTTACAGTACCCTC---	CC	---ATCACCTTCGGCCA JK5	V1-17	GGATGACAGCCTGAGTGGTCC		---GGGTGTTCCG Jλ3
012/02	ACAGAGTTACAGTACCCTC---	CCTC	---GTACACTTTTGGCCA JK2	V1-17	GGATGACAGCCTGAGTGGTCC	CC	---TGTTCGG Jλ2/3/7
012/02	ACAGAGTTACAGTACCCTC		---ACTTTTGGCCA JK2	V1-19	GGATGACAGCCTGAGTGGTCC		---GGTATTCCG Jλ2
012/02	ACAGAGTTACAGTACCCTC	CC	---TTCCGCGG JK4	V1-20	GGACAGCAGCTGAGTGGTCC	A	---GGTATTCCG Jλ3
014/04	ACGGACTTACAATGCCCTC---	ACC	---ACACTTTTGGCCA JK2	V2-11	AGACAGCAGTGGTACTTTA---		---GGTATTCCG Jλ2
014/04	ACGGACTTACAATGCCCTCCTC		---GTACACTTTTGGCCA JK2	V2-13	GGACAGCAGTGGTAACTT---	T	TTGGGTGTTCCG Jλ3
014/04	ACGGACTTACAATGCCCTCCTC	G	---ACACTTTTGGCCA JK2	V2-13	GGACAGCAGTGGTAACTTCT		---GGTATTCCG Jλ2
014/04	ACGGACTTACAATGCCCTCCTC	G	---ACITTTGGCCA JK2	V2-13	GGACAGCAGTGGTAACTTCT	GGTC	---TTCCG Jλ2/3/7
014/04	ACGGACTTACAATGCCCTC---	CCGGAG	---GTACACTTTTGGCCA JK2	V2-13	GGACAGCAGTGGTAACTTCT	CCCAA	---GGGTGTTCCG Jλ3
018/08	ACAGTATGATAATCTCCCTCC		---CACTTTTGGCCA JK2	V2-13	GGACAGCAGTGGTAACTTCT		---GGTATTCCG Jλ2
018/08	ACAGTATGATAATCACTCCCTC	GGG	---GTACACTTTTGGCCA JK2	V2-13	GGACAGCAGTGGTAACTTCT	TTCTGG	TGTGGTATTCCG Jλ2
018/08	ACAGTATGATAATCTCCCTC---		---GTACACTTTTGGCCA JK2	V2-14	GGATAGTAGTAGTGAATCATC-	TT	TTATGCTTCCG Jλ1
018/08	ACAGTATGATAATCTCCCTC---	CCC	---GTACACTTTTGGCCA JK2	V2-7	AGACAGCAGTGGTAACTTCCATG	CTA	---TGGGTGTTCCG Jλ3
018/08	ACAGTATGATAATCTCCCTC---	GG	---CACTTTTGGCCA JK2	V2-7	AGACAGCAGTGGTAACTTCCATG	TGGGAA	---GGTATTCCG Jλ2
018/08	ACAGTATGATAATCTCCCTC---	TT	---CACCTTCGGCCA JK5	V2-17	AGACAGCAGTGGTAACTTCCATC-	A	---GGTATTCCG Jλ3
018/08	ACAGTATGATAATCTCCCTC---	AT	---CACCTTCGGCCA JK5	V2-17	AGACAGCAGTGGTAACTTCCATC-	GTCT	---TGTTCGG Jλ3/7
018/08	ACAGTATGATAATCTCCCTC		---CACTTTTGGCCA JK2	V2-17	AGACAGCAGTGGTAACTTCCATC	TAA	---GGTATTCCG Jλ2

Fig. 6. Analysis of CDR3 sequences of V_LJ_L rearrangements of endogenous κ and λ light chain gene loci. (a) 50 CDR3 sequences of V_KJ_K rearrangements and 50 CDR3 sequences of V_λJ_L rearrangements from one NBS patient. The names of the V_L and J_L elements used in the rearrangements are given at the right and left sides of the rearrangements. Missing nucleotides from either coding end are indicated by dashes, non-germline sequences are given in the middle of the column, with potential P-nucleotides underlined. Nucleotides at coding ends that could belong to either coding end, and therefore represent microhomologies, are printed in boldface type. (b) 50 CDR3 sequences of V_KJ_K rearrangements and 50 CDR3 sequences of V_λJ_L rearrangements from two healthy donors as indicated.

formation of either SJ or CJ formation is significantly affected by a mutation in the *nbs1* gene. A role of the Nbs1/Mre11/Rad50 protein complex in the opening or processing of hairpinned coding end intermediates would have been conceivable, because the purified proteins were able to hydrolyze DNA hairpin substrates in a biochemical assay in vitro (Paull and Gellert, 1999). Any involvement of Nbs1/Mre11/Rad50 in the opening of hairpinned coding end intermediates in V(D)J recombination in vivo should be detectable at the level of P nucleotide sequences in CJs. However, comparison of 150 CJ sequences from an NBS cell line to 150 CJ sequences of WT and AT control cell lines revealed no statistically significant difference in the frequency of CJs containing of P-nucleotides. In addition, we were unable to detect significant differences in the occurrence of P nucleotides in each 100 CJ se-

quences from the endogenous Ig κ and λ L chain gene loci derived from an NBS patient and healthy individuals. This clearly suggests that Nbs1, and therefore most likely, also the complex of Nbs1/Mre11/Rad50 is not involved for coding end processing in V(D)J recombination in vivo.

Apart from the biochemical activity of the Nbs1/Mre11/Rad50 complex, there was another important observation that suggested a role of these proteins in V(D)J recombination. The *Saccharomyces cerevisiae* homologues of the mammalian DNA repair proteins, *Sc-xrs2*, *Sc-mre11* and *Sc-Rad50*, are involved in NHEJ in yeast (Moore and Haber, 1996). So far, all known DNA repair components that are essential for NHEJ, have been found to be equally important for the DNA end joining phase of V(D)J recombination. As an extension from this, it would have been likely that the

b)

Healthy individual 1: V_kJ_k rearrangements				Healthy individual 2: V_kJ_k rearrangements			
A17	GCAAGGTACACACTGGCCCT--	AGGGG	---ACACTTTGGCCA JK2	A3/A19	GCAAGCTCTACAAAC	Δ	---ACACTTTGGCCA JK2
A17	GCAAG-----	CTCTACAA	---ACACTTTGGCCA JK2	A27	GCGGTATGGTAGCT-----	TT	---ACTTTGGCCA JK2
A17	GCAAGGTACACACTGGCC--		-GTACACTTTGGCCA JK2	A27	GCAGTATGGTAGCTCACC---	GAAG	---ACTTTGGCCA JK2
A18	GCAAGGTATACACCT-----		---ACACTTTGGCCA JK2	A27	GCGGTATG-----	TTACTTCACQ	-GTACACTTTGGCCA JK2
A18	GCAAGGTATACACCTTCCT--		---ACACTTTGGCCA JK2	A30	ACAGCATAATAGTTACCC---	CGT	---CACTCTGGCCA JK2
A23	GCAAGGTACACAATTCCTCA	G	---ACACTTTGGCCA JK2	L1	ACAGTATAATAGTTACCCTC-	G	---CACTTTGGCCA JK2
A27	GCAGTATGGTAGCT-----	CATC	-GTACACTTTGGCCA JK2	L1	ACAGTATAATAGTTACCCCTCC	GA	---ACCTTCGGCCA JK5
A3/A19	GCAAGCTCTACAAAC	CCC	-GTACACTTTGGCCA JK2	L6	GCAACGTAGCAACTGGCC---		-GTACACTTTGGCCA JK2
A3/A19	GCAAGGTCTACAAACT----	AT	-GTACACTTTGGCCA JK2	L9	ACAGTATAATAGTTACCCTC-	GG	---CTTTGGCCA JK2
L2	GCAGGATTATAACT-----	TACCT	TGTACACTTTGGCCA JK2	L12	ACAGTCTCATAGT-----	CTCCQ	-GTACACTTTGGCCA JK2
L8	ACAGCATAATAGTTACCC---	C	-GATCACCTTCGGCCA JK5	L12	ACAGTATAATAG-----	GGGAA	---ACACTTTGGCCA JK2
L6	GCAGCGTAGCAACTGGCCTC-	GGC	---CACTTTGGCCA JK2	L12	ACAGTATAATAGTTA-----	CCQ	-GTACACTTTGGCCA JK2
L6	GCAGCGTAGCAACTGGCCCT--	TC	-GTACACTTTGGCCA JK2	L25	GCAGAATTATAACTT-----		---TTGGCCA JK2
L11	ACACGATTATACA-----	GTAAGCC	-GTACACTTTGGCCA JK2	012/02	ACAGAGTTACAGTACC----		-TACACTTTGGCCA JK2
L12	ACAGTATAATAGTTATTCCT--		-GTACACTTTGGCCA JK2	012/02	ACAGAGTTACAGTACCC--		-GTACACTTTGGCCA JK2
L12	ACAGTATAATAGTTATTC---		-GTACACTTTGGCCA JK2	012/02	ACAGAGTTACAGT-----	TCTCTTTACT	---CTTTGGCCA JK2
L23	ACAGTATTATAGTACCCT---		-GATCACCTTCGGCCA JK5	012/02	ACAGAGTTACA-----	TCGGGGTC	---TTGGCCA JK2
L25	GCAGGATTATACTTACCT---		TGTACACTTTGGCCA JK2	012/02	ACAGAGTTACAGTACCCCT--		---ACACTTTGGCCA JK2
L25	GCAGGATTATACTTACCT---	CC	-GTACACTTTGGCCA JK2	012/02	AC-----	TTCCGGAGT	---ACTTTGGCCA JK2
011/01	GCAACGTATAGAGTTTCCT--	C	TGTACACTTTGGCCA JK2	014/04	ACGGACTTACAATGCCCC---	TC	-GTACACTTTGGCCA JK2
011/01	GCAACGTATAGAGTTTCCT--		---ACACTTTGGCCA JK2	014/04	ACGGACTTACAATGCCCTC-		---TTGGCCA JK5
012/02	ACAGAGTTACAGTGGCCCT---		-GTACACTTTGGCCA JK2	018/08	ACAGTATGATAATCTCCC---	CC	-GTACACTTTGGCCA JK2
012/02	ACAGAGTTACAGTGGCCCT---	C	TGTACACTTTGGCCA JK2	018/08	ACAGTATGATA-----	CTTTC	-TACACTTTGGCCA JK2
018/08	ACAGTATGATAATCTCCCT---	GG	---TTGGCCA JK2	018/08	CCAGTATGATAATCTCCCTCC	TTCT	TGTACACTTTGGCCA JK2
018/08	ACAGTATGATAATCTCCCT---	GG	---CACTTTGGCCA JK2	018/08	ACAGTATGATAATCTCCCT---		-GTACACTTTGGCCA JK2
Healthy individual 1: V_λJ_λ rearrangements				Healthy individual 2: V_λJ_λ rearrangements			
V1-2	TATGCAGG-----	TAGTAGCCTC	-TGGTGTTCGG Jλ3	V1-3	TATGCAGGCAGC-----	CACACCCTT	-----TTFCGG Jλ2/3/7
V1-2	TATG-----	TCGGCAGTAACACTTTGA	----TATTCCGG Jλ2	V1-7	TATGCAGGTAGTAGC-----	CCCTCTC	-----TTFCGG Jλ2/3/7
V1-3	TATGCAGGCAGCTACTCTT--		---GGTGTTCGG Jλ3	V1-7	CMTCGA-----	TATATTCCA	----TATTCCGG Jλ2
V1-4	TATA-----	GAATCACCAGCAAT	---GGTGTTCGG Jλ3	V1-7	TATGCAGGTAGTAGCA-----	GTCCGGAG	---GGTGTTCGG Jλ3
V1-7	TATGCAGGTAGTA-----	ATATTTT	---GGTGTTCGG Jλ3	V1-4	TATACAGCAGCAGCACTC-	QAGGTΔ	-----TCGG Jλ2/3/7
V1-7	TATGCAGGTAGTAGC-----	GT	TTGGGTGTTCGG Jλ3	V1-11	GGATGACAGGCTGAATGGT--		-TATGCTTCGG Jλ1
V1-7	TATGCAGGTAGTAGCACTTT--		---GGTATTCCGG Jλ2	V1-16	GGATGACAGGCTGAATGGT--	G	TTGGGTGTTCGG Jλ3
V1-13	TGACAGCAGCCTGAGTGGTTC		---GGTGTTCGG Jλ3	V1-16	GGATGACAGCCTGAATGG--	CGTT	---GTATTCCGG Jλ2
V1-13	TGACAGCAGCCTGAGTGGTTC	AA	---GGTATTCCGG Jλ2	V1-16	GGATGACAGCCTCAATGGT--		-TGGGTGTTCGG Jλ3
V1-17	GGATGACAGCCTGAGTGGTC-	G	TTGGGTGTTCGG Jλ3	V1-17	GGATGACAGCCTGAGTGG--	CT	TTGGGTGTTCGG Jλ3
V1-17	GGATGACAGCCTGAGTGG--	GTAA	TTGGGTGTTCGG Jλ3	V1-17	GGATGACAGCTGAGTGGTC-		---GGTATTCCGG Jλ2
V1-17	GGATGACAGCCTGAGTGGTC-	GGG	---GGTGTTCGG Jλ3	V1-17	GGATGACAGCCTGAGTGG--	C	---GGTATTCCGG Jλ2
V1-17	GGATGACAGCCTGAGTGGTC-		---GGTATTCCGG Jλ3	V1-17	GGATGGCAGCCTGAGTGGT--	TA	TTGGGTGTTCGG Jλ3
V1-17	GGATGACAGCCTGAGTGGT--		-GTGTATTCCGG Jλ2	V1-20	GGACAGCAGCCTCAGTGG--		-GTGGTATTCCGG Jλ2
V2-7	AGACAGCAGTGGTAATC---	GG	---GGTATTCCGG Jλ2	V2-7	AGACAGCAGTGGTAATCATAG	GGGA	---GGTATTCCGG Jλ2
V2-13	GGACAGCAGTGGTAACCATCT	AAA	TTGGGTGTTCGG Jλ3	V2-7	AGACAGCAGTGGTAATCA---	CCCC	TTGGGTGTTCGG Jλ3
V2-13	GGACAGCAGTGGTAACCATCT	AAA	---GGTATTCCGG Jλ2	V2-7	AGACAGCAGTGGTAATCATA-	AA	---GGTATTCCGG Jλ2
V2-13	GGACAGCAGTGGTAACCAT---	GT	---GGTGTTCGG Jλ3	V2-11	AGACAACAGTGGTA-----	GCC	TTGGGTGTTCGG Jλ3
V2-13	GGACA-----	ATGGTGGTAGTACC	-TGGGTGTTCGG Jλ3	V2-13	GGACAGCAGTGGTAACCATCT	AA	---GGTATTCCGG Jλ2
V2-13	GGACAGCAGTGGTAACCAT---	TGGGGA	---GTATTCCGG Jλ2	V2-13	GGACAGCAGTGGTAACCAT---		-TGGGTGTTCGG Jλ3
V2-13	GGACAGCAGTGGTAACCATCT		---GGTGTTCGG Jλ3	V2-17	AGACAGCAGTGGTACTTT--		---GGTGTTCGG Jλ3
V2-17	AGACAGCAGTGGTACTTTAT--		-TGGTATTCCGG Jλ2	V2-17	AGACACCAGTGGTACTTTAT--	TCQ	-GTGGTATTCCGG Jλ2
V3-4	GTATATGGGTAGTGGCATT--		---TGGTGTTCGG Jλ7	V4-2	ATTTGGTACAGCAGCACTT--		-TGGTATTCCGG Jλ2
V4-2	ATTTGGTACAGCAGC-----	ACTT	-TGGTATTCCGG Jλ2	V4-2	ATTTGGCAGCAGCAGCACTT--		---GGTGTTCGG Jλ3
V4-3	ATTTGGCAGCAGCAGT-----	CATTG	---GGTGTTCGG Jλ3	V5-2	AGTGGGAGCAACTCTCGTGT--	TAAGG	---GGTGTTCGG Jλ3

Fig. 6. (Continued)

mammalian homologues play a part in NHEJ and thus also in V(D)J recombination.

Therefore the question arises as to whether the mammalian Nbs1/Rad50/Mre11 proteins, like their yeast counterparts, are directly involved in NHEJ and if so, would they therefore be the first NHEJ components not involved in DNA end joining in V(D)J recombination? Our own analysis of DNA repair might provide an answer to this question. Cytogenetic analysis of cells challenged with low doses of ionizing radiation clearly demonstrates that both AT and NBS cell lines accumulate chromosomal translocations at almost equally increased levels compared to wild-type control cells. This is the basis for the increased radiosensitivity of AT and NBS cells and for the genetic instability of AT and NBS patients.

However, the kinetics of DNA repair demonstrate an important difference between AT and NBS cells. While AT cells retain some unrepairable DNA damage even after long-term DNA repair, NBS cells repair their DSB

as efficiently as wild-type controls, such that no residual DNA damage is detectable above the background of control cells (Fig. 3 and Kraakman-van der Zwet et al., 1999).

These findings would suggest that Nbs1 in complex with Mre11 and Rad50 are not directly required to activate DNA end joining in NHEJ, but that they might rather have an important function in keeping chromosomal breaks tethered together, in order to assure that the correct ends will be rejoined instead of DNA ends from different chromosomes. This possibility would be consistent with the observed localization of these proteins to IRIF and to sites of DNA breakage (Maser et al., 1997; Nelms et al., 1998). Loss of Nbs1 expression has been shown to impair the localization of the remaining Mre11/Rad50 proteins to IRIF (Carney et al., 1998). It is therefore conceivable that a defect in localization and in tethering of DNA ends by these proteins, associated with a wild-type efficiency to rejoin DNA ends, results in an increased manifestation of chromosomal translocations.

Table 3
Characteristics of CJ from endogenous IgL chain loci

NBS	Patient	Healthy controls	Literature ^c
Number of sequences	100	100	100
CJ with non-GL ^a additions	65%	68%	54%
CJ with P nucleotides	29%	39%	34%
Nucleotide loss/end	2.58 nt ^b	3.38 nt ^b	2.01 nt
N-, P-additions per CJ	2.18 nt ^b	2.98 nt ^b	2.50 nt
Microhomology CJs	12.0% (12/100)	12.0% (12/100)	18.0% (18/100)

^a GL = germline.

^b nt = nucleotide.

^c DNA sequences were cited from the EMBL data bank; accession numbers Z85398-Z85453 (50 V_HJ_H sequences) and AJ230234-AJ230299 (50 V_λJ_λ sequences).

In addition, it has been shown that NBS cells are characterized by a reduced p53 response upon induction of DNA damage (Antoccia et al., 1999; Jongmans et al., 1997). A role of Nbs1 for a p53 mediated G₁/S checkpoint control appears to be mediated by a phosphorylation via the ATM kinase (Wu et al., 2000; Zhao et al., 2000). A failure to efficiently activate the G₁/S checkpoint has the consequence that, in NBS cells, untethered DSBs can persist as the cell cycle progresses into S phase and mitosis, further increasing the probability of fixing chromosomal translocations.

Taken together, the Nbs1/Mre11/Rad50 proteins might, therefore, not be required to activate DNA end joining by NHEJ, but might rather be responsible for assuring the fidelity of the end joining process. For V(D)J recombination this function of these proteins might be less critical, because signal and coding ends are already tethered in a postcleavage complex composed of RAG-proteins and components of the DNA-PK holoenzyme (Agrawal and Schatz, 1997).

The possibility that the yeast Xrs2/Mre11/Rad50 and the mammalian Nbs1/Mre11/Rad50 complexes might have a different significance for NHEJ could have its basis in the very limited sequence homology between the human *nbs-1* and its yeast analogue *xrs-2* genes, which share only 12% sequence identity. On the protein level, the only significant homology is restricted to 87 amino acids close to the N-terminus of Nbs1 containing a fork-head-associated domain, where 46% sequence similarity and 28% sequence identity can be found (Carney et al., 1998). The difference in the primary sequence of human Nbs1 and yeast Xrs2 proteins might therefore explain a different role of the human and yeast proteins for NHEJ.

NBS patients are often characterized by immunodeficiencies, most often associated with impaired T cell responses to antigens, reduced percentages of CD³⁺ and CD⁴⁺ T cells, and in some cases coupled with agammaglobulinemia (35%) and IgA deficiency (20%). Our finding that V(D)J recombination is quantitatively and qualitatively normal in a NBS cell line suggests that the immunodeficiency in NBS patients is not associated with any defects in the mechanism of V(D)J recombination. Nevertheless, a mildly leaky defect in V(D)J recombination in NBS patients could remain undetected, because endogenous rearrangements are selected for productive joints limiting unusual rearrangements. The direct analysis of coding end resolution in NBS cells by ligation mediated PCR could be a more direct way to assess a mechanistic role of the Nbs1 protein in V(D)J recombination. However, based on our data we would like to suggest that the reduction in certain lymphocyte populations is the result of misrepaired/undetected DSBs that are carried through different cell cycle stages during rapid proliferative expansion phases of lymphocyte precursors, as they are selected for functional antigen receptors. During these early differentiation phases precursor lymphocytes are extremely susceptible to apoptosis, and cells with unrepaired breaks might quickly get removed from the pool of differentiating cells.

Some of these unrepaired DSBs are certainly caused by V(D)J recombination events in the endogenous Ig and TCR gene loci as evidenced by the fact that the majority of chromosomal translocations found in mitogen stimulated lymphocytes involve chromosomes 7 and 14, which include the immunoglobulin and T cell receptor gene loci. Furthermore, most malignancies occurring in NBS patients are lymphomas, with the majority of them being B cell lymphomas.

More work is certainly desirable for elucidating the exact mechanism, by which defects in the Nbs1/Mre11/Rad50 DNA repair complex cause genetic instability in mammalian cells, as it is possible that subtle mutations in any of these factors might contribute to predisposition for certain malignancies. Because homozygous null mutations in these genes lead to early embryonic lethality and might even be cell autonomously lethal, partially inactivating mutations could be created in cell lines or in the mouse germ line. In this regard it would also be of interest to extend a functional analysis of cell lines from recently identified patients carrying mutations in the *mre11* gene to cell lines from patients carrying mutations in *nbs-1*.

Acknowledgements

We would like to thank Drs Alexandre Akhmedov and Dominic van Essen for critical reading of the

manuscript. Further thanks go to Professor E. Gebhart for providing us with AT cell lines. We are also grateful to R. Sieber for technical assistance with the DNA repair assay and to David Zimmer for many discussions. The Basel Institute was founded and is supported by F. Hoffmann-La Roche, Basel, Switzerland.

References

- Agrawal, A., Schatz, D.G., 1997. RAG1 and RAG2 form a stable postcleavage synaptic complex with DNA containing signal ends in V(D)J recombination. *Cell* 89, 43–53.
- Antoccia, A., Stumm, M., Saar, K., Ricordy, R., Maraschio, P., Tanzarella, C., 1999. Impaired p53-mediated DNA damage response, cell-cycle disturbance and chromosome aberrations in Nijmegen breakage syndrome lymphoblastoid cell lines. *Int. J. Radiat. Biol.* 75, 583–591.
- Besmer, E., Mansilla-Soto, J., Cassard, S., Sawchuk, D.J., Brown, G., Sadofsky, M., Lewis, S.M., Nussenzweig, M.C., Cortes, P., 1998. Hairpin coding end opening is mediated by RAG1 and RAG2 proteins. *Mol. Cell* 2, 817–828.
- Blocher, D., Sigut, D., Hannan, M.A., 1991. Fibroblasts from ataxia telangiectasia (AT) and AT heterozygous show enhanced levels of residual DNA double-strand breaks after low dose-rate g-irradiation as assayed by pulsed field gel electrophoresis. *Int. J. Radiat. Biol.* 60, 791–802.
- Boulton, S.J., Jackson, S.P., 1998. Components of the Ku-dependent non-homologous end-joining pathway are involved in telomeric length maintenance and telomeric silencing. *EMBO J.* 17, 1819–1828.
- Carney, J.P., Maser, R.S., Olivares, H., Davis, E.M., Le Beau, M., Yates III, J.R., Hays, L., Morgan, W.F., Petrini, J.H., 1998. The hMre11/hRad50 protein complex and Nijmegen breakage syndrome: linkage of double-strand break repair to the cellular DNA damage response. *Cell* 93, 477–486.
- Critchlow, S.E., Bowater, R.P., Jackson, S.P., 1997. Mammalian DNA double-strand break repair protein XRCC4 interacts with DNA ligase IV. *Curr. Biol.* 7, 588–598.
- Digweed, M., Reis, A., Sperling, K., 1999. Nijmegen breakage syndrome: consequences of defective DNA double strand break repair. *Bioessays* 21, 649–656.
- Farner, N.L., Dörner, T., Lipsky, P.E., 1999. Molecular mechanisms and selection influence the generation of the human V_HJ repertoire. *J. Immunol.* 162, 2137–2145.
- Foray, N., Priestley, A., Alsbeih, G., Badie, C., Capulas, E.P., Arlett, C.F., Malaise, E.P., 1997. Hypersensitivity of ataxia telangiectasia fibroblasts to ionizing radiation is associated with a repair deficiency of DNA double-strand breaks. *Int. J. Radiat. Biol.* 72, 271–283.
- Foster, S.J., Brezinschek, H.P., Brezinschek, R.I., Lipsky, P.E., 1997. Molecular Mechanisms and selective influences shape the kappa gene repertoire of IgM+ B cells. *J. Clin. Invest.* 99, 1614–1627.
- Frank, K.M., Sekiguchi, J.M., Seidl, K.J., Swat, W., Rathbun, G.A., Cheng, H.L., Davidson, L., Kangaloo, L., Alt, F.W., 1998. Late embryonic lethality and impaired V(D)J recombination in mice lacking DNA ligase IV. *Nature* 396, 173–177.
- Gao, Y., Chaudhuri, J., Zhu, C., Davidson, L., Weaver, D.T., Alt, F.W., 1998a. A targeted DNA-PKcs-null mutation reveals DNA-PK-independent functions for KU in V(D)J recombination. *Immunity* 9, 367–376.
- Gao, Y., Sun, Y., Frank, K.M., Dikkes, P., Fujiwara, Y., Seidl, K.J., Sekiguchi, J.M., Rathbun, G.A., Swat, W., Wang, J., Bronson, R.T., Malynn, B.A., Bryans, M., Zhu, C., Chaudhuri, J., Davidson, L., Ferrini, R., Stamato, T., Orkin, S.H., Greenberg, M.E., Alt, F.W., 1998b. A critical role for DNA end-joining proteins in both lymphogenesis and neurogenesis. *Cell* 95, 891–902.
- Gauss, G.H., Lieber, M.R., 1993. Unequal signal and coding joint formation in human V(D)J recombination. *Mol. Cell. Biol.* 13, 3900–3906.
- Gauss, G.H., Domain, I., Hsieh, C.L., Lieber, M.R., 1998. V(D)J recombination activity in human hematopoietic cells: correlation with developmental stage and genome stability. *Eur. J. Immunol.* 28, 351–358.
- Gilfillan, S., Dierich, A., Lemeur, M., Benoist, C., Mathis, D., 1993. Mice lacking TdT: mature animals with an immature lymphocyte repertoire. *Nature* 261, 1175–1178.
- Grawunder, U., Schatz, D.G., Leu, T.M.J., Rolink, A.G., Melchers, F., 1996. The half-life of RAG-1 protein in precursor B cells is increased in the absence of RAG-2 expression. *J. Exp. Med.* 183, 1731–1737.
- Grawunder, U., Wilm, M., Wu, X., Kulesza, P., Wilson, T.E., Mann, M., Lieber, M.R., 1997. Activity of DNA ligase IV stimulated by complex formation with XRCC4 protein in mammalian cells. *Nature* 388, 492–495.
- Grawunder, U., Zimmer, D., Fugmann, S., Schwarz, K., Lieber, M.R., 1998. DNA ligase IV is essential for V(D)J recombination and DNA double-strand break repair in human precursor lymphocytes. *Mol. Cell* 2, 477–484.
- Gu, Y., Seidl, K.J., Rathbun, G.A., Zhu, C., Manis, J.P., van der Stoep, N., Davidson, L., Cheng, H.L., Sekiguchi, J.M., Frank, K., Stanhope-Baker, P., Schlissel, M.S., Roth, D.B., Alt, F.W., 1997. Growth retardation and leaky SCID phenotype of Ku70-deficient mice. *Immunity* 7, 653–665.
- Hesse, J.E., Lieber, M.R., Gellert, M., Mizuuchi, K., 1987. Extrachromosomal DNA substrates in pre-B cells undergo inversion or deletion at immunoglobulin V-(D)-J joining signals. *Cell* 49, 775–783.
- Hsieh, C.L., Arlett, C.F., Lieber, M.R., 1993. V(D)J recombination in *Ataxia telangiectasia*, Bloom's syndrome, and a DNA ligase I-associated immunodeficiency disorder. *J. Biol. Chem.* 268, 20105–20109.
- Jongmans, W., Vuillaume, M., Chrzanowska, K., Smeets, D., Sperling, K., Hall, J., 1997. Nijmegen breakage syndrome cells fail to induce the p53-mediated DNA damage response following exposure to ionizing radiation. *Mol. Cell. Biol.* 17, 5016–5022.
- Komori, T., Okada, A., Stewart, V., Alt, F.W., 1993. Lack of N regions in antigen receptor variable region genes of TdT-deficient lymphocytes. *Science* 261, 1171–1175.
- Kraakman-van der Zwet, M., Overkamp, W.J., Friedl, A.A., Klein, B., Verhaegh, G.W., Jaspers, N.G., Midro, A.T., Eckardt-Schupp, F., Lohman, P.H., Zdzienicka, M.Z., 1999. Immortalization and characterization of Nijmegen Breakage syndrome fibroblasts. *Mutat. Res.* 434, 17–27.
- Luo, G., Yao, M.S., Bender, C.F., Mills, M., Bladl, A.R., Bradley, A., Petrini, J.H., 1999. Disruption of mRad50 causes embryonic stem cell lethality, abnormal embryonic development, and sensitivity to ionizing radiation [In Process Citation]. *Proc. Natl. Acad. Sci. USA* 96, 7376–7381.
- Maser, R.S., Monsen, K.J., Nelms, B.E., Petrini, J.H., 1997. hMre11 and hRad50 nuclear foci are induced during the normal cellular response to DNA double-strand breaks. *Mol. Cell. Biol.* 17, 6087–6096.
- Matsuura, S., Tauchi, H., Nakamura, A., Kondo, N., Sakamoto, S., Endo, S., Smeets, D., Solder, B., Belohradsky, B.H., Der Kaloustian, V.M., Oshimura, M., Isomura, M., Nakamura, Y., Komatsu, K., 1998. Positional cloning of the gene for Nijmegen breakage syndrome. *Nat. Genet.* 19, 179–181.
- McBlane, J.F., van Gent, D.C., Ramsden, D.A., Romeo, C., Cuomo, C.A., Gellert, M., Oettinger, M.A., 1995. Cleavage at the V(D)J recombination signal requires only RAG1 and RAG2 proteins and occurs in two steps. *Cell* 83, 387–395.

- Moore, J.K., Haber, J.E., 1996. Cell cycle and genetic requirements of two pathways of nonhomologous end-joining repair of double-strand breaks in *Saccharomyces cerevisiae*. *Mol. Cell. Biol.* 16, 2164–2173.
- Neizel, H., 1986. A routine method for the establishment of permanent growing lymphoblastoid cell lines. *Hum. Genet.* 73, 320–326.
- Nelms, B.E., Maser, R.S., MacKay, J.F., Lagally, M.G., Petrini, J.H., 1998. In situ visualization of DNA double-strand break repair in human fibroblasts. *Science* 280, 590–592.
- Neubauer, S., Gebhart, E., Schmitt, G., Birkenhake, S., Dunst, J., 1996. Is chromosome in situ suppression (CISS) hybridization suited as a predictive test for intrinsic radiosensitivity in cancer patients? *Int. J. Oncol.* 8, 707–712.
- Nussenzweig, A., Chen, C., da Costa Soares, V., Sanchez, M., Sokol, K., Nussenzweig, M.C., Li, G.C., 1996. Requirement for Ku80 in growth and immunoglobulin V(D)J recombination. *Nature* 382, 551–555.
- Paull, T.T., Gellert, M., 1999. Nbs1 potentiates ATP-driven DNA unwinding and endonuclease cleavage by the Mre11/Rad50 complex. *Genes Dev.* 13, 1276–1288.
- Roth, D.B., Menetski, J.P., Nakajima, P.B., Bosma, M.J., Gellert, M., 1992. V(D)J recombination: Broken DNA molecules with covalently sealed (hairpin) coding end in scid mouse thymocytes. *Cell* 70, 983–991.
- Sadofsky, M.J., Hesse, J.E., McBlane, J.F., Gellert, M., 1993. Expression and V(D)J recombination activity of mutated RAG-1 proteins. *Nucl. Acids Res.* 21, 5644–5650.
- Sadofsky, M.J., Hesse, J.E., Gellert, M., 1994. Definition of a core region of RAG-2 that is functional in V(D)J recombination. *Nucl. Acids Res.* 22, 1805–1809.
- Savage, J.R.K., 1975. Classification and relationship of induced chromosomal structural changes. *J. Med. Genet.* 12, 103–122.
- Savitsky, K., Bar-Shira, A., Gilad, S., Rotman, G., Ziv, Y., Vanagaite, L., Tagle, D.A., Smith, S., Uziel, T., Sfez, S., Ashkenazi, M., Pecker, I., Frydman, M., Harnik, R., Patanjali, S.R., Simmons, A., Clines, G.A., Sartiel, A., Gatti, R.A., Chessa, L., Sanal, O., Lavin, M.F., Jaspers, N.G.J., Taylor, M.R., Arlett, M.F., Miki, T., Weissman, S.M., Lovett, M., Collins, F.C., Shiloh, Y., 1995. A single ataxia telangiectasia gene with a product similar to PI-3 kinase. *Science* 268, 1749–1753.
- Shockett, P.E., Schatz, D.G., 1999. DNA hairpin opening mediated by the RAG1 and RAG2 proteins. *Mol. Cell. Biol.* 19, 4159–4166.
- Stewart, G.S., Maser, R.S., Stankovic, T., Bressan, D.A., Kaplan, M.I., Jaspers, N.G., Raams, A., Byrd, P.J., Petrini, J.H., Taylor, A.M., 1999. The DNA double-strand break repair gene hMRE11 is mutated in individuals with an ataxia-telangiectasia-like disorder. *Cell* 99, 577–587.
- Taccioli, G.E., Amatucci, A.G., Beamish, H.J., Gell, D., Xiang, X.H., Torres-Arzayus, M.I., Priestley, A., Jackson, S.P., Marshak Rothstein, A., Jeggo, P.A., Herrera, V.L., 1998. Targeted disruption of the catalytic subunit of the DNA-PK gene in mice confers severe combined immunodeficiency and radiosensitivity. *Immunity* 9, 355–366.
- Tonegawa, S., 1983. Somatic generation of antibody diversity. *Nature* 302, 575–581.
- van Gent, D.C., McBlane, J.F., Ramsden, D.A., Sadofsky, M.J., Hesse, J.E., Gellert, M., 1995. Initiation of V(D)J recombination in a cell-free system. *Cell* 81, 925–934.
- Varon, R., Vissinga, C., Platzer, M., Cerosaletti, K.M., Chrzanosowska, K.H., Saar, K., Beckmann, G., Seemanova, E., Cooper, P.R., Nowak, N.J., Stumm, M., Weemaes, C.M., Gatti, R.A., Wilson, R.K., Digweed, M., Rosenthal, A., Sperling, K., Concannon, P., Reis, A., 1998. Nibrin, a novel DNA double-strand break repair protein, is mutated in Nijmegen breakage syndrome. *Cell* 93, 467–476.
- Wu, X., Ranganathan, V., Weisman, D.S., Heine, W.F., Ciccone, D.N., O'Neill, T.B., Crick, K.E., Pierce, K.A., Lane, W.S., Rathbun, G., Livingston, D.M., Weaver, D.T., 2000. ATM phosphorylation of Nijmegen breakage syndrome protein is required in a DNA damage response. *Nature* 405, 477–482.
- Xiao, Y., Weaver, D.T., 1997. Conditional gene targeted deletion by Cre recombinase demonstrates the requirement for the double-strand break repair Mre11 protein in murine embryonic stem cells. *Nucl. Acids Res.* 25, 2985–2991.
- Yamaguchi-Iwai, Y., Sonoda, E., Sasaki, M.S., Morrison, C., Haraguchi, T., Hiraoka, Y., Yamashita, Y.M., Yagi, T., Takata, M., Price, C., Kakazu, N., Takeda, S., 1999. Mre11 is essential for the maintenance of chromosomal DNA in vertebrate cells. *EMBO J.* 18, 6619–6629.
- Zhao, S., Weng, Y.C., Yuan, S.S., Lin, Y.T., Hsu, H.C., Lin, S.C., Gerbino, E., Song, M.H., Zdzienicka, M.Z., Gatti, R.A., Shay, J.W., Ziv, Y., Shiloh, Y., Lee, E.Y., 2000. Functional link between ataxia-telangiectasia and Nijmegen breakage syndrome gene products. *Nature* 405, 473–477.
- Zhu, C., Bogue, M.A., Lim, D.S., Hasty, P., Roth, D.B., 1996. Ku86-deficient mice exhibit severe combined immunodeficiency and defective processing of V(D)J recombination intermediates. *Cell* 86, 379–389.

2.1 Addendum

2.1.1 The hairpin opening activity

The first hint to answer the question, which factor is responsible for opening hairpinned coding ends gave the analysis of a group of patients with T-B-SCID, characterized by the absence of T and B cells and an increased sensitivity to DNA damaging agents (RS-SCID) (Nicolas et al., 1998). This study together with the characterization of cells of A-SCID patients (a SCID variant with a very high incidence in Athabascan-speaking Navajo and Apache Native Americans) substantiated the idea of an additional, yet unknown NHEJ factor (Li et al., 1998). Soon it was discovered that RS-SCID and A-SCID are caused by the same genetic defect (Moshous et al., 2000). Involvement of the *RAG1/2* genes as well as *Ku80*, *Ku70*, *DNA-PK_{cs}*, *ligase IV* and *XRCC4* had been ruled out in these patients by means of genetic linkage analysis of all known NHEJ factors (Li et al., 1998; Nicolas et al., 1998), the A-SCID locus showing linkage to markers on chromosome 10p (Li et al., 1998). Cells of these patients were shown to be deficient for V(D)J recombination, result of the failure in coding joint formation but not signal joint formation. This phenotype was remarkably similar to that seen in *DNA-PK_{cs}*-deficient SCID mice, in which also hairpin coding ends accumulate. Eventually, the corresponding gene, termed *Artemis*, was identified and sequence analysis suggested that it belonged to the β -lactamase family (Moshous et al., 2001). Artemis was soon shown to possess single-strand-specific 5' to 3' exonuclease activity and, upon complex formation with *DNA-PK_{cs}* and activation, also to acquire endonucleolytic activity on DNA overhangs and, most interestingly, also on hairpins (Ma et al., 2002). These properties strongly suggest that Artemis is the long sought hairpin opening activity, the V(D)J deficiency of *Artemis*^{-/-} mice supporting this assumption (Rooney et al., 2002). The general role of Artemis in DNA repair is probably based on its exo- and endonucleolytic activities, processing DNA ends at DNA double strand breaks (DSBs) for NHEJ repair (Rooney et al., 2003).

2.1.2 The role of Nbs1

The first critical step in the cellular response to DSBs is sensing the DNA lesions. In this process several factors are involved including the phosphatidylinositol 3-kinase like kinase (PIKK), like ATM, and Nbs1 as part of the Mre11/Rad50/Nbs1 (MRN) complex (Bakkenist and Kastan, 2003; Petrini and Stracker, 2003). Upon DSBs generated by irradiation ATM is activated, phosphorylating subsequently first itself and then a wide range of proteins functionally implicated in the genome integrity network, like the histone variant H2AX (resulting in γ H2AX). The latter immediately forms discrete foci in response to DSBs and has been suggested to function as a scaffold for the assembly of protein complexes involved in the subsequent cellular responses (Fernandez-Capetillo et al., 2004). Nbs1, also phosphorylated by ATM (Wu et al., 2000), colocalizes with γ H2AX (Kobayashi et al., 2002), thereby bringing in the other components of the MRN complex. But Nbs1 is not only involved as a downstream target of ATM, it has also been implicated in the modulation of ATM activation and thereby also of the general DNA repair response (Horejsi et al., 2004). Additionally, other DSB repair factors, like BRCA1, are recruited to the foci to subsequently initiate together critical downstream steps in the cellular response to DSB, i.e. either the activation of a cell cycle checkpoint to facilitate DNA repair or the induction of p53 mediated apoptosis. Nbs1 together with the MRN complex has been implicated in the intra-S phase and G2/M checkpoint, lying downstream of ATM (Buscemi et al., 2001; Falck et al., 2002). Additionally, the biochemical activities of Mre11 in the context of the ternary M/R/N complex are probably directly involved in the processing of DNA ends preparing them for DNA repair (D'Amours and Jackson, 2002). Rad50, in turn, belongs to the family of structural maintenance proteins and has been suggested to bind to DNA ends and hold them in close proximity to facilitate religation (D'Amours and Jackson, 2002). Nbs1 as part of the MRN complex seems therefore to be involved in sensing DSBs, signaling of the induced cellular response as well as directly in the repair of DNA breaks.

Originally, it was thought that the DSBs, generated during VDJ recombination, would not be detected by the cellular repair machinery, because of its sequestration into the postcleavage complexes by the RAG1/2 proteins (Agrawal and Schatz, 1997; Hiom and Gellert, 1998). However, it could be shown that the histone variant H2AX and Nbs1 form RAG dependent foci at the the TCR α locus (Chen et al., 2000), implying

the detection of the DSBs by the repair factors. The high frequency of chromosomal translocations involving the Ig and TCR loci seen in humans deficient in ATM, Nbs1 or Mre11 (Kobayashi et al., 2004; Taylor et al., 2004) together with the increased inter-chromosomal V(D)J recombination in Nbs1 mutant mice (Kang et al., 2002) suggest additionally a link between V(D)J recombination and Nbs1 and the other DNA repair factors, even if they are not needed to perform the rearrangement. This has led to the proposal that RAG initiated DNA damage is sensed and generates signals to suppress oncogenic translocations. Additionally, H2AX and the MRN complex could function as an anchor for the assembly of DNA/protein complexes that prevent the dissociation and potential misrepair of the broken DNA ends at the DSBs. Class switch recombination (CSR) is a second genomic recombination reaction, that B lymphocytes can undergo in response to antigenic stimulation. This reaction replaces one Ig constant gene for another, thereby changing the effector function of the Ig. Interestingly, V(D)J recombination and CSR seem to have differential requirements for certain components of the cellular DSB response machinery. Although, Nbs1 and H2AX foci are formed during both processes (Chen et al., 2000; Petersen et al., 2001), only CSR is impaired in H2AX deficient mice (Celeste et al., 2002; Reina-San-Martin et al., 2003). Also Nbs1 is thought to be involved in CSR (Digweed and Sperling, 2004; Pan et al., 2002), explaining the agammaglobulinaemia often seen in Nbs1 patients (van Engelen et al., 2001). This differential requirement for DNA repair factors may reflect the fact that RAG liberated DNA ends are stably held and actively linked to downstream factors by the RAG proteins in the postcleavage complex. In contrast, DSBs initiated during CSR may not be similarly held by specific synapsis factors, depending therefore on factors, like the MRN complex, to tether the generated DNA ends in close proximity.

Additionally, Nbs1 has been implicated in telomere maintenance (Lombard and Guarente, 2000; Ranganathan et al., 2001) as well as in meiotic recombination, together with Mre11 and Rad50 (Ivanov et al., 1992; Tsubouchi and Ogawa, 1998).

Altogether, Nbs1 in a complex with Mre11 and Rad50 has been shown to be important in multiple cellular mechanisms maintaining genomic integrity of a cell. Concerning V(D)J recombination, as Nbs1 is not directly involved in the rearrangement mechanism, we did not detect any defect in the rearrangement process in cells of NBS patients. Nonetheless, there seems to be a residual dependence of

V(D)J recombination on Nbs1, a kind of additional backup system to ensure correct joining of the RAG associated DNA ends. Deficiency in any of the involved factors is not enough to result in an obvious defect in the cellular assays we employed, but suffices to cause the frequent chromosomal translocations of the Ig and TCR loci seen in NBS patients.

2.1.3 References

- Agrawal, A., and Schatz, D. G. (1997). RAG1 and RAG2 form a stable postcleavage synaptic complex with DNA containing signal ends in V(D)J recombination. *Cell* *89*, 43-53.
- Bakkenist, C. J., and Kastan, M. B. (2003). DNA damage activates ATM through intermolecular autophosphorylation and dimer dissociation. *Nature* *421*, 499-506.
- Buscemi, G., Savio, C., Zannini, L., Micciche, F., Masnada, D., Nakanishi, M., Tauchi, H., Komatsu, K., Mizutani, S., Khanna, K., *et al.* (2001). Chk2 activation dependence on Nbs1 after DNA damage. *Mol Cell Biol* *21*, 5214-5222.
- Celeste, A., Petersen, S., Romanienko, P. J., Fernandez-Capetillo, O., Chen, H. T., Sedelnikova, O. A., Reina-San-Martin, B., Coppola, V., Meffre, E., Difilippantonio, M. J., *et al.* (2002). Genomic instability in mice lacking histone H2AX. *Science* *296*, 922-927.
- Chen, H. T., Bhandoola, A., Difilippantonio, M. J., Zhu, J., Brown, M. J., Tai, X., Rogakou, E. P., Brotz, T. M., Bonner, W. M., Ried, T., and Nussenzweig, A. (2000). Response to RAG-mediated VDJ cleavage by NBS1 and gamma-H2AX. *Science* *290*, 1962-1965.
- D'Amours, D., and Jackson, S. P. (2002). The Mre11 complex: at the crossroads of dna repair and checkpoint signalling. *Nat Rev Mol Cell Biol* *3*, 317-327.
- Digweed, M., and Sperling, K. (2004). Nijmegen breakage syndrome: clinical manifestation of defective response to DNA double-strand breaks. *DNA Repair (Amst)* *3*, 1207-1217.
- Falck, J., Petrini, J. H., Williams, B. R., Lukas, J., and Bartek, J. (2002). The DNA damage-dependent intra-S phase checkpoint is regulated by parallel pathways. *Nat Genet* *30*, 290-294.
- Fernandez-Capetillo, O., Lee, A., Nussenzweig, M., and Nussenzweig, A. (2004). H2AX: the histone guardian of the genome. *DNA Repair (Amst)* *3*, 959-967.
- Hiom, K., and Gellert, M. (1998). Assembly of a 12/23 paired signal complex: a critical control point in V(D)J recombination. *Mol Cell* *1*, 1011-1019.
- Horejsi, Z., Falck, J., Bakkenist, C. J., Kastan, M. B., Lukas, J., and Bartek, J. (2004). Distinct functional domains of Nbs1 modulate the timing and magnitude of ATM activation after low doses of ionizing radiation. *Oncogene* *23*, 3122-3127.
- Ivanov, E. L., Korolev, V. G., and Fabre, F. (1992). XRS2, a DNA repair gene of *Saccharomyces cerevisiae*, is needed for meiotic recombination. *Genetics* *132*, 651-664.
- Kang, J., Bronson, R. T., and Xu, Y. (2002). Targeted disruption of NBS1 reveals its roles in mouse development and DNA repair. *Embo J* *21*, 1447-1455.

Kobayashi, J., Antoccia, A., Tauchi, H., Matsuura, S., and Komatsu, K. (2004). NBS1 and its functional role in the DNA damage response. *DNA Repair (Amst)* 3, 855-861.

Kobayashi, J., Tauchi, H., Sakamoto, S., Nakamura, A., Morishima, K., Matsuura, S., Kobayashi, T., Tamai, K., Tanimoto, K., and Komatsu, K. (2002). NBS1 localizes to gamma-H2AX foci through interaction with the FHA/BRCT domain. *Curr Biol* 12, 1846-1851.

Li, L., Drayna, D., Hu, D., Hayward, A., Gahagan, S., Pabst, H., and Cowan, M. J. (1998). The gene for severe combined immunodeficiency disease in Athabaskan-speaking Native Americans is located on chromosome 10p. *Am J Hum Genet* 62, 136-144.

Lombard, D. B., and Guarente, L. (2000). Nijmegen breakage syndrome disease protein and MRE11 at PML nuclear bodies and meiotic telomeres. *Cancer Res* 60, 2331-2334.

Ma, Y., Pannicke, U., Schwarz, K., and Lieber, M. R. (2002). Hairpin opening and overhang processing by an Artemis/DNA-dependent protein kinase complex in nonhomologous end joining and V(D)J recombination. *Cell* 108, 781-794.

Moshous, D., Callebaut, I., de Chasseval, R., Corneo, B., Cavazzana-Calvo, M., Le Deist, F., Tezcan, I., Sanal, O., Bertrand, Y., Philippe, N., *et al.* (2001). Artemis, a novel DNA double-strand break repair/V(D)J recombination protein, is mutated in human severe combined immune deficiency. *Cell* 105, 177-186.

Moshous, D., Li, L., Chasseval, R., Philippe, N., Jabado, N., Cowan, M. J., Fischer, A., and de Villartay, J. P. (2000). A new gene involved in DNA double-strand break repair and V(D)J recombination is located on human chromosome 10p. *Hum Mol Genet* 9, 583-588.

Nicolas, N., Moshous, D., Cavazzana-Calvo, M., Papadopoulo, D., de Chasseval, R., Le Deist, F., Fischer, A., and de Villartay, J. P. (1998). A human severe combined immunodeficiency (SCID) condition with increased sensitivity to ionizing radiations and impaired V(D)J rearrangements defines a new DNA recombination/repair deficiency. *J Exp Med* 188, 627-634.

Pan, Q., Petit-Frere, C., Lahdesmaki, A., Gregorek, H., Chrzanowska, K. H., and Hammarstrom, L. (2002). Alternative end joining during switch recombination in patients with ataxia-telangiectasia. *Eur J Immunol* 32, 1300-1308.

Petersen, S., Casellas, R., Reina-San-Martin, B., Chen, H. T., Difilippantonio, M. J., Wilson, P. C., Hanitsch, L., Celeste, A., Muramatsu, M., Pilch, D. R., *et al.* (2001). AID is required to initiate Nbs1/gamma-H2AX focus formation and mutations at sites of class switching. *Nature* 414, 660-665.

Petrini, J. H., and Stracker, T. H. (2003). The cellular response to DNA double-strand breaks: defining the sensors and mediators. *Trends Cell Biol* 13, 458-462.

Ranganathan, V., Heine, W. F., Ciccone, D. N., Rudolph, K. L., Wu, X., Chang, S., Hai, H., Ahearn, I. M., Livingston, D. M., Resnick, I., *et al.* (2001). Rescue of a

telomere length defect of Nijmegen breakage syndrome cells requires NBS and telomerase catalytic subunit. *Curr Biol* *11*, 962-966.

Reina-San-Martin, B., Difilippantonio, S., Hanitsch, L., Masilamani, R. F., Nussenzweig, A., and Nussenzweig, M. C. (2003). H2AX is required for recombination between immunoglobulin switch regions but not for intra-switch region recombination or somatic hypermutation. *J Exp Med* *197*, 1767-1778.

Rooney, S., Alt, F. W., Lombard, D., Whitlow, S., Eckersdorff, M., Fleming, J., Fugmann, S., Ferguson, D. O., Schatz, D. G., and Sekiguchi, J. (2003). Defective DNA repair and increased genomic instability in Artemis-deficient murine cells. *J Exp Med* *197*, 553-565.

Rooney, S., Sekiguchi, J., Zhu, C., Cheng, H. L., Manis, J., Whitlow, S., DeVido, J., Foy, D., Chaudhuri, J., Lombard, D., and Alt, F. W. (2002). Leaky Scid phenotype associated with defective V(D)J coding end processing in Artemis-deficient mice. *Mol Cell* *10*, 1379-1390.

Taylor, A. M., Groom, A., and Byrd, P. J. (2004). Ataxia-telangiectasia-like disorder (ATLD)-its clinical presentation and molecular basis. *DNA Repair (Amst)* *3*, 1219-1225.

Tsubouchi, H., and Ogawa, H. (1998). A novel mre11 mutation impairs processing of double-strand breaks of DNA during both mitosis and meiosis. *Mol Cell Biol* *18*, 260-268.

van Engelen, B. G., Hiel, J. A., Gabreels, F. J., van den Heuvel, L. P., van Gent, D. C., and Weemaes, C. M. (2001). Decreased immunoglobulin class switching in Nijmegen Breakage syndrome due to the DNA repair defect. *Hum Immunol* *62*, 1324-1327.

Wu, X., Ranganathan, V., Weisman, D. S., Heine, W. F., Ciccone, D. N., O'Neill, T. B., Crick, K. E., Pierce, K. A., Lane, W. S., Rathbun, G., *et al.* (2000). ATM phosphorylation of Nijmegen breakage syndrome protein is required in a DNA damage response. *Nature* *405*, 477-482.

3 Targeting of the *KRC* locus

Introduction

KRC for Kappa B and RSS recognition component was identified in a screen for RSS binding proteins (Wu et al., 1993). The cDNA was cloned by searching a mouse thymocyte expression library with a DNA probe harboring alternating RSS heptamers and nonamers for proteins with RSS binding specificity. Also in nuclear extracts of B lymphocytes KRC was found to be the major RSS binding protein (Wu et al., 2001). Additionally, KRC was shown to bind the κ B motif of the Ig κ light chain enhancer and related sequences.

Molecular cloning and sequencing of the KRC cDNA identified long 5'- and 3'- untranslated regions and a large open reading frame encoding nearly 2,300 amino acids. The deduced protein sequence revealed multiple DNA and protein-protein interaction domains. Most characteristic are the two ZAS domains which consist of tandem zinc fingers, followed by an acidic motif and a Ser/Thr-rich region. The ZAS domains are located at the C-terminus and at the N-terminus. Flanked by the two ZAS domains are a single zinc finger, an acidic motif, a Ser-rich region, a putative nuclear localization signal and several GTPase motifs (see figure 3.1, Wu et al., 1996).

Both isolated ZAS domains were expressed as recombinant protein fragments and were shown to form ordered, multimeric complexes (Mak et al., 1994). It was also demonstrated that both ZAS domains bind, independently of each other, the κ B motif as well as the RSS (Mak et al., 1998; Wu et al., 1993). A site selection study performed on random nucleotide sequences with each of the two ZAS domains specifically selected RSS-like sequences (Allen et al., 2002a).

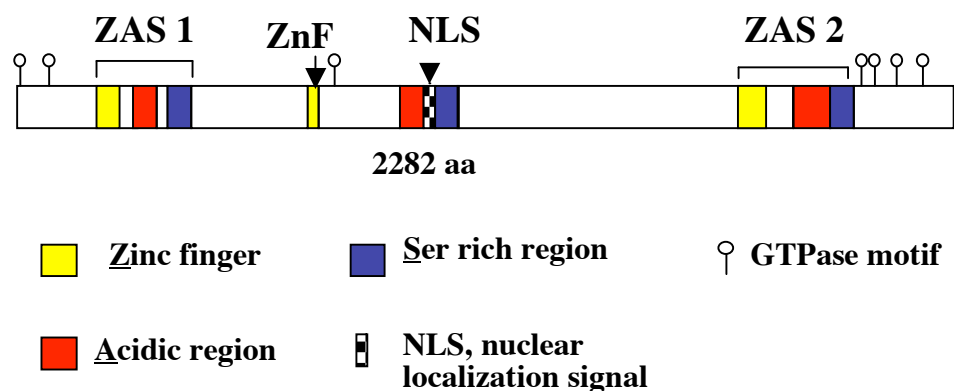


Figure 3.1: Schematic representation of the KRC protein

Interestingly, the DNA binding properties of KRC are modulated by post-translational modifications. Bachmeyer and coworkers showed that preincubation of recombinant protein with nuclear, but not cytoplasmic, extract of a pre-B cell line increased DNA binding (Bachmeyer et al., 1999). Induction of V(D)J recombination decreases the affinity of KRC to the RSS (Hicar et al., 2002; Wu et al., 2001) making it conceivable that KRC is involved in V(D)J recombination either in the mechanism itself or its regulation through modifying its accessibility to the RSS.

KRC is expressed most prominently in thymus and brain but also present in spleen and bone marrow (Hicar et al., 2002; Wu et al., 1996; Wu et al., 1993). Interestingly, multiple differential splicing transcripts were identified with a different splicing pattern in thymus and brain. The prevalent KRC transcripts in the thymus are the full length version and a spliced form lacking the second exon which includes ZAS1 and a significant portion of the middle part of KRC with the putative nuclear localization signal. In the brain the most abundant transcript lacks exon IV which comprises amongst other regions the ZAS2 domain (Mak et al., 1998). These alternative splicing events could result in the production of KRC isoforms with varying DNA and protein binding properties, suggesting that KRC may have different functions in lymphoid and neuronal tissues.

One known function of KRC is its ability to positively regulate the transcription of the *S100A4/mts1* gene, which is linked to its κ B (and related motifs) binding specificity (Hjelmsoe et al., 2000). S100A4/mts1 is a small acidic Ca^{2+} -binding protein which has been implicated in metastasis formation probably through its interaction with p53 (Grigorian et al., 2001) and nonmuscle myosin (Kriajevska et al., 2000). *S100A4/mts1* was shown to be expressed, similarly to *KRC*, in lymphoid tissues (Ebralidze et al., 1989) and in the central nervous system (Aberg and Kozlova, 2000).

KRC, itself, has also been implicated in proliferation. Introduction of antisense *KRC* mRNA into HeLa cells resulted in lower protein expression levels, induced proliferation, anchorage independence growth and mitotic cell death (Allen and Wu, 2000). If this observation is linked to the function of KRC as a positive transcriptional activator of the *S100A4/mts1* gene is unknown.

Additionally, to the regulatory function of KRC in gene expression, it was also shown that KRC participates directly in signaling events through protein-protein interactions. Altered expression of KRC modulates tumor necrosis factor α (TNF- α) driven

responses (Oukka et al., 2002). Overexpression of *KRC* inhibited, while antisense *KRC* c-DNA or a dominant negative form of the protein enhanced NF κ B activation as well as Jun N-terminal kinase (JNK) phosphorylation and consequently apoptosis and cytokine expression. Regulation of the TNF-receptor downstream signaling seemed to occur via direct protein-protein interaction of KRC with TRAF2.

KRC's binding specificity to the RSS, but also its modulatory function of inflammatory and apoptotic responses seemed very interesting. Together with its lymphoid expression pattern it made it conceivable that KRC plays a role in lymphoid cells early on in development during V(D)J recombination and/or later during immune responses. To address this question we decided to generate *KRC* deficient mice.

Results

Cloning of the targeting construct

The *KRC* locus spans over 70 kb genomic sequence and consists of 7 exons (Wu et al., 1996). Exon II is with its ca. 5.5 kb size extraordinarily large. It comprises the start codon together with the coding region for a significant portion of the protein including the first ZAS domain and the putative nuclear localization sequence. Therefore we designed a targeting vector which would lead, upon homologous recombination, to the deletion of nearly the complete coding region of exon II, encoding the N-terminal and central region of KRC, as well as part of exon III including the splice acceptor site to prevent splicing from exon I to III (see figure 3.2).

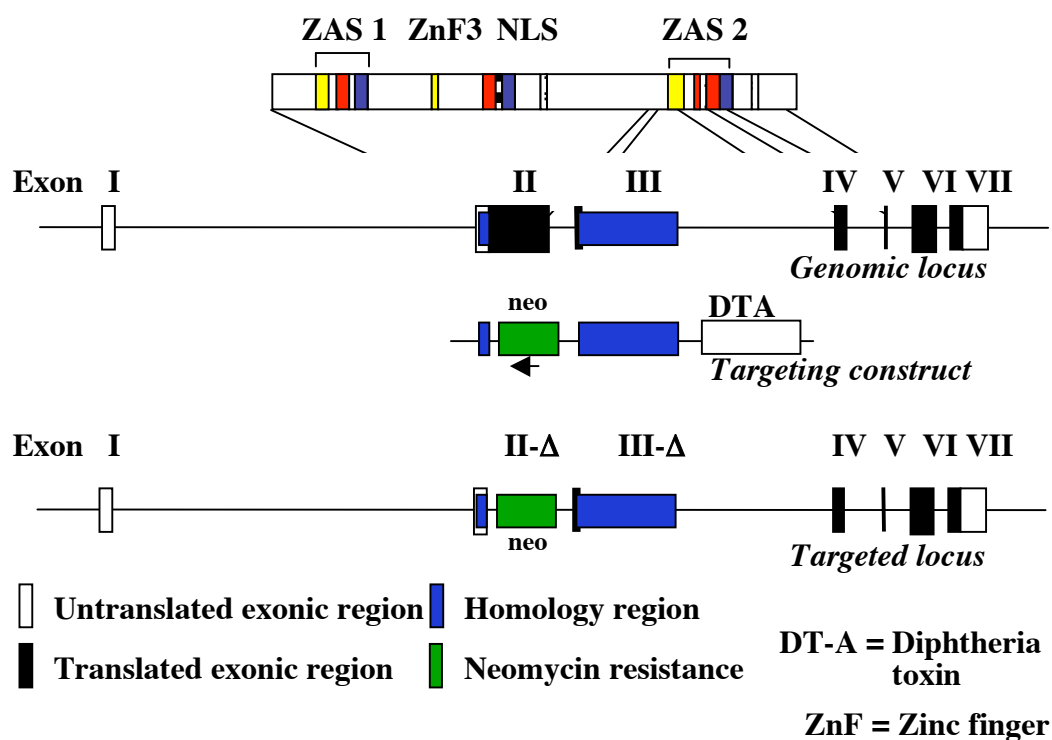


Figure 3.2: Schematic representation of the targeting construct, genomic and targeted locus

The targeting construct carried a neomycin resistance marker inside the targeting cassette as a positive selection marker. Additionally, for negative selection against randomly integrated DNA constructs the diphtheria toxin A expression cassette was placed beside the long arm of homology. Two homology regions flanked the targeting cassette. The 5' homology region consisted of 1 kb of the upstream 5' UTR of exon II. The 7 kb long 3' homology region consisted of downstream intronic region of

exon III including the splice donor site of exon III. Both homology regions were cloned by PCR amplification with 129/Ola genomic DNA as template. The primers for the amplification of the 5' arm could be readily designed based on the known sequence of exon II whereas the intronic sequence downstream of exon III was not known. Therefore the 3' intronic sequence was assembled using an *in silico* genome walking approach (see methods 7.11).

Targeting of the *KRC* locus

Targeting was done in the 129/Ola derived E14 ES cell line. ES cells were transfected with the linearized targeting construct and selected with G418. 450 resistant ES cell clones were screened by PCR for homologous integration of the construct first as pools of 8-10 clones and then the corresponding single clones. Screening PCR was designed to detect homologous integration of the short arm, with one primer lying upstream of the 5' homology region in the genomic locus and the second lying in the construct. One positive ES cell clone was detected. Homologous integration was

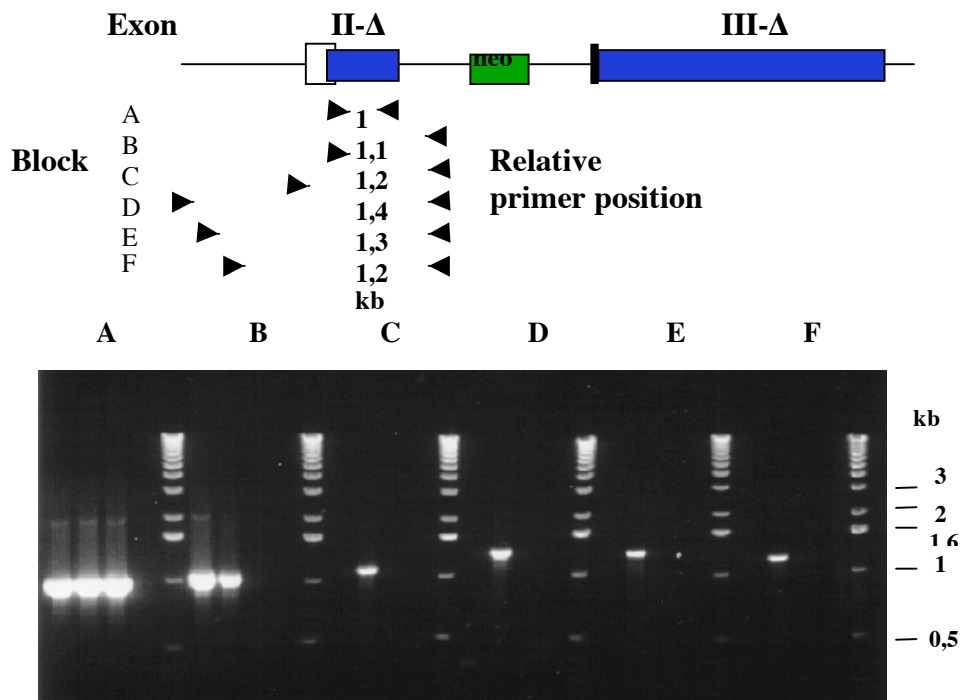


Figure 3.3: PCR Screening of G418 resistant ES cell clones. Upper part shows a schematic representation of the locus and the PCR strategy. Clone #57 positive for homologous recombination, clone #58 with random integration of the targeting construct. Lanes 1: clone #58; Lane 2: clone #57 Lane; Lane 3: WT DNA; Lane 4: no DNA; 5: standard.

verified with different primer combinations (see figure 3.3) and by additionally sequencing the complete amplificate of the screening PCR to exclude false positives. This targeted ES cell clone was injected into BDF1 blastocysts which were then transplanted into pseudopregnant females. 40 agouti offspring mice with varying degrees of chimerism, judging from fur colour, were born. Eventually various chimeric mice were bred to C57Bl/6 animals to obtain offspring of ES cell origin carrying the targeted locus. One of the chimeric mice gave germline transmission. The heterozygous offspring was then either intercrossed to obtain homozygous *KRC* knock-out mice or backcrossed with C57Bl/6 mice.

Characterization of the Integration Event

While heterozygous mice were bred the integration event was further genomically characterized. Southern blot analysis of the 5' region of the targeted locus confirmed that the construct had homologously integrated with the short arm into the *KRC* locus (see figure 3.4).

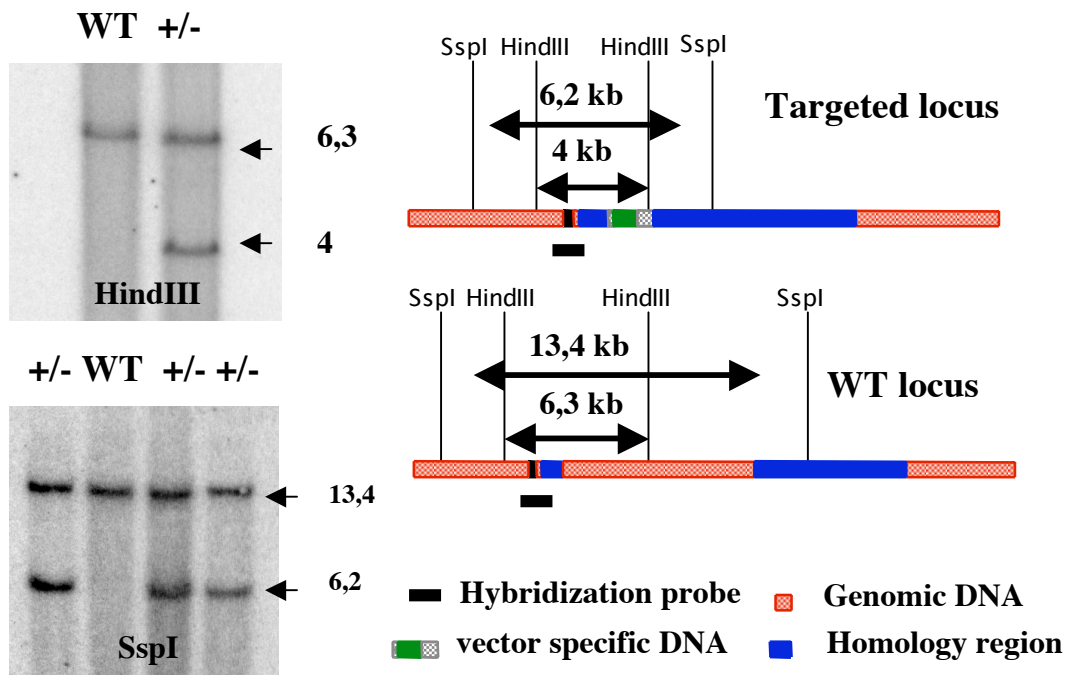


Figure 3.4: Southern blot analysis of the targeting construct integration at the 5' prime homology region.

In contrast, southern blot analysis of the 3' region in the selected ES cell clone revealed that the long arm had not homologously but randomly integrated into the locus (see figure 3.5). Quantitation with Real Time PCR showed that the exonic region directly downstream of the 5'-homology region had not been deleted (Data not shown). Southern blot analysis of the intronic region between exon II and II showed no modification of this region (Data not shown).

Altogether this suggested that the 3'-homology sequence had been joined to the genomic 5'-DNA end which was created during homologous recombination of the short targeting arm. Thereby exon II would not have been deleted. Nonetheless, one would expect that the integration event should interfere substantially with the transcription and translation of the locus. First of all, vector sequence is integrated into the locus which interrupts the *KRC* open reading frame. Additionally, the vector region include the neomycin resistance cassette which is transcribed in opposite direction to the locus thereby producing a kind of „antisense“ RNA. Furthermore, correct splicing should be hampered. The long homology region includes at its 5' end the splice donor site of exon III. Therefore splicing should occur from exon I to the targeted start of exon II and then again from the 5'-end of the right homology arm with the splice donor site of exon III to the splice acceptor site of the genomic exon III omitting thereby the residual genomic region of exon II.

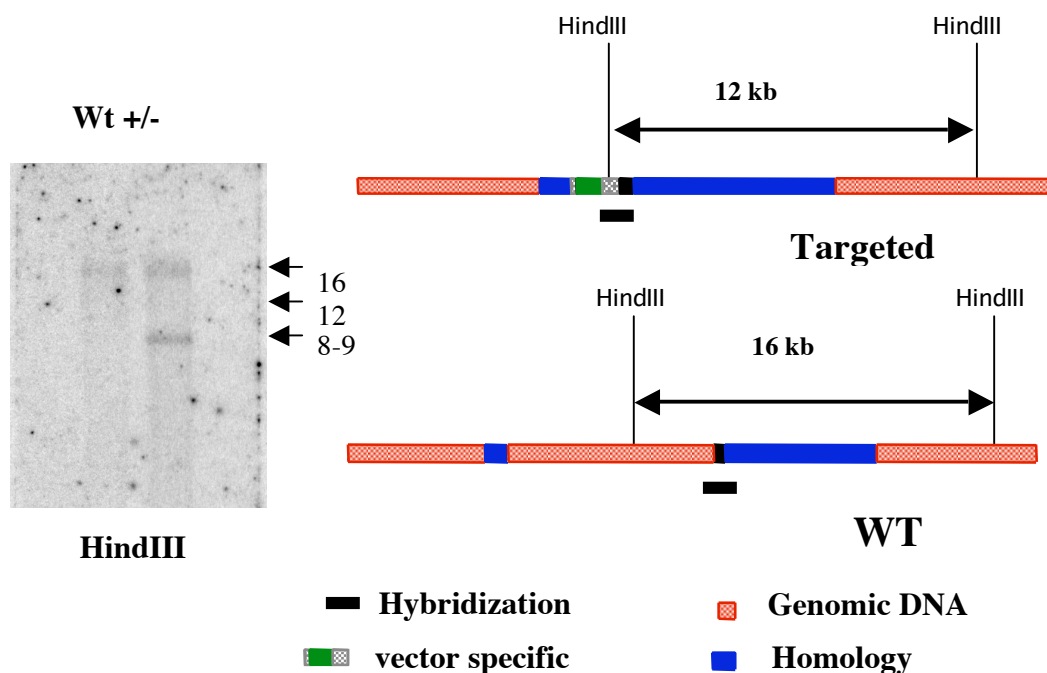


Figure 3.5: Southern blot analysis of the 3' prime region of the targeted locus with a construct specific probe.

Southern blot analysis performed with construct specific oligonucleotides additionally detected a second integration event of the targeting construct (see figure 3.6). The fact that all heterozygous mice also carried the second integration led to the conclusion that the second integration occurred on the same chromosome. Using an inverted PCR approach the 3' site of the second integration could be localized to the first intron of the *KRC* locus itself, more precisely about 5 kb upstream of exon II. Judging on basis of the currently known features of this genomic region (www.ncbi.nlm.nih.gov/mapview/) and if no larger rearrangements or translocations took place the second integration should not affect any other gene than the *KRC* gene itself. The fact that germline transmission was seen also suggests that no major rearrangements on the chromosomal level took place.

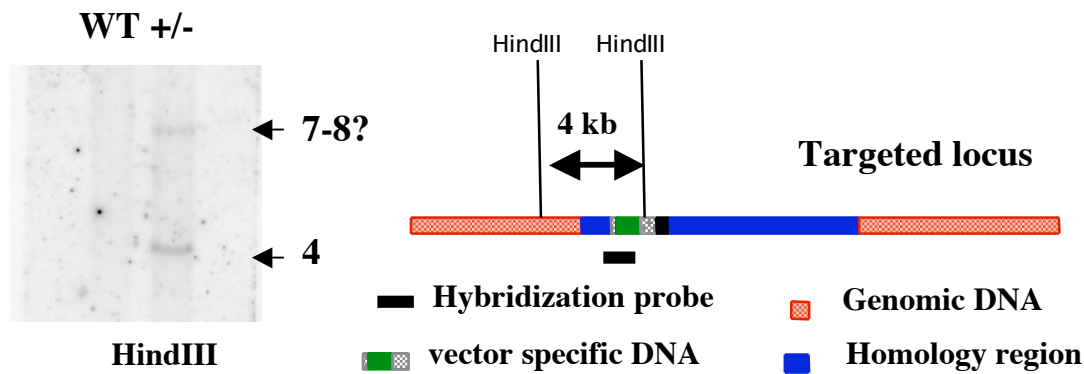


Figure 3.6: Southern blot analysis of the targeted locus with a construct specific probe.

Developmental consequences of the targeted *KRC* locus

Heterozygous mice were mated to obtain homozygous offspring for analysis of the effect of homozygosity of the targeted locus. We analyzed 44 3-week-old offspring of the heterozygous crosses and found no homozygous progeny. The average litter size was 5. One mouse died before weaning. Genotyping detected 9 WT and 35 heterozygous mice. Altogether this suggested that homozygosity of the mutation was embryonically lethal.

To investigate this question time matings were set up of heterozygous mice to analyze embryos at different timepoints of gestation. Embryos of day 14.5 pc (n = 24) and day 11.5 pc (n =12) were analyzed by southern blotting (see figure 3.7). Embryos of day 9.5 pc were genotyped (n = 10) with PCR. No homozygous embryo could be detected.

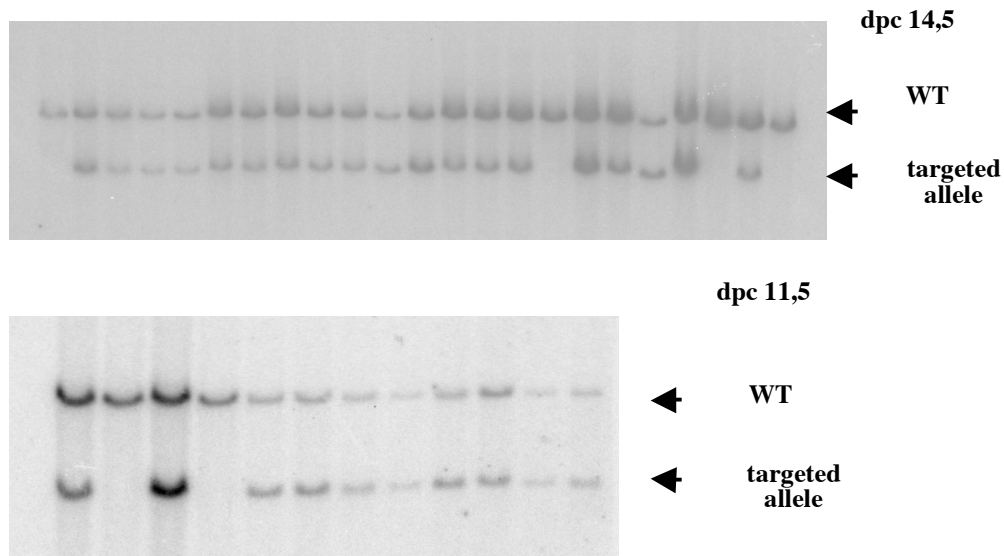


Figure 3.7: Genotyping of embryos by southern blot analysis with an 5' genomic probe.

To determine whether the embryonic lethality was post- or preimplantational we analyzed 67 embryos of the blastocyst stage (3.5 dpc) with a nested PCR approach for the presence of homozygotes (see figure 3.8). We did not detect any homozygous embryos indicating either preimplantation or cell-autonomous lethality of the homozygous mutation.

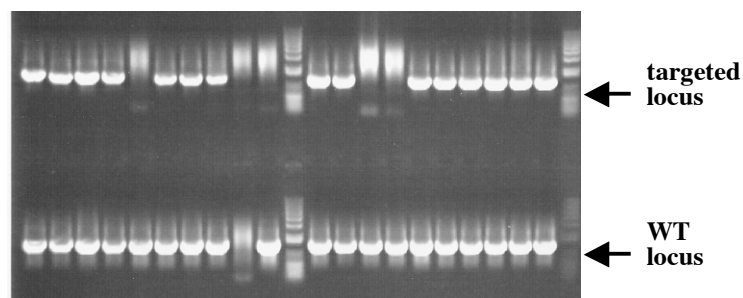


Figure 3.8: Genotyping 3.5 dpc blastocysts by nested PCR analysis, representatives results.

Characterization of heterozygous mice

In crosses between heterozygous and WT C57Bl/6 mice the ratio of wild type to heterozygous offspring that were obtained was close to 1:1. The heterozygotes were of comparable size to their WT siblings, healthy and without fertility problems. Considering that homozygosity of the mutation caused embryonic lethality we

decided to analyze the lymphoid compartment of heterozygous mice to see if haploinsufficiency would lead to detectable defects in the heterozygotes.

Therefore different lymphoid organs of 9 week old heterozygous mice (n = 4) were analyzed. Figures 3.9-11 show representative FACS analysis of the different organs and cell populations. In the thymus normal proportions of CD4⁺ and CD8⁺ DN, DP and SP thymocyte subpopulations were present. Also in the mesenteric lymph nodes no effect of heterozygosity on the CD4⁺ or CD8⁺ SP thymocyte populations was detected. The bone marrow contained a normal percentage of immature B220⁺/IgM⁺ and recirculating mature B220^{high}/IgM⁺ B cells. Analysis of the CD19⁺ compartment of the spleen detected normal percentages of immature T1 (493⁺/CD23⁻), immature T2+T3 (493⁺/CD23⁺), follicular (CD21⁺/CD23⁺) and marginal zone B cells (CD21⁺/CD23⁻). In conclusion, no obvious defect was found in heterozygous animals.

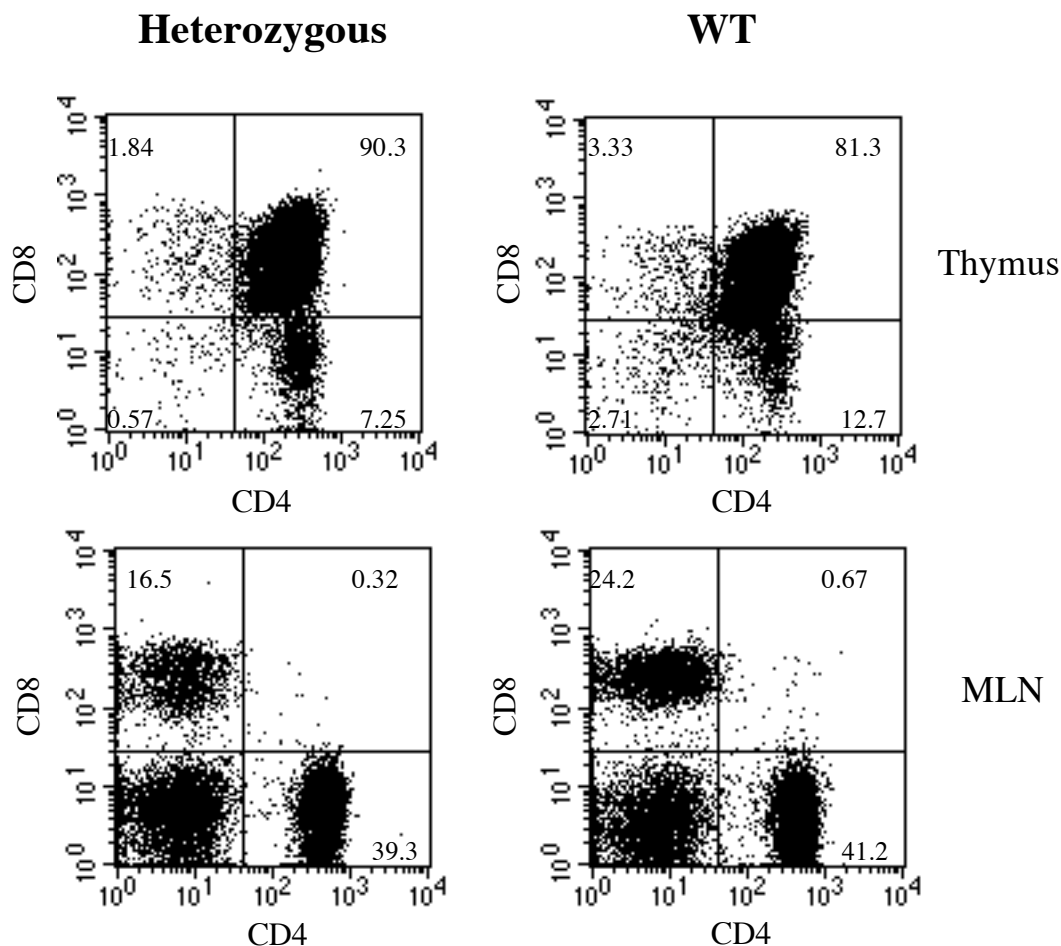


Figure 3.9: Representative FACS profiles of different organs of WT and heterozygous mice. The cells of all organs are gated on the lymphoid FSC and SSC gate. MLN = mesenteric lymph node

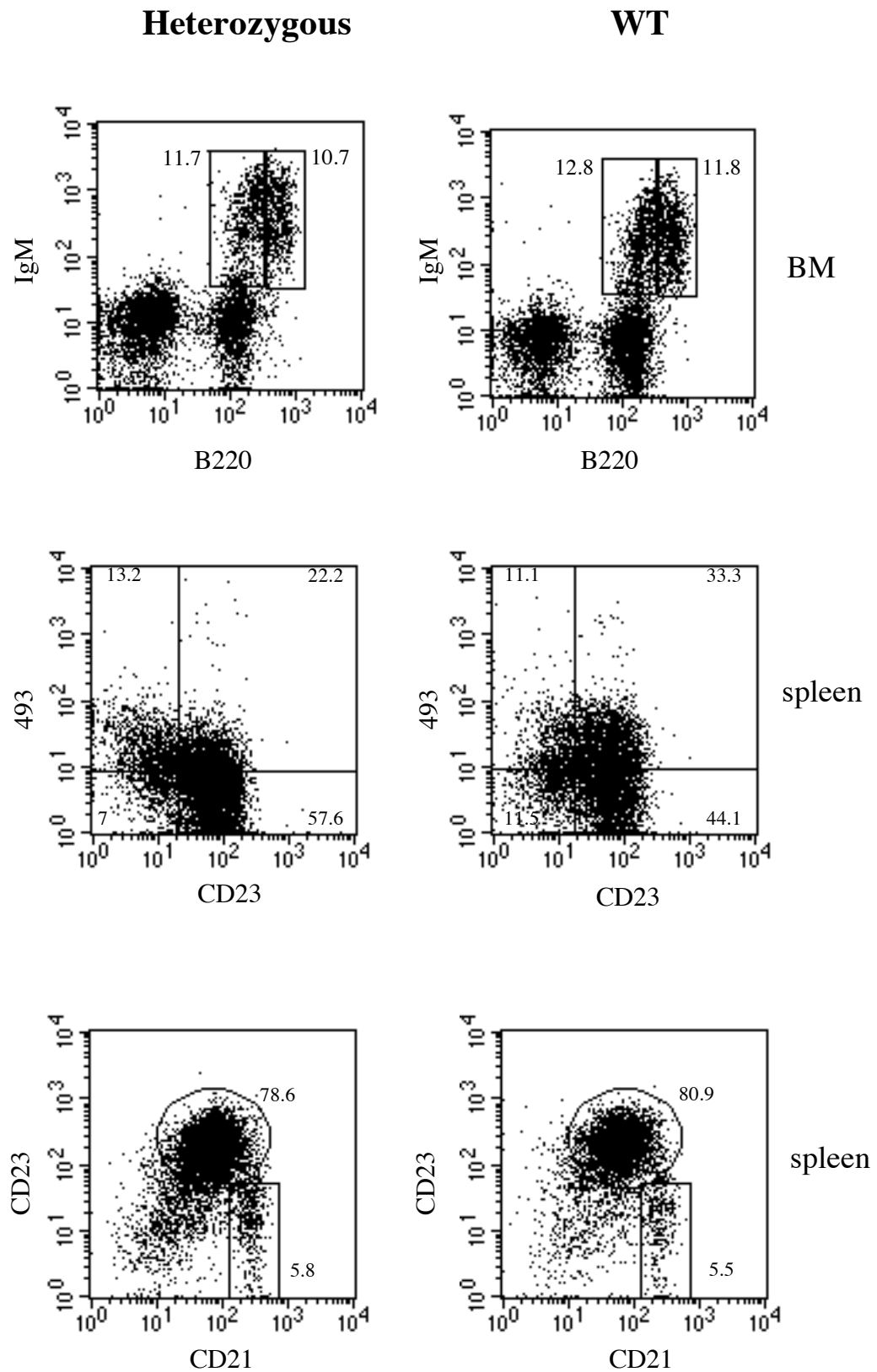


Figure 3.10: Representative FACS profiles of spleen cells of WT and heterozygous mice. The cells are gated on the lymphoid FSC and SSC gate and additionally on CD19⁺ cells. BM = bone marrow

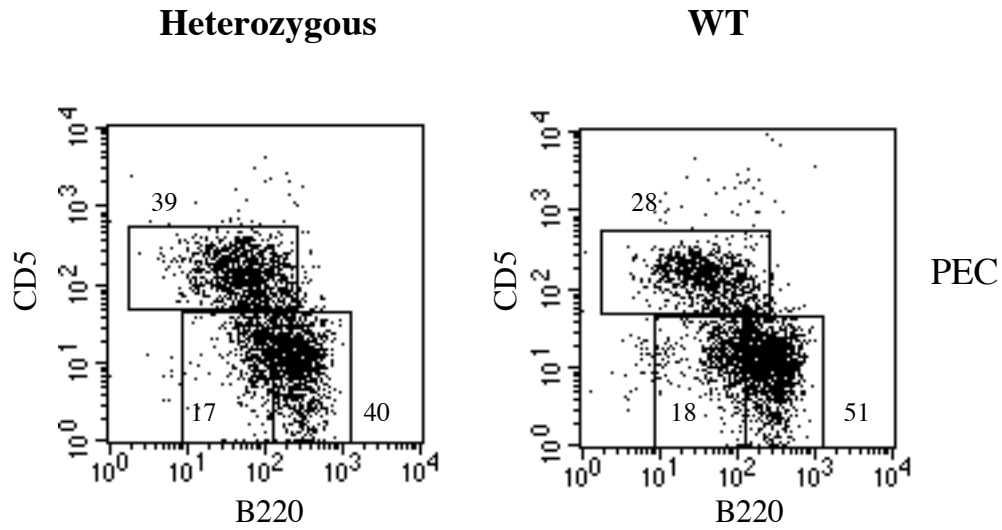


Figure 3.11: Representative FACS profiles of peritoneal cells of WT and heterozygous mice. The cells are gated on the lymphoid FSC and SSC gate and additionally on CD19⁺ cells. PEC = peritoneal cells

Discussion

KRC belongs to a family of large DNA binding proteins. Based on sequence similarities, these proteins are divided into three classes (Wu et al., 1993) represented by HIV-EP1 (also known as Schnurri-1, MBP-1, PRDII-BF1 and α A-CRYBP1), HIV-EP2 (also known as Schnurri-2, MBP-2, AGIE-BP1 and MIBP1) and *KRC* (Schnurri-3, HIV-EP3, KBP1). The different names are indicative of the large spectrum of functions the different protein family members are involved in. Human HIV-EP1 has been shown to activate transcription of the human immunodeficiency virus enhancer (human immunodeficiency virus type I enhancer binding protein 1) (Seeler et al., 1994). Its mouse counterpart α A-crystallin binding protein 1 (α A-CRYBP1) acts as transcription activator for the α A-crystallin gene during the development of the eye lens (Brady et al., 1995). The *Drosophila* orthologue Schnurri plays a role in dorsal ectodermal patterning as part of the decapentaplegic (Dpp)/TGF β signaling pathway (Arora et al., 1995; Grieder et al., 1995). HIV-EP2 in mouse has been shown to be required for positive selection of thymocytes (Takagi et al., 2001). This groups *KRC* into a protein family whose members are involved in diverse developmental processes including transcriptional regulation and signaling. Due to its lymphoid expression pattern and its RSS binding ability we wanted to further characterize the role of *KRC* in lymphocyte development including V(D)J recombination.

To address this question we targeted the *KRC* locus. Targeting was done in 129/Ola ES cells and homologous recombination was tested by PCR screening and subsequent sequencing of the amplified products. One clone out of 450 was tested positive for homologous recombination. Closer characterization of the targeted locus verified the correct integration of the short homology region but also revealed random integration of the the long (3'-) homology region of the targeting construct. Integration of the targeting construct into the 5' region of exon II presumably led to an interruption of transcription, translation and/or interference with the correct splicing of the *KRC* messenger RNA mimicking a deletion of exon II. Additionally, a second integration of the targeting construct into the first exon of the *KRC* locus was detected. Taken together these results argue for a successful disruption of the *KRC* locus.

The clone positive for homologous recombination was injected into BDF1 blastocysts and these were subsequently transplanted into pseudopregnant females. Chimeric

mice were backcrossed to C57BL/6 and the heterozygous offspring was subsequently intercrossed to allow homozygosity of the targeted *KRC* locus.

The offspring was genotyped and none of the 44 tested littermates was homozygous for the targeted *KRC* locus indicating that homozygosity of the targeted locus led to embryonic lethality. We therefore genotyped embryos between day 9.5 pc and 14.5 pc of embryonic development. No homozygous embryos were detected, demonstrating that homozygosity of the targeted locus causes embryonic lethality before day 9.5 pc. To narrow down the time frame of embryonic lethality 3.5 dpc blastocysts were genotyped by PCR, but again no homozygous embryo was detected leading to the conclusion that homozygosity of the mutation causes either preimplantational or cell-autonomous lethality.

Preimplantational development of mouse embryos proceeds through a series of critical steps: the transition from oocyte to embryo, the first cell divisions, the establishment of cellular contacts and the first lineage differentiation. Global expression profiles revealed two major waves of *de novo* transcription, one corresponding to the zygote gene activation and the second to the mid-preimplantation gene activation (Hamatani et al., 2004; Wang et al., 2004). These analysis also showed that mouse oocytes and early embryos (analyzed till blastocyst stage) express components of multiple signaling pathways like Wnt and Notch and most interestingly of the bone morphogenetic protein (BMP) signaling machinery. BMP signaling, involved in nearly all aspects of embryonic development and organogenesis, is in turn closely related to the Dpp signaling in *Drosophila* where the *KRC* orthologue Schnurri is part of (Zhao, 2003). Therefore it would be conceivable that *KRC* deficiency causes preimplantational lethality by interfering with essential signaling processes in the very-early embryo development. Alternatively, the implication of *KRC* in proliferative processes (Allen and Wu, 2000), demonstrated by its effect on the growth of HeLa cells, could have adverse effects on embryonic preimplantational development. Preimplantation lethality has been shown to occur, like in the case of the *mixed lineage leukemia* gene (*MLL*), which is involved in *Hox* gene regulation. *MLL* deficient embryos do not progress to the 2-cell stage *in vivo* (Ayton et al., 2001) only *in vitro*.

Results published during the course of the project by Allen et al. would also argue against cell-autonomous lethality. In this report, 500 bp of the coding region of

exon II were replaced with a neomycin resistance cassette (Allen et al., 2002b). Homozygous ES cell clones were generated by subjecting the heterozygous clones to more stringent G418 selection. These cells were then analyzed in a *RAG2*^{-/-} blastocyst complementation system. The authors do not comment on why no heterozygous and subsequently homozygous mice were generated with the help of these ES cells. This suggests that while *KRC* deficient cells were viable also this targeting might have resulted in embryonic lethality. Analysis of the *RAG2*^{-/-};*KRC*^{-/-} chimeras showed that B and T lymphocytes developed leading to the conclusion that *KRC* deficiency had no effect on V(D)J recombination. Nonetheless, it is noteworthy that only exon II was targeted in this approach leaving open the possibility that an isoform of the protein, excluding exon II, plays a role in V(D)J recombination, since it had been shown that especially the thymus naturally expressed such a splice variant (Mak et al., 1998). Although reconstitution of the lymphoid system took place in the *RAG2*^{-/-};*KRC*^{-/-} chimeras, analysis of older chimeras revealed a marked deficit of CD4⁺/CD8⁺ double positive thymocytes. Since BMP signaling was also shown to be involved in T lymphocyte development one could speculate again about a correlation of *KRC* and BMP signaling (Graf et al., 2002; Hager-Theodorides et al., 2002). Furthermore, Oukka et al. published a report in which they characterized *KRC* deficient T cells and showed that *KRC* is involved in the regulation of the IL-2 gene in T cells via interaction with c-Jun (Oukka et al., 2004). As this report referred to unpublished data regarding the generation of the analyzed cells it is unclear what kind of targeting approach the authors chose and if it caused embryonic lethality. Taken together, the results of this work suggested that complete disruption of the *KRC* gene locus leads to very early embryonic lethality, provided that no other essential genes were affected by the targeting.

References

Aberg, F., and Kozlova, E. N. (2000). Metastasis-associated mts1 (S100A4) protein in the developing and adult central nervous system. *J Comp Neurol* 424, 269-282.

Allen, C. E., Mak, C. H., and Wu, L. C. (2002a). The kappa B transcriptional enhancer motif and signal sequences of V(D)J recombination are targets for the zinc finger protein HIVEP3/KRC: a site selection amplification binding study. *BMC Immunol* 3, 10.

Allen, C. E., Muthusamy, N., Weisbrode, S. E., Hong, J. W., and Wu, L. C. (2002b). Developmental anomalies and neoplasia in animals and cells deficient in the large zinc finger protein KRC. *Genes Chromosomes Cancer* 35, 287-298.

Allen, C. E., and Wu, L. C. (2000). Downregulation of KRC induces proliferation, anchorage independence, and mitotic cell death in HeLa cells. *Exp Cell Res* 260, 346-356.

Arora, K., Dai, H., Kazuko, S. G., Jamal, J., O'Connor, M. B., Letsou, A., and Warrior, R. (1995). The *Drosophila* schnurri gene acts in the Dpp/TGF beta signaling pathway and encodes a transcription factor homologous to the human MBP family. *Cell* 81, 781-790.

Ayton, P., Sneddon, S. F., Palmer, D. B., Rosewell, I. R., Owen, M. J., Young, B., Presley, R., and Subramanian, V. (2001). Truncation of the *Mll* gene in exon 5 by gene targeting leads to early preimplantation lethality of homozygous embryos. *Genesis* 30, 201-212.

Bachmeyer, C., Mak, C. H., Yu, C. Y., and Wu, L. C. (1999). Regulation by phosphorylation of the zinc finger protein KRC that binds the kappaB motif and V(D)J recombination signal sequences. *Nucleic Acids Res* 27, 643-648.

Brady, J. P., Kantorow, M., Sax, C. M., Donovan, D. M., and Piatigorsky, J. (1995). Murine transcription factor alpha A-crystallin binding protein I. Complete sequence, gene structure, expression, and functional inhibition via antisense RNA. *J Biol Chem* 270, 1221-1229.

Ebralidze, A., Tulchinsky, E., Grigorian, M., Afanasyeva, A., Senin, V., Revazova, E., and Lukanidin, E. (1989). Isolation and characterization of a gene specifically expressed in different metastatic cells and whose deduced gene product has a high degree of homology to a Ca²⁺-binding protein family. *Genes Dev* 3, 1086-1093.

Graf, D., Nethisinghe, S., Palmer, D. B., Fisher, A. G., and Merckenschlager, M. (2002). The developmentally regulated expression of Twisted gastrulation reveals a role for bone morphogenetic proteins in the control of T cell development. *J Exp Med* 196, 163-171.

Grieder, N. C., Nellen, D., Burke, R., Basler, K., and Affolter, M. (1995). Schnurri is required for *Drosophila* Dpp signaling and encodes a zinc finger protein similar to the mammalian transcription factor PRDII-BF1. *Cell* 81, 791-800.

- Grigorian, M., Andresen, S., Tulchinsky, E., Kriajevska, M., Carlberg, C., Kruse, C., Cohn, M., Ambartsumian, N., Christensen, A., Selivanova, G., and Lukanidin, E. (2001). Tumor suppressor p53 protein is a new target for the metastasis-associated Mts1/S100A4 protein: functional consequences of their interaction. *J Biol Chem* 276, 22699-22708.
- Hager-Theodorides, A. L., Outram, S. V., Shah, D. K., Sacedon, R., Shrimpton, R. E., Vicente, A., Varas, A., and Crompton, T. (2002). Bone morphogenetic protein 2/4 signaling regulates early thymocyte differentiation. *J Immunol* 169, 5496-5504.
- Hamatani, T., Carter, M. G., Sharov, A. A., and Ko, M. S. (2004). Dynamics of global gene expression changes during mouse preimplantation development. *Dev Cell* 6, 117-131.
- Hicar, M. D., Robinson, M. L., and Wu, L. C. (2002). Embryonic expression and regulation of the large zinc finger protein KRC. *Genesis* 33, 8-20.
- Hjelmsoe, I., Allen, C. E., Cohn, M. A., Tulchinsky, E. M., and Wu, L. C. (2000). The kappaB and V(D)J recombination signal sequence binding protein KRC regulates transcription of the mouse metastasis-associated gene S100A4/mts1. *J Biol Chem* 275, 913-920.
- Kriajevska, M., Bronstein, I. B., Scott, D. J., Tarabykina, S., Fischer-Larsen, M., Issinger, O., and Lukanidin, E. (2000). Metastasis-associated protein Mts1 (S100A4) inhibits CK2-mediated phosphorylation and self-assembly of the heavy chain of nonmuscle myosin. *Biochim Biophys Acta* 1498, 252-263.
- Mak, C. H., Li, Z., Allen, C. E., Liu, Y., and Wu, L. (1998). KRC transcripts: identification of an unusual alternative splicing event. *Immunogenetics* 48, 32-39.
- Mak, C. H., Strandtmann, J., and Wu, L. C. (1994). The V(D)J recombination signal sequence and kappa B binding protein Rc binds DNA as dimers and forms multimeric structures with its DNA ligands. *Nucleic Acids Res* 22, 383-390.
- Oukka, M., Kim, S. T., Lugo, G., Sun, J., Wu, L. C., and Glimcher, L. H. (2002). A mammalian homolog of *Drosophila schnurri*, KRC, regulates TNF receptor-driven responses and interacts with TRAF2. *Mol Cell* 9, 121-131.
- Oukka, M., Wein, M. N., and Glimcher, L. H. (2004). Schnurri-3 (KRC) Interacts with c-Jun to Regulate the IL-2 Gene in T Cells. *J Exp Med* 199, 15-24.
- Seeler, J. S., Muchardt, C., Suessle, A., and Gaynor, R. B. (1994). Transcription factor PRDII-BF1 activates human immunodeficiency virus type 1 gene expression. *J Virol* 68, 1002-1009.
- Takagi, T., Harada, J., and Ishii, S. (2001). Murine Schnurri-2 is required for positive selection of thymocytes. *Nat Immunol* 2, 1048-1053.
- Wang, Q. T., Piotrowska, K., Ciemerych, M. A., Milenkovic, L., Scott, M. P., Davis, R. W., and Zernicka-Goetz, M. (2004). A genome-wide study of gene activity reveals

developmental signaling pathways in the preimplantation mouse embryo. *Dev Cell* 6, 133-144.

Wu, L. C., Hicar, M. D., Hong, J., and Allen, C. E. (2001). The DNA-binding ability of HIVEP3/KRC decreases upon activation of V(D)J recombination. *Immunogenetics* 53, 564-571.

Wu, L. C., Liu, Y., Strandtmann, J., Mak, C. H., Lee, B., Li, Z., and Yu, C. Y. (1996). The mouse DNA binding protein Rc for the kappa B motif of transcription and for the V(D)J recombination signal sequences contains composite DNA-protein interaction domains and belongs to a new family of large transcriptional proteins. *Genomics* 35, 415-424.

Wu, L. C., Mak, C. H., Dear, N., Boehm, T., Foroni, L., and Rabbitts, T. H. (1993). Molecular cloning of a zinc finger protein which binds to the heptamer of the signal sequence for V(D)J recombination. *Nucleic Acids Res* 21, 5067-5073.

Zhao, G. Q. (2003). Consequences of knocking out BMP signaling in the mouse. *Genesis* 35, 43-56.

4 Analysis of the mature B cell compartments in $\lambda 5$ deficient mice

Introduction

Developing B lymphocytes rearrange their V, sometimes D and J segments of their *IgH* and *L* chain gene loci in an ordered, stepwise fashion (Alt et al., 1984; ten Boekel et al., 1995; ten Boekel et al., 1998). The first segments to be rearranged at the transition of the proB cell to the preB-I cell stage are the D_H and J_H gene segments of the *IgH* locus. Both *IgH* alleles are rearranged resulting in preB-I cells carrying two *IgH* DJ rearrangements. Late stage preB-I cells start to rearrange V_H to DJ_H , first only on one allele. If the V_H to DJ_H rearrangement is productive and the resulting μH protein is able to pair with the surrogate light chain (SL) a pre-Bcell receptor (preBCR) is formed and expressed on the cell surface. The SL is composed of the noncovalently associated VpreB and $\lambda 5$ proteins, forming a λL -chain-like structure that is able to pair and form disulfide bridges with μH chains. Only if a non-productive rearrangement occurs on the first allele or if the synthesized μH protein is unable to pair with the SL, will the second allele be rearranged. Thus, it is ensured that a single B cell expresses only one type of IgH on the cell surface (Nussenzweig et al., 1987), a phenomenon termed allelic exclusion. Deposition of a preBCR on the cell surface allows the cells to become large preB-II cells which undergo two to five rounds of cell division (Rolink et al., 2000). Thereby, only clones with a SL pairing μH are expanded, whereas other cells with nonpairing μH chains are not. Successful pairing with the SL could therefore be seen as a μH quality control checkpoint. Eventually, the cells become small resting preB-II cells, rearranging their κL and/or λL chain loci. In the case of a productive L chain rearrangement cells develop into surface IgM-bearing immature B cells. These sIgM⁺ B cells, after having been negatively selected against autoreactive cells, leave the bone marrow and home to the spleen. There they go through different phenotypically characterized stages of the transitional compartment finally becoming mature B cells (reviewed in Rolink et al., 2004). The most prominent mature B cells in the spleen are the follicular B cells, mainly involved in thymus-dependent (TD) immune responses. Marginal zone B (MZB) cells, located at the outer rim of the follicles, represent a smaller fraction of splenic B cells, their origin being still a matter of debate (Lopes-Carvalho and

Kearney, 2004; Martin and Kearney, 2002). They are considered to be a first line of defense against blood-borne antigens (Martin et al., 2001) participating in TI immune responses. Another peripheral mature B cell population, the B1 B cells, represents in the spleen only a minor fraction, but is the main B cell population in peritoneal and pleural cavities. B1 B cells develop prior to weaning and persist thereafter, in contrast to conventional B2 B cells, as a self-replenishing population. Two subpopulations are differentiated based on their CD5 expression, the B1a being CD5⁺ and the B1b CD5⁻^{low}. A high proportion of the serum IgM, including the natural antibodies (produced without apparent antigenic stimulus) is produced by the B1 B cells. They are thought to participate mainly in thymus-independent (TI) immune responses (Herzenberg, 2000).

Several mutations affecting the early development of B cells are known. In 1992 Kitamura and coworkers generated $\lambda 5$ deficient mice to analyze the role of the SL component in B cell development. $\lambda 5^{-/-}$ mice, also referred to as $\lambda 5T$ mice, showed, as expected, a block in early B cell development, more precisely at the transition from preB-I cells to preB-II cells. In contrast to other deficiencies for e.g. like in the μMT mutant mice, in which the exon encoding the transmembrane domain of the μH chain was disrupted (Kitamura et al., 1991), the developmental block observed in $\lambda 5^{-/-}$ mice was incomplete. As a consequence cells of the following developmental stages were largely reduced but not completely absent and a low number of B2 cells could be detected in the periphery. These cells were shown to be functional concerning their ability to respond to TD as well as TI immunizations. Analysis of the B1 B cell compartment revealed, apart from an initial reduction of cell numbers in neonates, no significant differences to wild type mice.

In the past few years many new phenotypic markers and marker combinations have been characterized allowing to distinguish B cell populations like transitional B cells or MZB by flow cytometric means. In 1992 these marker combinations were not yet known and as a consequence, no detailed analysis of the different B cell compartments in the $\lambda 5^{-/-}$ mice could be made. Several different mice with mutations affecting the generation of B cells have been characterized, also concerning their mature B cell populations. Thereby it became apparent that a whole variety of molecules are involved in the shaping of the mature B cell pool. Thus, mutations affecting the BCR co-receptors, BCR signaling regulators or Notch signaling

pathways influence the formation of a mature B cell populations in different ways. Interestingly, it was observed that there is a tendency to preferentially propagate and maintain activated and/or highly responsive cells, like MZB, in B lymphopenic mice (Carvalho et al., 2001; Hao and Rajewsky, 2001).

This raised the question whether $\lambda 5$ deficient animals would also show a proportional expansion of B cell compartments, considered to be more innate. To address this we decided to analyze B cell populations in $\lambda 5$ deficient mice in more detail. Additionally, we studied the turnover of the different B cell populations in wild type and mutant mice, the secondary immune response and the ability of $\lambda 5^{-/-}$ progenitor cells to reconstitute in competition with wild type cells in mixed bone marrow chimeras.

Results

Characterization of B cell populations in $\lambda 5$ deficient mice

B cell compartments in bone marrow, peritoneal cavity and spleen of adult wild type and $\lambda 5$ deficient mice were analyzed by flow cytometry.

As it was previously described (Kitamura et al., 1992; Rolink et al., 1994), analysis of the $c\text{-kit}^+/B220^+$ compartment in the bone marrow, comprising the early pre/pro-B, pro-B and pre-BI cells, showed a slight enlargement in $\lambda 5^{-/-}$ mice compared to wild type (see figure 4.1 A). This was most probably due to the block in development at the transition of the pre-BI cell to the pre-BII cell, resulting in the accumulation of $c\text{-kit}^+/B220^+$ cells. As a consequence of the block there was a pronounced decrease of the following pre-BII compartment ($B220^+/CD25^+$) (see figure 4.1). Also the $IgM^+/B220^+$ B cell fraction comprising the immature ($IgM^+/B220^{int}$) and mature

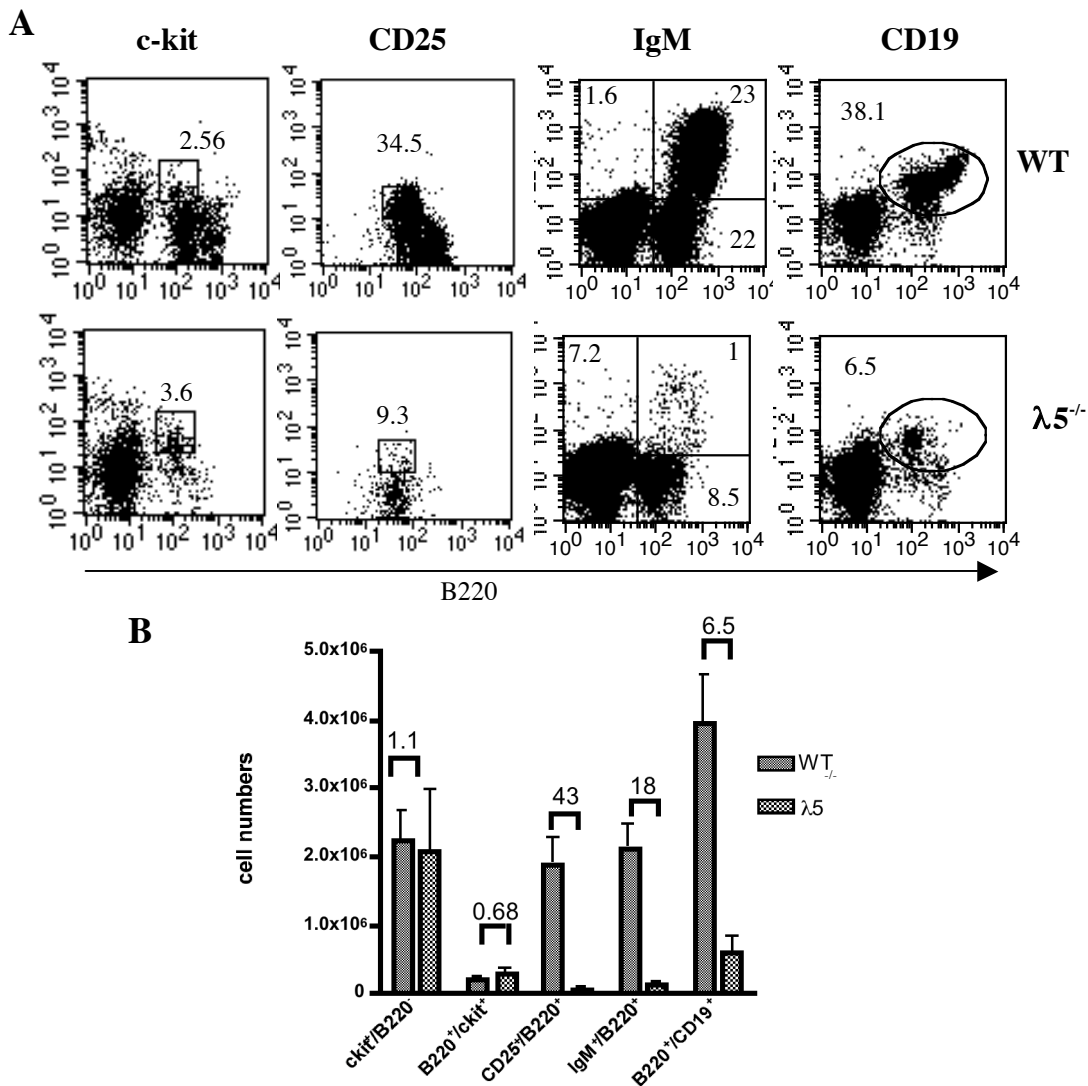


Figure 4.1: Representative flow cytometric analysis (A) and total cell numbers (B) of bone marrow viable cells of 9 week old wild type and $\lambda 5^{-/-}$ mice. A) In the CD25 panel only CD19⁺ lymphocytes are shown. Numbers indicate percentages of the subpopulations. B) Numbers above the bars indicate the x-fold difference in wild type and $\lambda 5^{-/-}$ mice (n = 6 each group).

recirculating ($\text{IgM}^+/\text{B220}^+$) B cells was markedly reduced (see figure 4.1). Overall there was a 6.5 fold reduction of the number of $\text{CD19}^+/\text{B220}^+$ B cells in the bone marrow of mutant mice due to $\lambda 5$ deficiency (see figure 4.1).

As the developmental block in $\lambda 5$ deficient mice is not absolute a low number of B cells were detectable in the periphery. Analysis of peritoneal cells in $\lambda 5$ deficient mice revealed, as described by Kitamura and coworkers (Kitamura et al., 1992), a marked reduction but not complete absence of the $\text{CD5}^-/\text{CD23}^+/\text{B220}^+/\text{CD19}^+$ B 2 compartment (see figure 4.2). The $\text{CD5}^+/\text{B220}^{\text{int}}$ B1a population, which seems to be less dependent on the preBCR (Kitamura et al., 1992), was present in normal numbers in the adult $\lambda 5^{-/-}$ mice (see figure 4.2 A/D). Instead the $\text{CD5}^{\text{low}}/\text{B220}^{\text{int}}$ B1b population, though normal in relative proportion, was reduced about twofold in terms of total cell numbers in mutant animals (see figure 4.2 A/C/D).

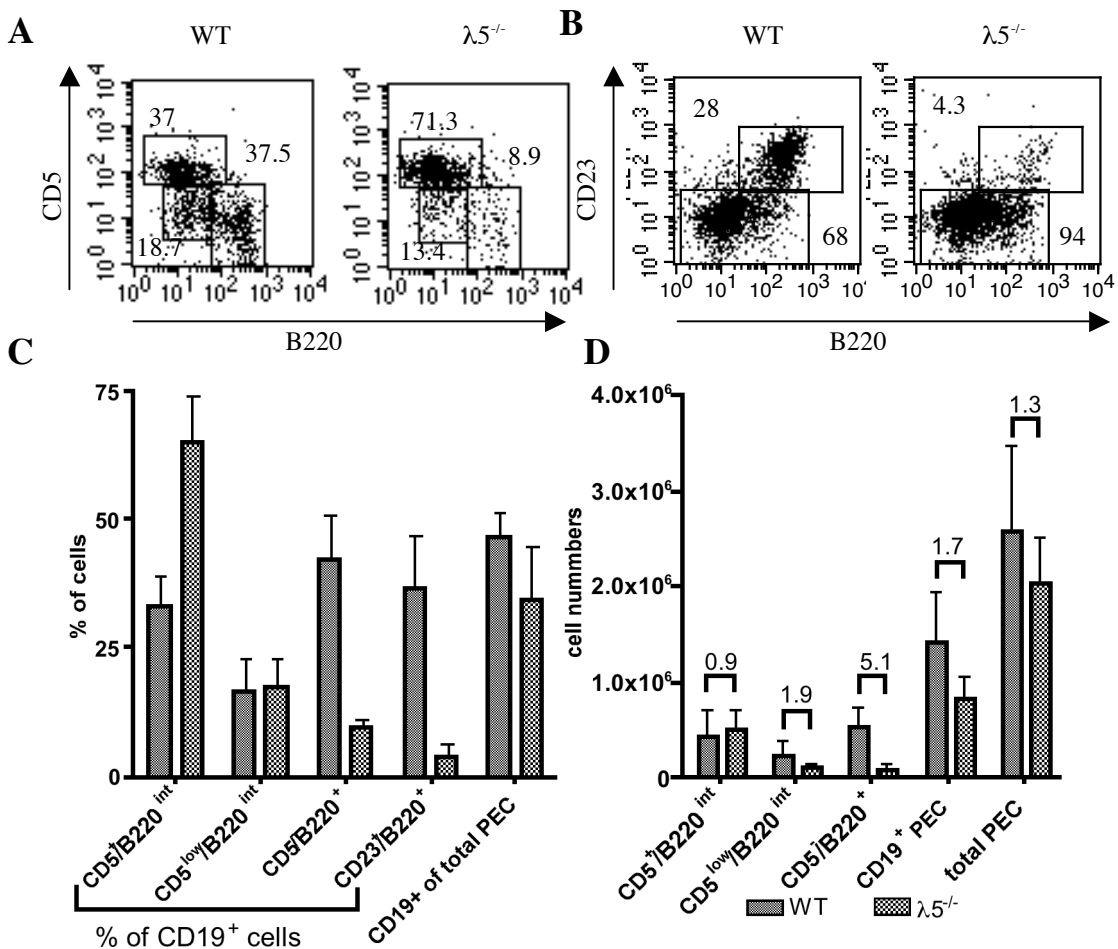


Figure 4.2: Analysis of peritoneal lymphocytes of 9 week old wild type and $\lambda 5^{-/-}$ mice. A) and B) representative flow cytometric analysis. Only CD19^+ cells are shown. Numbers indicate percentages of the subpopulations. C) and D) Relative proportions and total cell numbers of different B cell populations in the peritoneal cavity. Numbers above the bars in D) indicate the x-fold difference in wild type and $\lambda 5^{-/-}$ mice (n = 6 each group).

Analysis of the transitional B cell compartment in the spleen showed that T1 ($CD19^+/493^+/CD23^-$) as well as T2/T3 cells ($CD19^+/493^+/CD23^+$) were barely detectable (see figure 4.3 A/C/D). Also follicular B (FOB) cells ($CD19^+/493^-/CD23^+$) were proportionally and absolutely very much reduced (see figure 4.3 A/C/D). In contrast there was a relative increase of MZB cells in the $CD19^+$ compartment in $\lambda 5^{-/-}$ mice (see figure 4.3 B/C; $CD19^+/493^-/CD23^{-/low}/CD21^{high}$), but in terms of absolute numbers MZB cells were present in equal quantities in wild type and $\lambda 5$ deficient mice (see figure 4.3 D). Phenotypically the MZB cells in $\lambda 5^{-/-}$ mice showed a slightly reduced CD21 expression. The $CD21^{low}/CD23^-$ B cell population (see figure 4.3 B), apparently proportionally enriched in the $\lambda 5^{-/-}$ mice, has not yet been described before and is currently characterized phenotypically and functionally in our group.

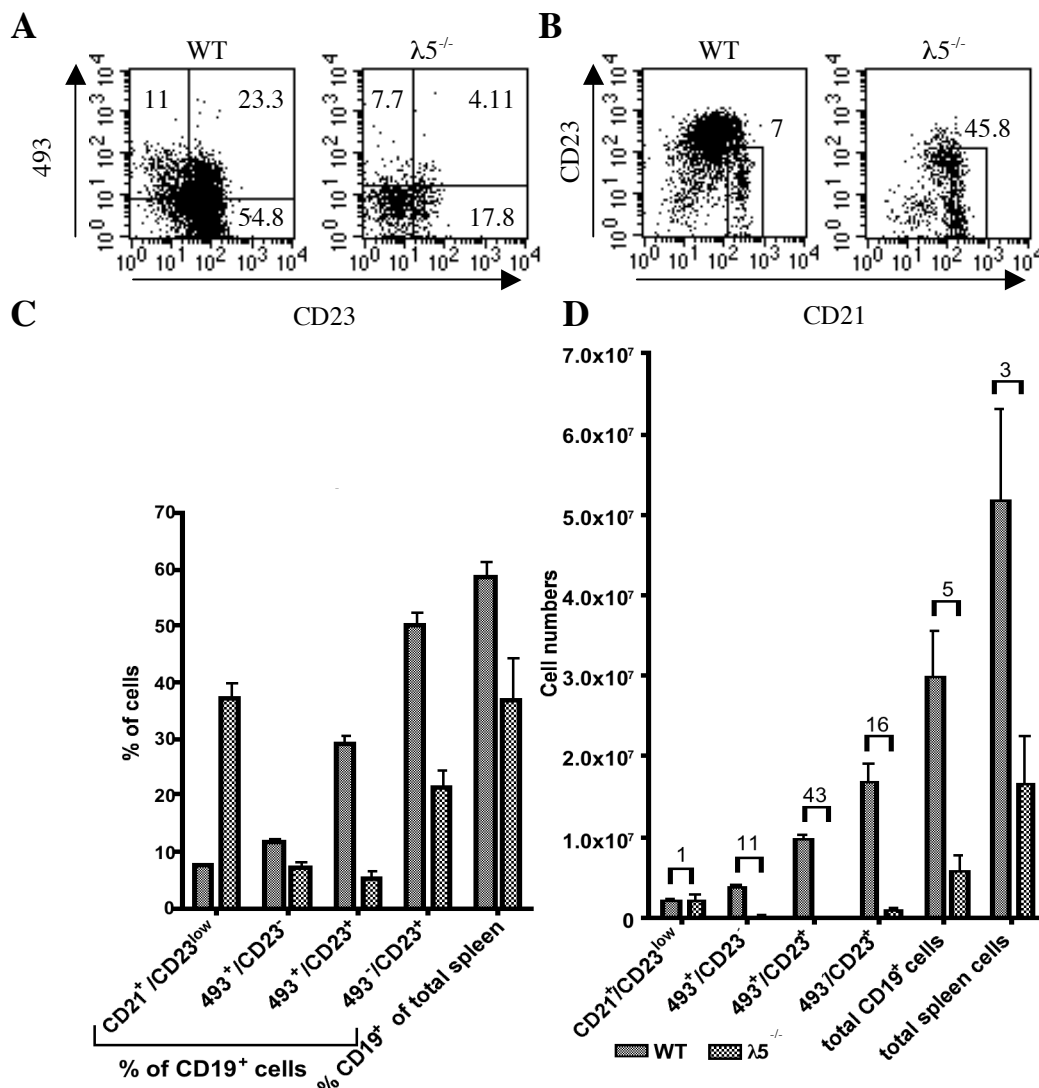


Figure 4.3: Analysis of splenic lymphocytes of 9 week old wild type and $\lambda 5^{-/-}$ mice. A) and B) representative flow cytometric analysis of splenocytes. Only $CD19^+$ cells are shown. Numbers indicate percentages of the subpopulations. Relative proportions (C) and total cell numbers (D) of different B cell populations in the spleen. Numbers above the bars in D) indicate the x-fold difference (n = 6 each group).

To corroborate the proportional differences between the mature B cell populations in mutant $\lambda 5^{-/-}$ and control mice we performed histological examination of spleen sections. Sections were stained for Thy-1⁺ T cells, IgM⁺ B cells and, to delineate the border between the marginal zone and the follicular area, MOMA-1⁺ metallophilic macrophages (see figures 4.4). In general, the size of follicles was smaller in $\lambda 5$ deficient animals than in control mice, corresponding to the reduced number of B cells. Especially the follicular area was diminished, in accordance with the lower FOB numbers, whereas the rim of marginal zone B cells was broadened reflecting the proportional increase of MZBs. Interestingly, we observed an elevated number of (bright IgM⁺) plasmablasts outside the follicles splenic sections of $\lambda 5$ deficient mice without prior immunization of the mice (see figure 4.4 B/D).

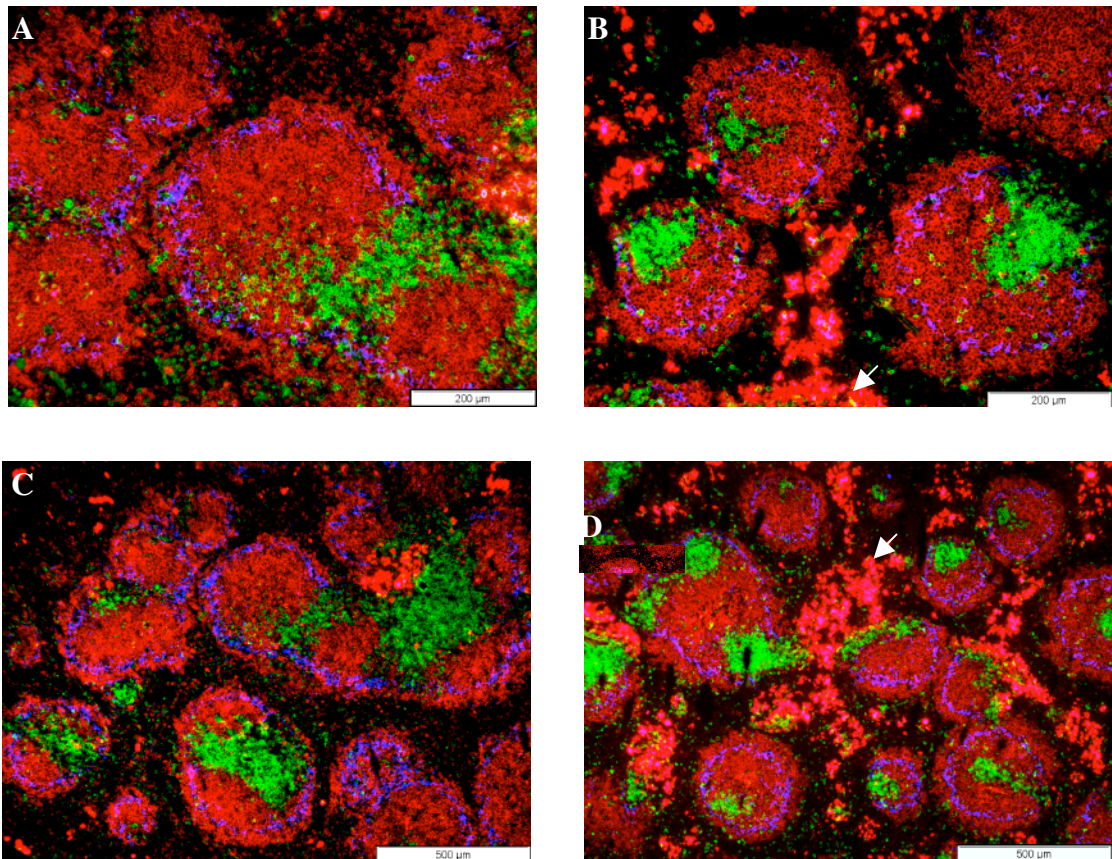


Figure 4.4: Representative spleen section of wild type and $\lambda 5^{-/-}$ mice. Sections were stained with anti-Thy1.1 (green), anti-IgM (red) and anti-MOMA-1 (blue). Arrows indicate plasma cells.

Turnover of mature peripheral B cells in $\lambda 5$ deficient mice

To assess the turnover of mature B cell populations in $\lambda 5$ deficient and control animals, mice were injected i.p. with the thymidine analogon BrdU and thereafter fed with drinking water containing BrdU for 11 days. BrdU incorporation into the DNA of splenic and peritoneal B cell populations was determined at day 4 and 11 during BrdU feeding and day 10 and 28 of the chase period (n = 3 each group).

Transitional B cells in wild type mice showed, in agreement with previously published data (Rolink et al., 1998), fast BrdU labeling which rapidly disappeared in the chase period indicating a high turnover of the cells (see figure 4.5 A). The lag in labeling of the T2/3 population compared to the T1 cells reflects the developmental chronology. Analysis of the BrdU labeling in the $\lambda 5^{-/-}$ mice of transitional populations was omitted due to the low numbers of these cells.

BrdU labeling of the FOB cell population occurred at a rate of about 1% per day in WT mice (see figure 4.5 B). In contrast, the labeling rate of FOB cells in $\lambda 5^{-/-}$ mice was only 0.5% per day, suggesting that FOB have a slower turnover in the mutant mice. The slower labeling kinetic was probably due to the largely diminished number of newly formed BrdU⁺ B cells entering the pool of FOB cells.

Analysis of the MZB cell compartment in wild type mice showed a labeling kinetic of about 6% per day (see figure 4.5 C), probably as a result of influx of BrdU⁺ cells as well as proliferation in the MZB population. In comparison to the wild type, only 2% of the MZB cells in the $\lambda 5$ deficient animals were labeled per day, probably due to a lowered influx of new BrdU⁺ cells into the compartment thereby reducing competition and consequently turnover of the cells.

Labeling kinetics of the self-replenishing peritoneal B1a population showed basically no differences between mutant and wild type mice with a labeling of about 4% of the cells per day and a slower decay of BrdU⁺ cells during the chase period (see figure 4.5 D). Analysis of the CD19⁺/CD5^{-low} population, comprising the conventional B2 B as well as B1b cells, showed very similar labeling kinetics in $\lambda 5$ deficient and wild type mice (see figure 4.5 E). The cells were labeled at about 1.5% per day, a large fraction of them being B1b cells in the $\lambda 5^{-/-}$ mice.

Comparing the labeling kinetics in $\lambda 5$ deficient mice and wild type mice it was evident that splenic B cell populations differed in their turnover of cells, being slower in the mutant mice, probably due to a reduced influx of newly formed B cells. Instead,

peritoneal cells of wild type and $\lambda 5^{-/-}$ origin showed very similar labeling kinetics and turnover.

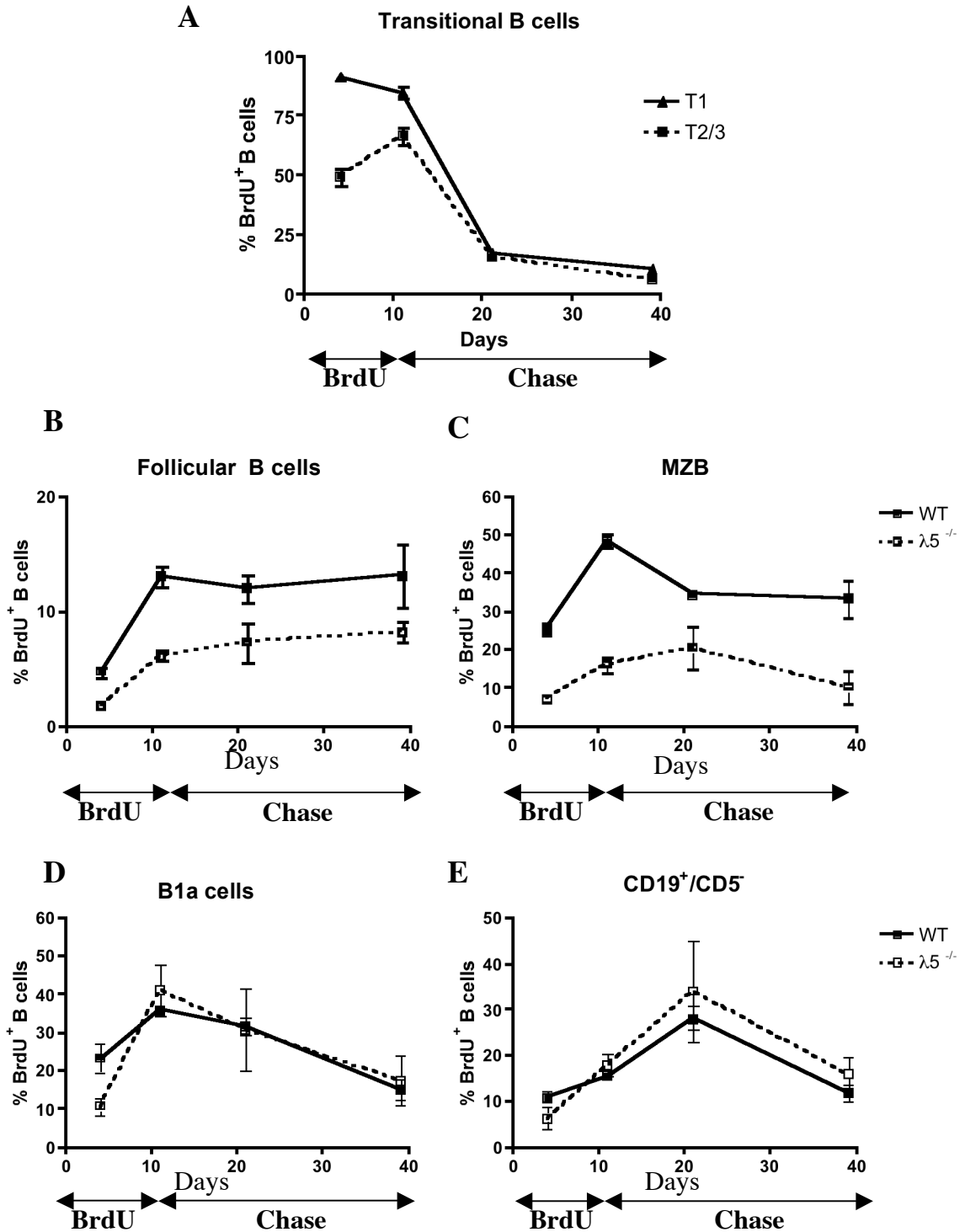


Figure 4.5: BrdU labeling of splenic and peritoneal B cell populations in wild type and $\lambda 5$ deficient mice. Cells were stained with phenotypic markers to distinguish A) transitional T1 and T2/3, B) follicular B cells, C) marginal zone B cells, D) peritoneal B1a cells and E) peritoneal CD5⁻ B cells i.e. B2 and B1b cells. BrdU⁺ cells were detected with an intracellular anti-BrdU staining. Represented are the means of the results of 3 wild type and $\lambda 5^{-/-}$ mice per timepoint. Bars represent the standard deviation.

Humoral primary and secondary immune responses in $\lambda 5$ deficient mice

To investigate the influence of $\lambda 5$ deficiency on primary and especially secondary immune responses, mice were immunized with the TD NIP-ovalbumin (s.c. with Freund's adjuvant) or the TI type 2 antigen NIP conjugated to Ficoll (i.v. in PBS). Nearly 4 months after the first immunization the TD immunized mice received a second dose of NIP-ovalbumin.

Hapten-specific antibodies of various isotypes and total IgM and IgG levels were determined in the sera of the mice at different timepoints before immunization, during the course of the primary immune response, after 2 month and 1 week after the secondary immunization.

Analysis of the total IgM levels during the TD response showed an approximately twofold higher IgM concentration in the $\lambda 5^{-/-}$ mice than in wild type controls, irrespective of the timepoint analyzed (see figure 4.6 A). The higher levels of IgM in $\lambda 5$ deficient animals might have originated from the increased number of plasma cells seen in the histological sections of non-immunized mice (see figure 4.4). In contrast, total IgG levels were lower in $\lambda 5$ deficient animals, most likely as a result of the decreased number of FOB cells (see figure 4.6 B). The amount of NIP specific IgM antibodies after TD immunization were higher in $\lambda 5$ deficient animals than in the controls but this probably rather reflected the increased steady state IgM levels in $\lambda 5$ mutant mice than an elicited anti-NIP IgM response (see figure 4.6 C). Levels of NIP specific IgG instead were, after TD immunization, two- to threefold lower in the mutant mice (see figure 4.6 D), most probably due to the reduction of FOB cell numbers. This was presumably also the reason for the lower anti-NIP IgG1 as well as IgG2b and IgG2a TD response in $\lambda 5$ deficient mice (see figure 4.6 E/F and 4.7 A). Upon TD immunization we could hardly detect any IgG3 response in control or in mutant animals (see figure 4.7 B). Reduced levels of the specific IgG responses (see figure 4.6 D/E/F and 4.7 A, between 2-5 fold reduction of the primary response) correlate with the about 5 fold reduction in number of B cells (see figure 4.3). Thus, the data indicate that $\lambda 5$ deficient animals are able to make a TD primary as well as secondary immune response, although at reduced levels compared to wild type animals.

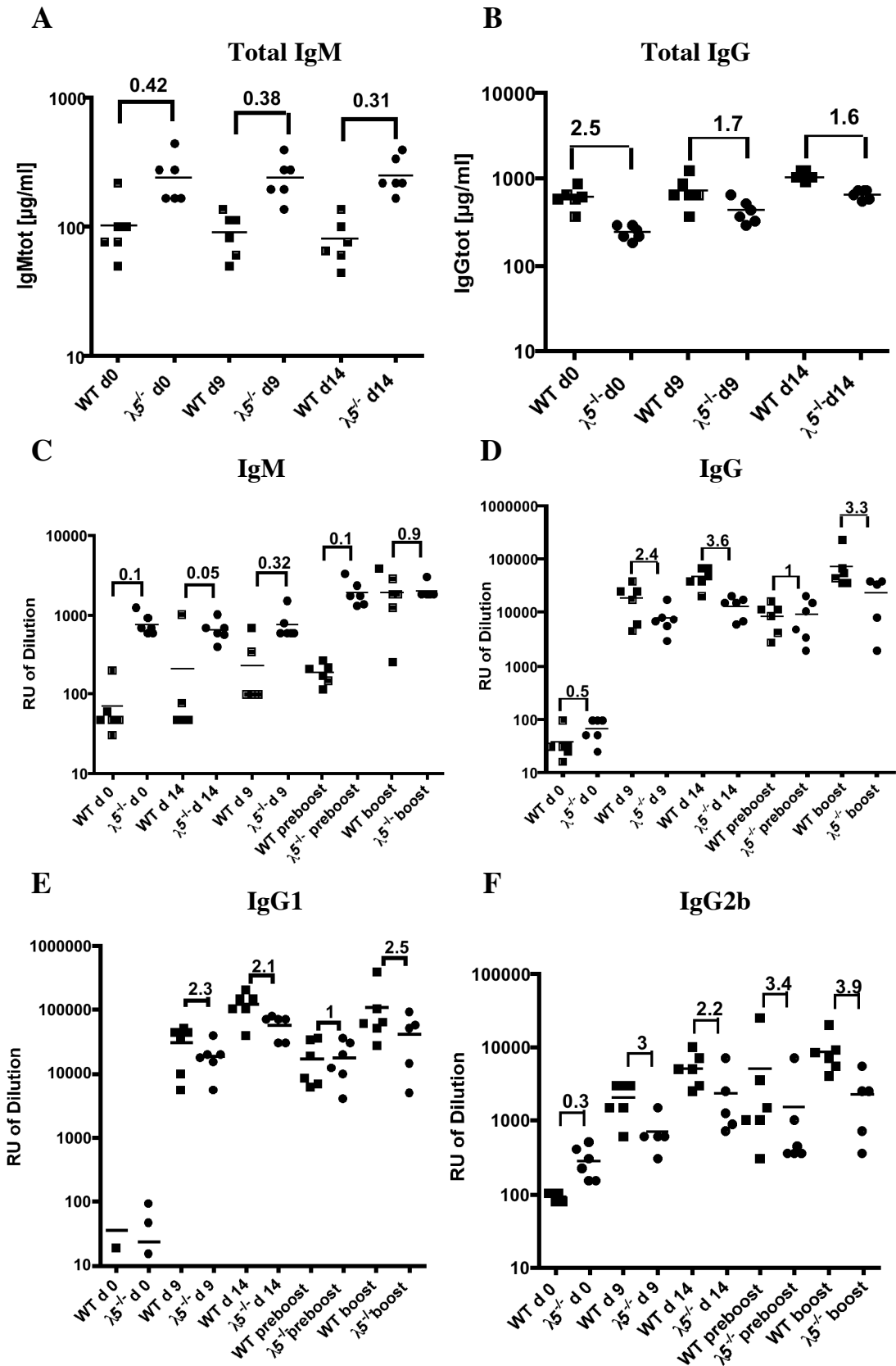


Figure 4.6: Total IgM (A) and IgG (B) concentrations in the sera of TD immunized wild type and $\lambda 5^{-/-}$ mice. NIP specific IgM (C), IgG (D), IgG1 (E) and IgG2b (F) levels in the sera of TD immunized wild type and $\lambda 5^{-/-}$ mice. The measurements are given in relative units of dilution. Squares represent serum Ig concentrations of single wild type and circles of single $\lambda 5^{-/-}$ mice.

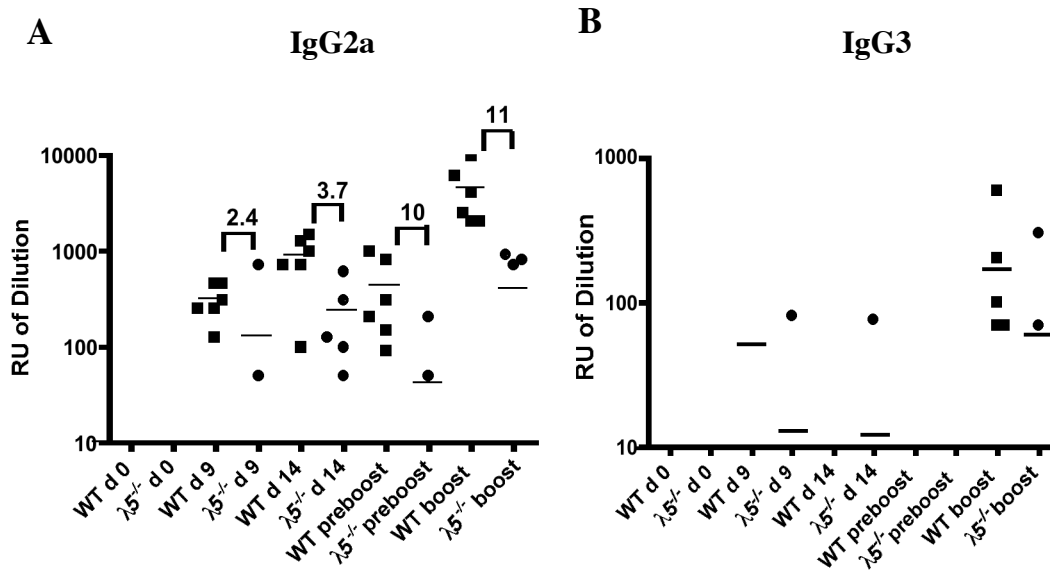


Figure 4.7: NIP specific IgG2a (A) and IgG3 (B) levels in the sera of TD immunized wild type and $\lambda 5^{-/-}$ mice. The measurements are given in relative units of dilution. Squares represent serum Ig levels of single wild type and circles of single $\lambda 5^{-/-}$ mice.

To further characterize the TD immune response in $\lambda 5$ deficient mice germinal center formation was examined in mutant and wild type mice after the secondary immunization. Germinal centers are typical structures formed in secondary lymphoid organs during the course of a TD immune response. They are the place where affinity maturation, class switching and memory cell formation takes place. After the secondary TD immunization the animals were sacrificed, spleen sections were taken and stained for Thy-1⁺ T cells, IgM⁺ B cells and with peanut agglutinin for the presence of germinal centers (see figure 4.8). The sections clearly showed germinal center formation in $\lambda 5$ deficient animals but in reduced number and size, corresponding to the data of the humoral TD immune response.

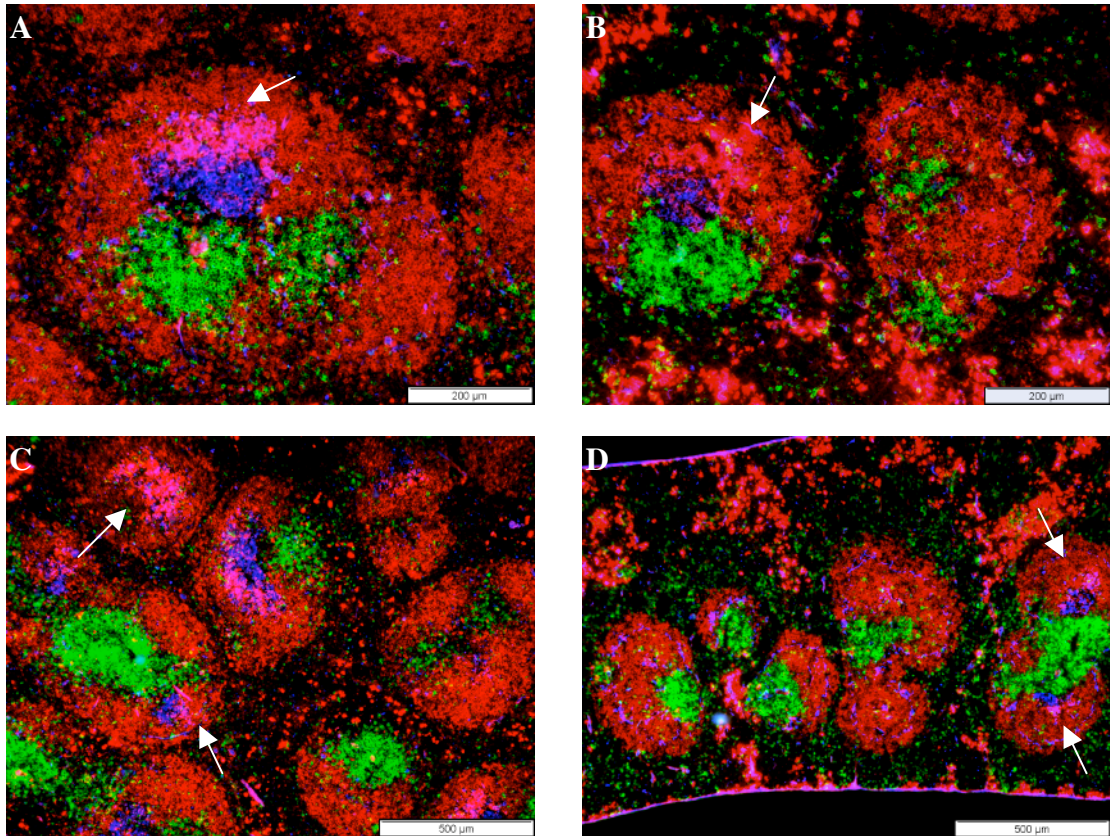


Figure 4.8: Representative spleen sections of wild type and $\lambda 5^{-/-}$ NIP immunized mice. Sections were stained with anti-Thy1.1 (green), anti-IgM (red) and with peanut agglutinin for germinal center cells (blue). IgM and peanut agglutinin double positive cells are represented in pink.

$\lambda 5$ deficient mice were also characterized regarding their ability to respond to a TI type 2 antigen. Total IgM and IgG levels were measured during the TI response, again showing higher total IgM levels and lower total IgG levels in the mutant animals in comparison to control mice (see figure 4.9 A/B). In terms of NIP specific IgM responses, there was a 2-3 fold reduction in the $\lambda 5$ deficient mice compared to the controls (see figure 4.9 C). Furthermore, the anti-NIP IgG, IgG1 and IgG3 (see figure 4.9 D/E/F) responses were decreased in the mutant mice. B1 B and MZB cells are thought to be a major source of IgM (Martin et al., 2001) and MZB cells were shown to readily secrete IgG3 (Oliver et al., 1997). But even though the B1a and MZB cells were present in normal numbers in the $\lambda 5^{-/-}$ mice, the animals showed a reduced TI response. Possibly the fact that the mice were immunized with soluble NIP-Ficoll skewed the TI type 2 response into other compartments like the FOB (van den Eertwegh et al., 1992), since MZB cells are known to respond to particulate antigens (Martin et al., 2001).

Altogether, these data indicate that $\lambda 5$ deficient animals can mount TI as well TD immune responses including secondary responses, albeit at somewhat reduced levels most probably due to the diminished numbers of follicular B and/or B1b cells.

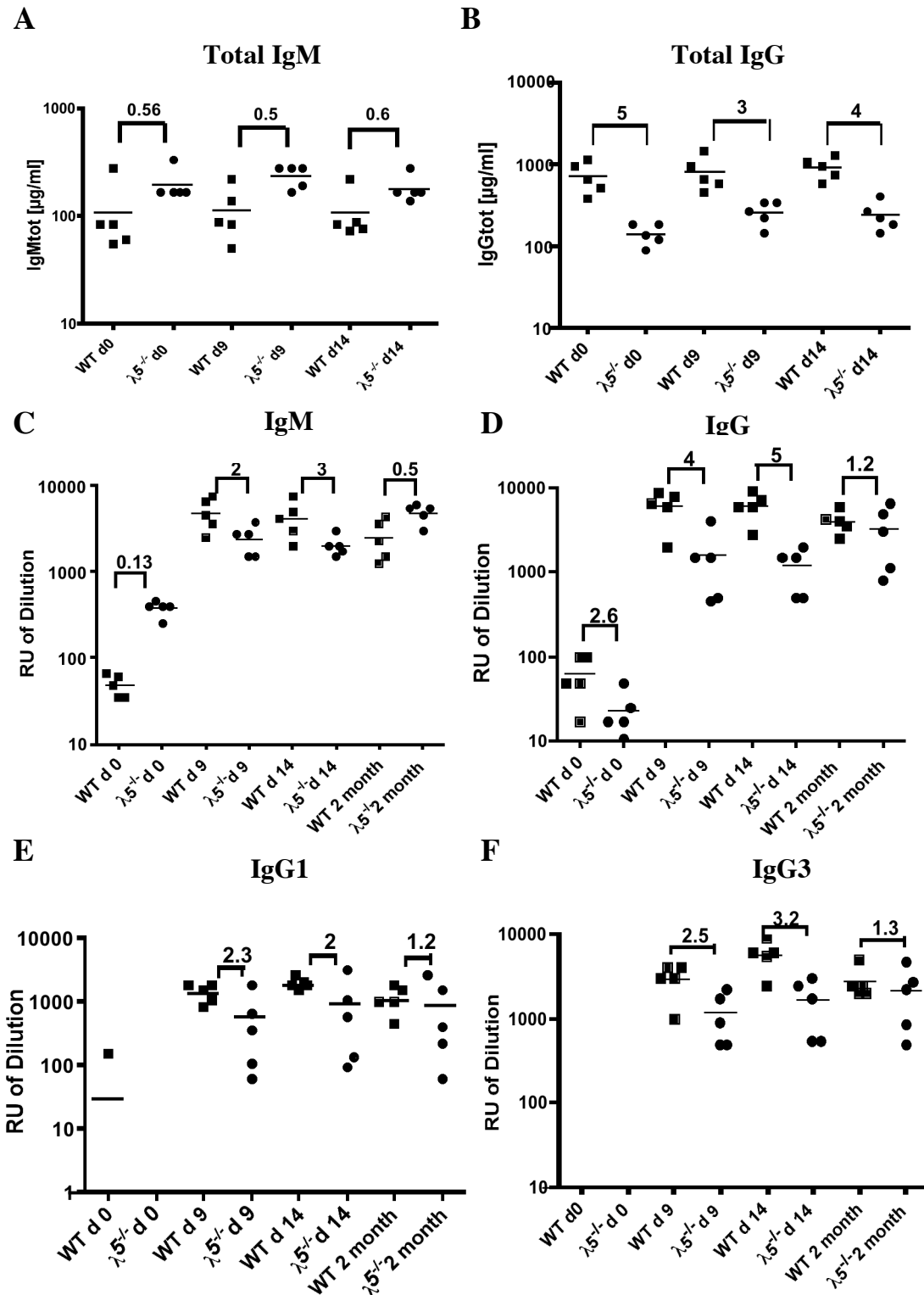


Figure 4.9: Total IgM (A) and IgG (B) and NIP specific IgM (C), IgG (D), IgG1 (E) and IgG3 (F) levels in the sera of TI immunized wild type and $\lambda 5^{-/-}$ mice. Squares represent serum Ig levels of single wild type and circles of single $\lambda 5^{-/-}$ mice. The measurements in C-F are given in relative units of dilution.

Wild type and $\lambda 5^{-/-}$ mixed bone marrow chimeras

To assess the ability of $\lambda 5$ deficient cells to reconstitute in competition with wild type cells, bone marrow cells of wild type (Ly5.1⁺) and $\lambda 5^{-/-}$ (Ly5.2⁺) origin were transferred into sublethally irradiated RAG2^{-/-} (450 rad) hosts. As control, mice were also reconstituted with either wild type or $\lambda 5^{-/-}$ cells alone. Four and a half weeks later the mice were analyzed for reconstitution of T and B cell compartments and the relative contribution of wild type and $\lambda 5^{-/-}$ cells. Unluckily, at that timepoint the mice started to become sick, probably due to a lack of regulatory T cells (A. Rolink personal communication), so that the data should be considered preliminary until experiments will be repeated with newborn mice as hosts.

Figure 4.10 A and B show the flow cytometric analysis of the T cell compartment in thymus and spleen. Phenotypical analysis of the organs showed normal T cell compartments in all three groups indicating successful reconstitution. Around 3 quarters of the T cells in the spleens of the mixed bone marrow chimeras were of $\lambda 5$ deficient origin (data not shown). This ratio probably reflected the relative contribution to reconstitution of $\lambda 5^{-/-}$ cells to compartments not affected by $\lambda 5$ deficiency. Analysis of splenic B cells in the wild type and the mixed bone marrow chimeras showed reconstitution also of the B cell compartments. A slight proportional enlargement of the MZB cells compartment compared to normal mice was detected (see figure 4.10 A/B). Mice, which had received bone marrow only of $\lambda 5$ deficient mice, also showed reconstitution of splenic B cell populations, albeit at largely reduced levels. A large proportion of the cells showed a MZB like phenotype although with a slightly reduced CD21 expression (see figure 4.10 C).

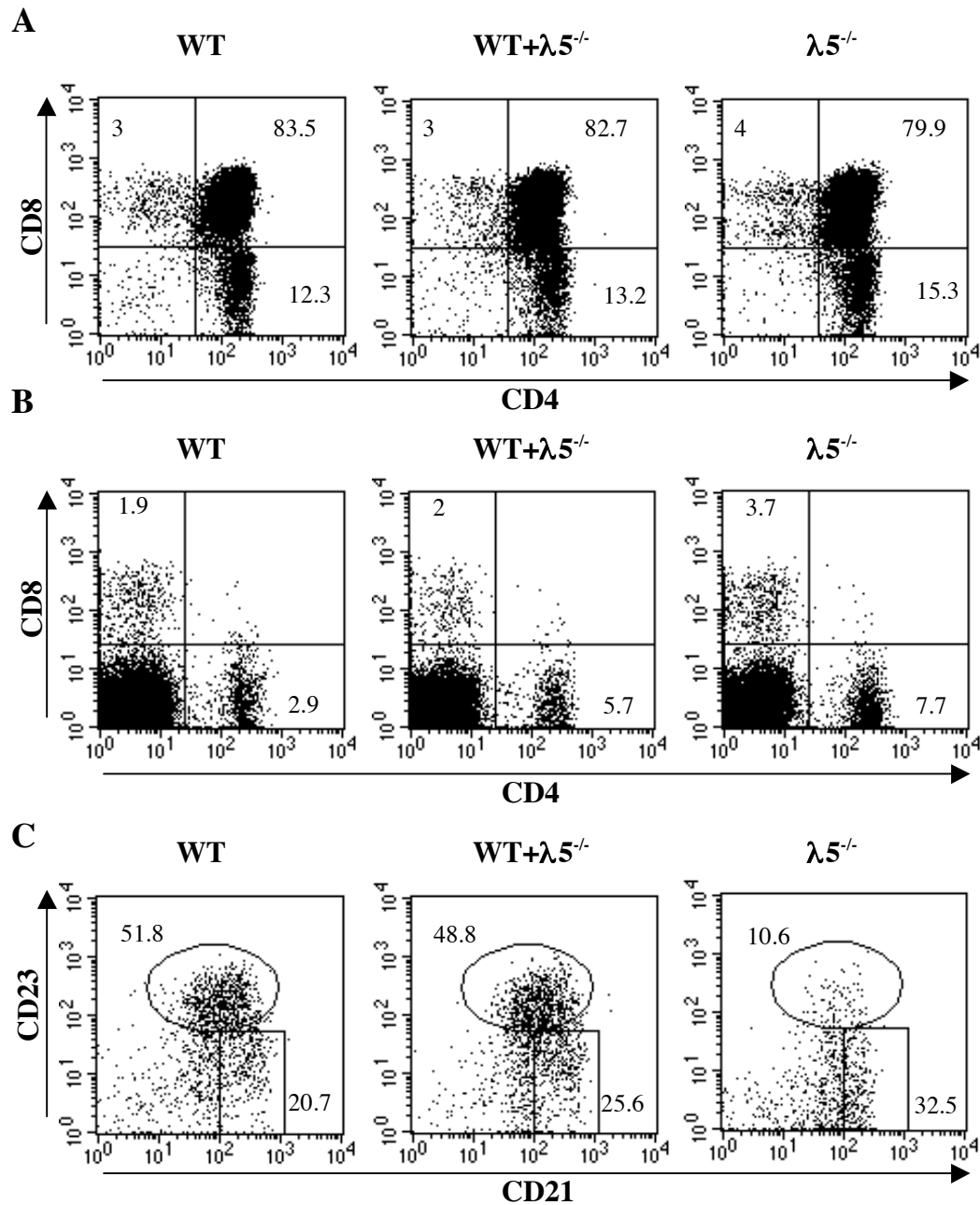


Figure 4.10: Representative FACS profiles of thymus (A) and spleen (B+C) of irradiated RAG-2^{-/-} mice reconstituted with WT, $\lambda 5^{-/-}$ or a 1:1 mixture of bone marrow. All profiles are gated on the lymphoid cells. C is additionally gated on CD19⁺ cells. Representatives profiles of the analysis 4-5 mice each group.

Analysis of the transferred cells concerning their origin showed that in the mixed bone marrow chimeras Ly5.1⁺ wild type cells mostly were CD21⁺/CD23⁺ i.e. FOB or T2/T3 cells. Around 20% of the CD19⁺/Ly5.1⁺ cells showed a MZB phenotype (see figure 4.11 B). The Ly5.2⁺ $\lambda 5$ deficient cells instead adopted mostly a MZB cell like phenotype. Closer characterization of the cells showed that they were large in size, CD9^{+/low} like typical MZBs but slightly lower in IgM and CD21 expression (data not

shown). The overall contribution of $\lambda 5$ deficient B cells to the splenic B cell compartment was about 10-12% which has to be seen in the context of the relative BM contributions of wild type and $\lambda 5^{-/-}$ being 1:3, based on analysis of the peripheral T cell compartment (see above).

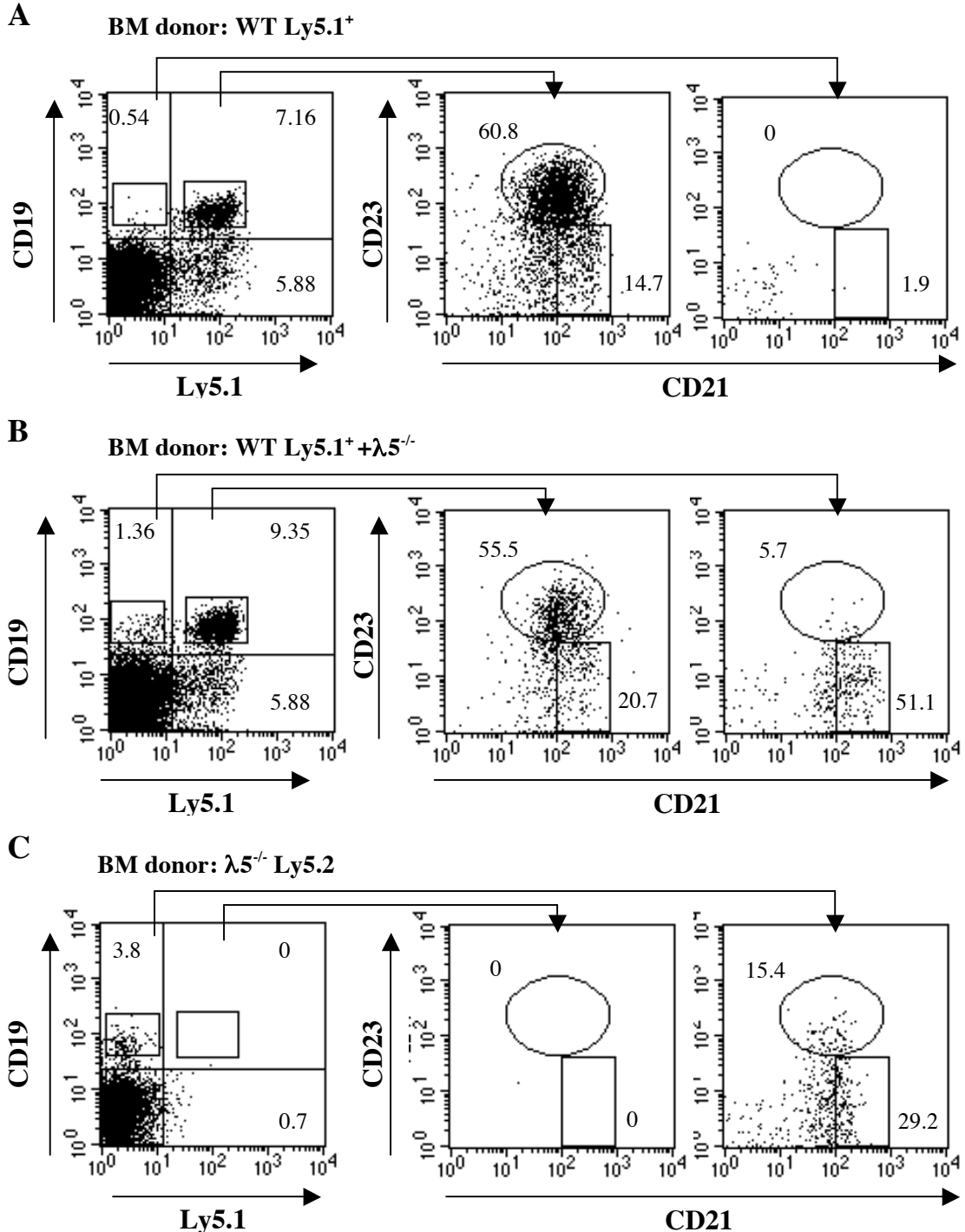


Figure 4.11: Representative FACS profiles of spleen (B/C) of mice reconstituted with WT (A), $\lambda 5^{-/-}$ (B) or a 1:1 mixture (C) of bone marrow. Profiles are gated on the lymphoid FSC/SSC gate. Representatives of the analysis 4-5 mice each group.

Additionally, spleens of mixed bone marrow chimeras were examined histologically to characterize the transferred cells also with regard to their splenic localization. The sections were stained for Thy1.1⁺ T cells, IgM⁺ B cells and Ly5.1⁺ or Ly5.2⁺ (see figure 4.12 and 4.13 A). To better define the MZB cells, the sections were stained with anti-IgM, anti-Ly5.1 or anti-Ly5.2 and additionally for MOMA-1⁺ cells (see figure 4.13 B/C). The ratio of Ly5.1⁺ to Ly5.2⁺ T cells corresponded to the 1:3 ratio of wild type to $\lambda 5$ deficient T cells detected by flow cytometry (see figure 4.12 and 4.13 A). The predominance of Ly5.1⁺/IgM⁺ cells in the follicular region was also obvious (see figure 4.12 and 4.13). Enrichment of Ly5.2⁺/Ly5.1⁻ and IgM⁺ cells in the marginal zone instead was not so pronounced but still detectable (see figure 4.12+ and 4.13, indicated with arrows). Splenic architecture, in particular the follicular structures, were altered in these mice so that often it was difficult to define clear marginal zones. However, the partial localization of $\lambda 5$ deficient Ly5.2⁺ cells in the outer rim of follicles is in accordance with the MZB like phenotype of these cells determined by flow cytometric analysis.

The data therefore suggest that $\lambda 5$ deficient cells can participate to some limited extent in the reconstitution of the mature B cell pool being channelled mostly into the MZB compartment.

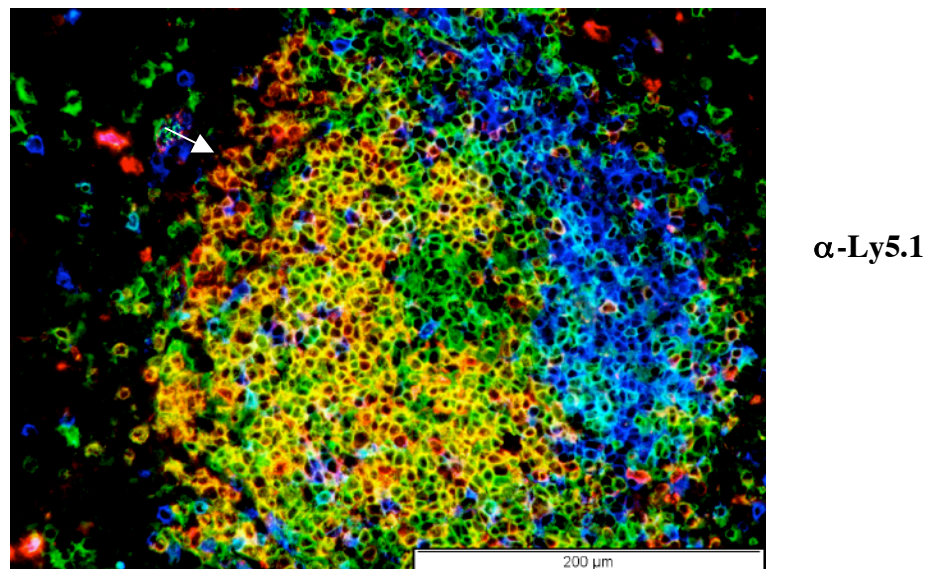


Figure 4.12: Localization of cells of wild type and $\lambda 5^{-/-}$ origin in spleen sections of mixed bone marrow chimeras. Sections were stained with anti-Thy1.1 (blue), anti-IgM (red) and anti-Ly5.1. IgM and Ly5.1 double positive cells are represented in yellow. Thy1.1 and Ly5.1 double positive cells are represented in cyan. Arrows indicate the presence of Ly5.1⁺/IgM⁺ cells in the marginal zone.

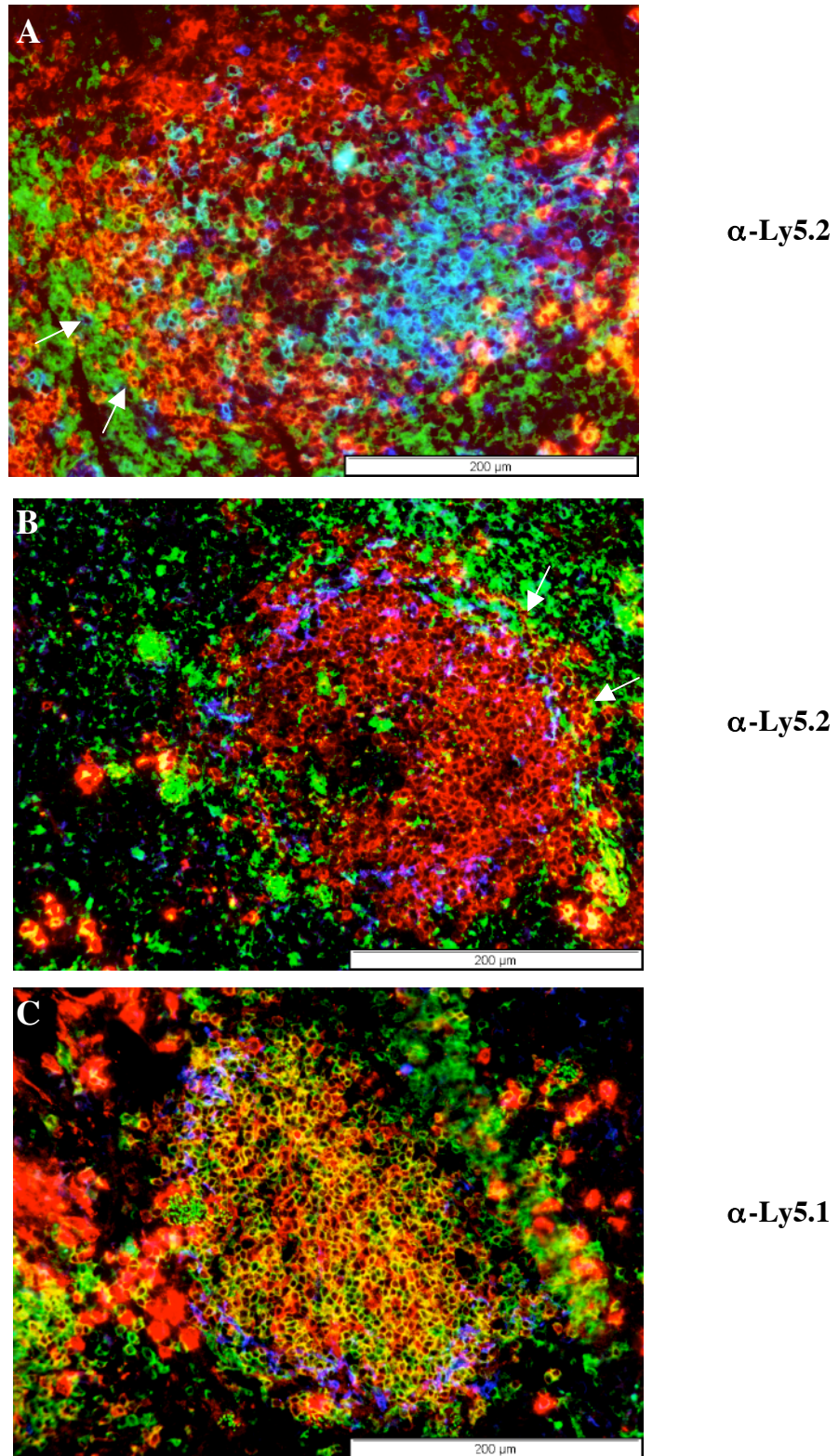


Figure 4.13: Localization of cells of wild type and $\lambda 5^{-/-}$ origin in spleen sections of mixed bone marrow chimeras. Sections were stained with anti-Thy1.1 (blue), anti-IgM (red) and anti-Ly5.2 (A). Sections were also stained with anti-MOMA-1 (blue), anti-IgM (red) and anti-Ly5.2 (B) or anti-Ly5.1 (C). Thy1.1 and Ly5.2 double positive cells are represented in cyan (A). IgM and Ly5.1 (B) or Ly5.2 (A,C) double positive cells are represented in yellow. Arrows indicate the presence of Ly5.2⁺/IgM⁺ cells in the marginal zone.

Discussion

At the time Kitamura et al. targeted the $\lambda 5$ locus, the prediction would have been that B cells would be completely absent like in the μ MT mice. However, analysis of the mutant mice revealed that the block in B cell development is not absolute and that mature B cells are found in the periphery. It was also shown that $\lambda 5$ deficient B cells still do allelically exclude at their Ig locus (Kitamura et al., 1992), although there is some debate about this subject (Loffert et al., 1996). Allelic exclusion at the Ig locus was also shown for a double knockout mouse which lacked both of the structurally very similar and partially redundant VpreB proteins (Mundt et al., 2001), VpreB1 and VpreB2 (Martensson et al., 1999). Finally, also the triple deficient mice lacking all components of the SL, showed the same phenotype (Shimizu et al., 2002). These results suggested that even though B cell generation is impaired in a SL deficient situation there seems to be a preBCR-independent mechanism allowing the maturation but not proliferative expansion of a small number of cells. This rescue mechanism is dependent on the membrane insertion of the μ H since in μ MT mice the developmental block is complete and in B cells heterozygous for the μ MT mutation allelic exclusion is lost. Recently two reports showed that a certain transgenic μ H can be expressed on the cell surface of preB cells in the absence of SL components and thereby promote IL-7 dependent growth and differentiation of preB cells (Galler et al., 2004; Schuh et al., 2003) as well as the downregulation of TdT and the RAG proteins. Additionally, endogenous μ H expression on CD19⁺ (SL⁻) BM cells of triple knockout mice could be detected showing that SL-independent μ H chain surface expression is also possible in a non-transgenic situation (Galler et al., 2004.) This could possibly represent the mechanism allowing the development of the B cells seen in the SL mutant mice. Generation of B cells would then depend on the frequency of μ H chains that can be expressed on the surface without associated SL. The mechanism by which a μ H can be expressed on the cell surface without associating with the SL remains completely unclear.

Due to the developmental block early in B cell development, the peritoneum of $\lambda 5$ deficient animals contained almost no conventional B2 B cells. In contrast, the B1a cells were present in the peritoneal cavity in normal numbers in adult mutant mice. Also the turnover of B1a cells, judged by BrdU labeling kinetics, was very similar in mutant and wild type animals. Experimental data suggest that B1 B cells are derived

from different progenitors than conventional B2 cells (reviewed in (Herzenberg, 2000)). They are formed early during ontogeny prior to weaning and persist thereafter as a self-replenishing population. Adult bone marrow fails to generate significant numbers of B1 cells. Several mutations, like e.g. IL7 deficiency, leading to a block in early B cell development in adult mice compromise formation of B2 B cells but still allow development of a normal B1 compartment (Carvalho et al., 2001). Also the V_H repertoire in B1 cells differs from the adult B2 V_H repertoire and the joining regions show less N-region insertion in B1 B cells. Wasserman and coworkers published data in which they showed that in fetal pre-B cells proliferation was rather inhibited by IgH transgenes efficiently forming a preBCR whereas expression of a fetal $VH11$ IgH transgene associating only incompletely with the SL, promoted pre-B cell development in fetal stages but not in adult stages (Wasserman et al., 1998). This would suggest that B1 B cell generation is either less or not at all preBCR dependent explaining why B1 B cells develop nearly normally in $\lambda 5$ deficient animals as well as in the triple knockout mice lacking all the SL components. This PreBCR-independent μH expression could be part of a mechanism that favors expression of a pure germline-encoded primordial repertoire biased toward certain specificities that bind for e.g. to common non-protein antigens as is seen in the B1 compartment. On the other hand, there is a time lag in the development of the B1 compartment in SL mutants arguing nonetheless for a role of the SL in B1 development. Additionally, the *in vitro* differentiation and proliferation potential of *ex vivo* isolated fetal liver preB-I is comparable to that of mature bone marrow preB-I (Rolink et al., 2000). $\lambda 5$ deficiency leads to strongly reduced survival, proliferation as well as differentiation in this *in vitro* system irrespectively whether the preB-I cells are of fetal or adult origin. This would implicate the preBCR also in fetal B cell development. The fact that the B1 compartment is nearly of normal size in $\lambda 5$ deficient animals would then rather be due to the self-replenishing capacity of B1 cells filling up their compartment by proliferation of a few initially generated cells.

B1 B cells can be further differentiated into $CD5^+$ B1a cells and $CD5^{low/-}$ B1b cells (Herzenberg, 2000). B1a and B1b are very similar nonetheless there is evidence accumulating that these cells constitute different lineages. B1b cells have been shown to be reconstituted to some extent by adult bone marrow whereas B1a are not. Additionally, adoptive transfer of B1a cells mainly reconstitutes the B1a compartment

whereas transferred B1b cells mostly remain B1b cells. Analysis of the peritoneal B1 compartment in $\lambda 5$ deficient mice showed a twofold reduction of B1b cells. It would be conceivable that in adult mice there is still some bone marrow influx into the B1b population, which is very much reduced in $\lambda 5$ deficient mice resulting in a smaller B1b compartment. Alternatively, the B1b cells are more dependent on the preBCR during their development than B1a.

Analysis of the mature B cell populations in the spleen revealed a large reduction of FOB cells as a result of the impaired generation of B cells in $\lambda 5^{-/-}$ mice. The turnover of cells was slower, probably due to the diminished influx of newly formed B cells. In contrast, there was a proportional, but not absolute, increase in the MZB compartment. The turnover of these cells was reduced suggesting that also the MZB compartment was affected by the diminished generation of B cells in $\lambda 5$ deficient mice. Origin and selection of MZB cells is still a matter of an ongoing debate (Lopes-Carvalho and Kearney, 2004; Saito et al., 2003). Some authors suggest that MZB are derived from the transitional compartment (Saito et al., 2003) others that they originate from FOB and/or memory B cells (Lopes-Carvalho and Kearney, 2004; Vinuesa et al., 2003). Interestingly, in B lymphopenic mice, for e.g. in animals in which B cell development is restricted to the perinatal period, the MZB compartment is often less or not affected at all (Carvalho et al., 2001; Hao and Rajewsky, 2001). This could be a result of the abundance of resources like growth factors, ligands for costimulatory and adhesion molecules etc. driving the cells into the “effector” branch of the B-cell system. In mice transgenic for the B cell survival factor BAFF (B- cell activating factor), for example, there is an particularly enlarged MZB compartment (Batten et al., 2000). Antigen, either self or environmental, has also been implicated in MZB enrichment (Julien et al., 2002). Enhanced antigenic selection could therefore be an alternative/additional mechanism leading to preferential selection of B cells into the MZB compartment. Reduced intercellular competition for antigens in B lymphopenic mice or lack of housekeeping Igs masking antigens could lead to enhanced antigen availability. Thus, experimental data showed that administration of polyclonal IgM to mice deficient in serum IgM reversed an observed MZB cell expansion in these mutant mice (Baker and Ehrenstein, 2002). Mutations affecting BCR-signaling properties are also known to influence the size of the MZB and FOB compartment differently (Martin and Kearney, 2002) substantiating that the selection

mechanisms are at least partially based on received BCR signals. Abundance of resources and/or antigens could therefore be an explanation why $\lambda 5$ deficient mice generate a proportionally enlarged MZB compartment.

On the other hand, an intrinsic propensity of $\lambda 5$ deficient cells to develop into MZB was observed in the analyzed mixed bone marrow chimeras. This disposition was also observed when wild type cells were cotransferred with the $\lambda 5^{-/-}$ cells, making abundance of antigens and resources less probable as sole driving force since both cell types encountered the same conditions. Assuming that the mature B cells were generated by the proposed rescue mechanism expressing SL independent μ H chains in the preB cell stage (see above) it could be conceivable that these μ H chains are part of a repertoire channelling the cells into the MZB compartment. The predisposition to develop into MZB cells could be the result of the specificities of the SL independent μ H chains, recognizing for e.g. common self- and foreign antigens. This would be in accordance with the enrichment for MZB cells found in transgenic mice expressing self-reactive heavy chains (Martin and Kearney, 2000).

Interestingly, although there seem to be forces driving the B cells into the MZB compartment in $\lambda 5^{-/-}$ and other lymphopenic mice, the absolute number of MZB cells is usually not increased. Also IL-7 transgenic mice, showing an enhanced generation of B cells, have normal numbers of MZB cells (Ceredig et al., 2003). This argues for a defined size of this compartment. It has been shown that the retention of MZB cells in the marginal zone is dependent on the presence of other cell types like the marginal zone macrophages (Karlsson et al., 2003). A direct interaction between the MZB cells and marginal zone macrophages was shown and its interruption led to relocation of the MZB cells. Therefore it would be conceivable that the maintenance of a certain number of MZB cells is defined by the number of interacting cells, like e.g. marginal zone macrophages. The fact that BAFF transgenic mice nonetheless have more MZB cells (Batten et al., 2000), could mean that BAFF not only acts on B cells but also on other cells, enlarging thereby the “compartment size” of MZB. Alternatively, BAFF could participate in the mechanisms establishing the “compartment size” (Lesley et al., 2004; Thien et al., 2004).

MZB cells are considered as a first line of defense joining in with the B1 B cells against bacterial and some viral pathogens thereby bridging the time gap between the innate and the adaptive immune response. The enrichment of specificities to common

non-protein antigens (not easily altered by organisms) in the MZB would be in accordance with the current view of MZB cells. In B lymphopenic mice, like the $\lambda 5^{-/-}$ mice, there is a tendency to maintain this first line of defense. The mechanisms by which this is achieved are not yet clear. It is not known if this is a result of enhanced antigenic selection or abundance of resources. In the case of SL deficient mice, inherent properties of the preBCR independent rescue mechanism could also be the reason. Finally, also a combination of the different mechanism could result in the formation of a fairly normal MZB and B1 compartment.

The experimental data, shown here, demonstrate that the limited number of B cells generated in $\lambda 5$ deficient mice are functional in terms of TI and TD immune responses including the secondary immune response. Detailed analysis shows that they are predominantly located in the B1 and MZB compartment. BrdU labeling kinetics reveal that the turnover of the splenic B cell populations, FOB as well as MZB, is reduced two- to threefold demonstrating that the decreased generation of B cells also influences the adult MZB compartment in $\lambda 5^{-/-}$ mice. Interestingly, $\lambda 5^{-/-}$ adult bone marrow cells seem to have a propensity to develop into MZB cells. Further experiments would have to be done analyzing for e.g. the μ H repertoire in wild type and $\lambda 5^{-/-}$ MZB cells. Furthermore, it would be informative to test the expressed μ H chains of MZB cells, developed in $\lambda 5^{-/-}$ mice, for SL independent expression to unravel the mechanisms behind the channeling of B cells into the “effector” branch of the B cell compartment in $\lambda 5$ deficient mice.

References

- Alt, F. W., Yancopoulos, G. D., Blackwell, T. K., Wood, C., Thomas, E., Boss, M., Coffman, R., Rosenberg, N., Tonegawa, S., and Baltimore, D. (1984). Ordered rearrangement of immunoglobulin heavy chain variable region segments. *Embo J* *3*, 1209-1219.
- Baker, N., and Ehrenstein, M. R. (2002). Cutting edge: selection of B lymphocyte subsets is regulated by natural IgM. *J Immunol* *169*, 6686-6690.
- Batten, M., Groom, J., Cachero, T. G., Qian, F., Schneider, P., Tschopp, J., Browning, J. L., and Mackay, F. (2000). BAFF mediates survival of peripheral immature B lymphocytes. *J Exp Med* *192*, 1453-1466.
- Carvalho, T. L., Mota-Santos, T., Cumano, A., Demengeot, J., and Vieira, P. (2001). Arrested B lymphopoiesis and persistence of activated B cells in adult interleukin 7(-/-) mice. *J Exp Med* *194*, 1141-1150.
- Ceredig, R., Bosco, N., Maye, P. N., Andersson, J., and Rolink, A. (2003). In interleukin-7-transgenic mice, increasing B lymphopoiesis increases follicular but not marginal zone B cell numbers. *Eur J Immunol* *33*, 2567-2576.
- Galler, G. R., Mundt, C., Parker, M., Pelanda, R., Martensson, I. L., and Winkler, T. H. (2004). Surface {micro} Heavy Chain Signals Down-Regulation of the V(D)J-Recombinase Machinery in the Absence of Surrogate Light Chain Components. *J Exp Med*.
- Hao, Z., and Rajewsky, K. (2001). Homeostasis of peripheral B cells in the absence of B cell influx from the bone marrow. *J Exp Med* *194*, 1151-1164.
- Herzenberg, L. A. (2000). B-1 cells: the lineage question revisited. *Immunol Rev* *175*, 9-22.
- Julien, S., Soulas, P., Garaud, J. C., Martin, T., and Pasquali, J. L. (2002). B cell positive selection by soluble self-antigen. *J Immunol* *169*, 4198-4204.
- Karlsson, M. C., Guinamard, R., Bolland, S., Sankala, M., Steinman, R. M., and Ravetch, J. V. (2003). Macrophages control the retention and trafficking of B lymphocytes in the splenic marginal zone. *J Exp Med* *198*, 333-340.
- Kitamura, D., Kudo, A., Schaal, S., Muller, W., Melchers, F., and Rajewsky, K. (1992). A critical role of lambda 5 protein in B cell development. *Cell* *69*, 823-831.
- Kitamura, D., Roes, J., Kuhn, R., and Rajewsky, K. (1991). A B cell-deficient mouse by targeted disruption of the membrane exon of the immunoglobulin mu chain gene. *Nature* *350*, 423-426.
- Lesley, R., Xu, Y., Kalled, S. L., Hess, D. M., Schwab, S. R., Shu, H. B., and Cyster, J. G. (2004). Reduced competitiveness of autoantigen-engaged B cells due to increased dependence on BAFF. *Immunity* *20*, 441-453.

- Loffert, D., Ehlich, A., Muller, W., and Rajewsky, K. (1996). Surrogate light chain expression is required to establish immunoglobulin heavy chain allelic exclusion during early B cell development. *Immunity* *4*, 133-144.
- Lopes-Carvalho, T., and Kearney, J. F. (2004). Development and selection of marginal zone B cells. *Immunol Rev* *197*, 192-205.
- Martensson, A., Argon, Y., Melchers, F., Dul, J. L., and Martensson, I. L. (1999). Partial block in B lymphocyte development at the transition into the pre-B cell receptor stage in Vpre-B1-deficient mice. *Int Immunol* *11*, 453-460.
- Martin, F., and Kearney, J. F. (2000). Positive selection from newly formed to marginal zone B cells depends on the rate of clonal production, CD19, and btk. *Immunity* *12*, 39-49.
- Martin, F., and Kearney, J. F. (2002). Marginal-zone B cells. *Nat Rev Immunol* *2*, 323-335.
- Martin, F., Oliver, A. M., and Kearney, J. F. (2001). Marginal zone and B1 B cells unite in the early response against T-independent blood-borne particulate antigens. *Immunity* *14*, 617-629.
- Mundt, C., Licence, S., Shimizu, T., Melchers, F., and Martensson, I. L. (2001). Loss of precursor B cell expansion but not allelic exclusion in VpreB1/VpreB2 double-deficient mice. *J Exp Med* *193*, 435-445.
- Nussenzweig, M. C., Shaw, A. C., Sinn, E., Danner, D. B., Holmes, K. L., Morse, H. C., 3rd, and Leder, P. (1987). Allelic exclusion in transgenic mice that express the membrane form of immunoglobulin mu. *Science* *236*, 816-819.
- Oliver, A. M., Martin, F., Gartland, G. L., Carter, R. H., and Kearney, J. F. (1997). Marginal zone B cells exhibit unique activation, proliferative and immunoglobulin secretory responses. *Eur J Immunol* *27*, 2366-2374.
- Rolink, A., Grawunder, U., Winkler, T. H., Karasuyama, H., and Melchers, F. (1994). IL-2 receptor alpha chain (CD25, TAC) expression defines a crucial stage in pre-B cell development. *Int Immunol* *6*, 1257-1264.
- Rolink, A. G., Andersson, J., and Melchers, F. (1998). Characterization of immature B cells by a novel monoclonal antibody, by turnover and by mitogen reactivity. *Eur J Immunol* *28*, 3738-3748.
- Rolink, A. G., Andersson, J., and Melchers, F. (2004). Molecular mechanisms guiding late stages of B-cell development. *Immunol Rev* *197*, 41-50.
- Rolink, A. G., Winkler, T., Melchers, F., and Andersson, J. (2000). Precursor B cell receptor-dependent B cell proliferation and differentiation does not require the bone marrow or fetal liver environment. *J Exp Med* *191*, 23-32.
- Saito, T., Chiba, S., Ichikawa, M., Kunisato, A., Asai, T., Shimizu, K., Yamaguchi, T., Yamamoto, G., Seo, S., Kumano, K., *et al.* (2003). Notch2 is preferentially

expressed in mature B cells and indispensable for marginal zone B lineage development. *Immunity* 18, 675-685.

Schuh, W., Meister, S., Roth, E., and Jack, H. M. (2003). Cutting edge: signaling and cell surface expression of a mu H chain in the absence of lambda 5: a paradigm revisited. *J Immunol* 171, 3343-3347.

Shimizu, T., Mundt, C., Licence, S., Melchers, F., and Martensson, I. L. (2002). VpreB1/VpreB2/lambda 5 triple-deficient mice show impaired B cell development but functional allelic exclusion of the IgH locus. *J Immunol* 168, 6286-6293.

ten Boekel, E., Melchers, F., and Rolink, A. (1995). The status of Ig loci rearrangements in single cells from different stages of B cell development. *Int Immunol* 7, 1013-1019.

ten Boekel, E., Melchers, F., and Rolink, A. G. (1998). Precursor B cells showing H chain allelic inclusion display allelic exclusion at the level of pre-B cell receptor surface expression. *Immunity* 8, 199-207.

Thien, M., Phan, T. G., Gardam, S., Amesbury, M., Basten, A., Mackay, F., and Brink, R. (2004). Excess BAFF rescues self-reactive B cells from peripheral deletion and allows them to enter forbidden follicular and marginal zone niches. *Immunity* 20, 785-798.

van den Eertwegh, A. J., Laman, J. D., Schellekens, M. M., Boersma, W. J., and Claassen, E. (1992). Complement-mediated follicular localization of T-independent type-2 antigens: the role of marginal zone macrophages revisited. *Eur J Immunol* 22, 719-726.

Vinuesa, C. G., Sze, D. M., Cook, M. C., Toellner, K. M., Klaus, G. G., Ball, J., and MacLennan, I. C. (2003). Recirculating and germinal center B cells differentiate into cells responsive to polysaccharide antigens. *Eur J Immunol* 33, 297-305.

Wasserman, R., Li, Y. S., Shinton, S. A., Carmack, C. E., Manser, T., Wiest, D. L., Hayakawa, K., and Hardy, R. R. (1998). A novel mechanism for B cell repertoire maturation based on response by B cell precursors to pre-B receptor assembly. *J Exp Med* 187, 259-264.

5 Summary

Antigen receptor variability is mostly generated by the V(D)J recombination mechanism. During V(D)J recombination hairpinned DNA ends are generated as intermediate reaction products, which have to be opened before religation can take place. One complex, which had been suggested to constitute the hairpin opening activity, was the Mre11/Rad50/Nbs1 (MRN) complex. This complex was known to be involved in DNA repair and hypothesized to participate in the non homologous end joining (NHEJ) pathway, the repair mechanism involved in V(D)J recombination. Additionally, it was shown that Mre11, as part of the ternary MRN complex, displayed hairpin opening activity *in vitro*, altogether making (Paull and Gellert, 1999) it conceivable that the complex is involved in V(D)J recombination.

To test whether or not the MRN complex, and accordingly Nbs1, is involved in hairpin opening at coding ends, we quantitatively and qualitatively analyzed V(D)J recombination with a cellular recombination assay in cells of healthy controls and cells of Nijmegen breakage syndrome (NBS) patients, the latter carrying a mutated *Nbs1* gene. No obvious difference was detected, neither in recombination frequencies nor in the quality of signal joint or coding joint formation. Endogenous CDR3 regions of the Ig κ and the Ig λ chain loci of lymphocytes of NBS patients also showed no differences compared to healthy controls. These results led to the conclusion that Nbs1, and as a consequence the MRN complex, is not directly involved in the processing of DNA ends during V(D)J recombination.

KRC, for kappa binding and RSS recognition component, was identified based on its ability to bind to the RSS (Wu et al., 1993). This RSS binding specificity was shown to be regulated by phosphorylation and to decrease upon RAG expression. Together with its mainly lymphoid expression pattern, it made it conceivable that KRC participates either in the V(D)J recombination mechanism itself or in the regulation of it. Additionally, KRC had been shown to be involved as a modulator in TNF- α signaling, suggesting an additional function for KRC in lymphocyte function and survival.

To investigate the role of KRC in lymphocytes the *KRC* locus was targeted in order to analyze the effects of KRC deficiency on V(D)J recombination and lymphoid cells in general. Heterozygous mice were obtained but no homozygous mice were born due to very early embryonic lethality caused by the introduced mutation. Closer

characterization of the targeted locus revealed that the integration of the targeting construct into the locus had occurred homologously only with one homology arm, whereas the other arm had integrated randomly. Additionally, a second integration into an intronic region of the *KRC* locus was detected. Whether the early embryonic lethality observed in our line of mice was due to *KRC* deficiency, based on a possible involvement of *KRC* in early zygotic/embryonic signaling, or rather due to the additional integration event, remains to be determined.

During B cell development the IgH chain locus is the first locus where V(D)J recombination takes place. The resulting μ H chain is subsequently tested for pairing with the surrogate light (SL) chain and for expression on the cell surface, as part of the preBCR. Deficiency in $\lambda 5$, one component of the SL, partially blocks early B cell development at the preB-I to preB-II stage transition, resulting in B lymphopenia (Kitamura et al., 1992). The rate of generation of B cells and also the size of the B cell compartment itself apparently influence, amongst other factors, both the composition and the size of peripheral B cell compartments. B lymphopenic situations, like in the case of $\lambda 5^{-/-}$ mice, seem to favour the development of B cell types, considered to be more innate, like marginal zone B cells (MZB). $\lambda 5$ deficient mice had not been analyzed in this respect, so that we decided to characterize the mature B cell compartments in $\lambda 5$ deficient mice.

Analysis of the peritoneal B cell compartment of $\lambda 5^{-/-}$ mice showed that conventional B2 B cells were hardly detectable and the B1b B cell population was reduced, whereas the B1a B cells were present in normal numbers. The splenic B cell compartment of $\lambda 5$ deficient animals was diminished, mainly due to the reduction of follicular B (FOB) cells. In contrast, MZB cells were present in normal numbers in $\lambda 5^{-/-}$ mice. BrdU labeling kinetics revealed a slower turnover of FOB as well as MZB cells in $\lambda 5$ deficient animals, probably due to lowered influx of newly generated B cells. Functionally, $\lambda 5^{-/-}$ mice were able to mount both primary and secondary thymus-dependent as well as thymus-independent responses, albeit mostly at reduced levels. Additionally, we tested the competitive reconstitution ability of $\lambda 5^{-/-}$ cells in mixed bone marrow chimeras between wild type and $\lambda 5^{-/-}$ bone marrow cells. The results are preliminary, but suggest that $\lambda 5$ deficient bone marrow can reconstitute to a limited extent, even in competition with wild type cells. Surprisingly, $\lambda 5^{-/-}$ deficient cells were enriched in the MZB compartment, implicating that they have an intrinsic propensity

to develop into MZB cells. In summary, the data show that in $\lambda 5$ deficient mice B cells preferentially develop into more innate-like B cell types.

5.1 References

Kitamura, D., Kudo, A., Schaal, S., Muller, W., Melchers, F., and Rajewsky, K. (1992). A critical role of lambda 5 protein in B cell development. *Cell* *69*, 823-831.

Paull, T. T., and Gellert, M. (1999). Nbs1 potentiates ATP-driven DNA unwinding and endonuclease cleavage by the Mre11/Rad50 complex. *Genes Dev* *13*, 1276-1288.

Wu, L. C., Mak, C. H., Dear, N., Boehm, T., Foroni, L., and Rabbitts, T. H. (1993). Molecular cloning of a zinc finger protein which binds to the heptamer of the signal sequence for V(D)J recombination. *Nucleic Acids Res* *21*, 5067-5073.

6 Abbreviations

aa	amino acid
ATM	ataxia telangiectasia mutated
BCR	B cell receptor
BM	bone marrow
BMP	bone morphogenetic protein
BrdU	5-bromo-2'-deoxyuridine
BSA	bovine serum albumine
CJ	coding joint
CD	cluster (complex) of differentiation
CDR	complementarity determining region
CSR	class switch recombination
DMSO	dimethylsulfoxide
DN	double negative
DP	double positive
dpc	days post coitus
DSB	DNA double strand break
DTT	dithiothreitol
EDTA	ethylenediamine-tetraacetate
ES cells	embryonic stem cells
FACS	fluorescence activated cell sorting
FCS	fetal calf serum
FITC	fluoresceinisoithiocyanate
FOB	follicular B cells
FSC	forward scatter
H chain	heavy chain
Ig	immunoglobulin
i.p.	intraperitoneally
i.v.	intravenously
kb	kilo bases
KRC	kappa B and RSS recognition component
L chain	light chain
min	minutes
MHC	major histocompatibility complex
MLN	mesenteric lymph nodes
MRN	Mre11/Rad50/Nbs1 complex
MZB	marginal zone B cells
MW	molecular weight
NBS	Nijmegen breakage syndrome
NIP	4-Hydroxy-3-iodo-5- nitrophenylacetyl
NHEJ	non homologous end joining
OD	optical density
ON	over night
pc	post coitus
PCR	polymerase chain reaction
PEC	peritoneal cells
PI	propidium iodide
preBCR	pre-B cell receptor
rpm	rounds per minute

Abbreviations

RAG	recombination activating gene
RSS	recombination signal sequence
RT	room temperature
RT-PCR	reverse transcriptase-PCR
SCID	severe combined immunodeficiency
SDS	sodium dodecylsulfate
sIgM	surface IgM
SJ	signal joint
SL	surrogate light chain
SP	single positive
SSC	side scatter
TCR	T cell receptor
TD	thymus dependent
Tdt	terminal deoxynucleotidyl transferase
TI	thymus independent
UTR	untranslated region
UV	ultra violett
WT	wild type
ZAS	zinc fingers/acidic motif/Ser/Thr-rich region domain
ZnF	zinc finger

7 Materials and Methods

7.1 General buffers and solutions

DNA loading buffer, 6x	0,25% bromophenol blue 0,25% xylyncyanol 1 mM EDTA 30% glycerol
PBS	137 mM NaCl 2.7 mM KCl 8 mM Na ₂ HPO ₄ 1.5 mM KH ₂ PO ₄ pH 7.2
20xSSC	3 M NaCl 300 mM sodium citrate pH 7.0
TAE	40 mM Tris-acetate pH 8.0 1 mM EDTA
TE	10 mM Tris/HCl pH 8.0 1 mM EDTA
5x PCR S buffer	50 mM Tris-HCL pH 8.8 250 mM KCl 7.5 mM MgCl ₂
ELISA buffer	4% BSA 0,1% Tween 10 mM NaN ₃ in PBS
ELISA-substrate buffer	0.1 g MgCl ₂ x 6 H ₂ O 800 ml ddH ₂ O 10 ml 1 M NaN ₃ 100 ml diethanolamine adjust to pH 9.8 with conc. HCl add to 1 l with ddH ₂ O
FACS-buffer	2%FCS 10 mM NaN ₃ in PBS
ACK red blood cell lysis buffer	0.15 M NH ₄ Cl 1.0 mM KHCO ₃ 0.1 mM EDTA filter through a 0.2 μm filter

Materials and Methods

PBST	0.1% Tween 20 in PBS
Proteinase K solution	10 mM Tris/HCl pH 8 5 mM EDTA pH 8 1 % SDS 300 mM sodium acetate pH 8 add fresh 200 μ g/ml Proteinase K
Mouse tail lysis buffer	50 mM Tris/Cl pH 8.0 5 mM EDTA 100 mM NaCl 0,5% SDS Add freshly 20 μ l / 750 μ l buffer 10 mg/ml proteinase K
Southern blot hybridization solution	171 ml 1 M Na ₂ HPO ₄ 79 ml 1 M NaH ₂ PO ₄ 175 ml 20% SDS 1 ml 0.5 M EDTA pH 8.0 Add to 500 ml Filter 0.45 μ m Keep at RT, heat in case of precipitate
Southern blot washing solution	54.72 ml 1 M Na ₂ HPO ₄ 25.28 ml 1 M NaH ₂ PO ₄ 100 ml 20 % SDS 4 ml 0.5 mM EDTA pH 8.0 Add to 2 l
Blastocyst digestion buffer	50 mM KCl 10 mM Tris/Cl (8.0) 2.5 mM MgCl ₂ 0.1 mg/ml gelatine 0.45% NP40 0.45% Tween

7.2 Bacterial media and supplements

LB	10 g tryptone 5 g yeast extract 10 g NaCl dissolved in 1 l H ₂ O autoclaved added 15 g agar for LB plates
ampicillin	sodium salt in H ₂ O stock 100 mg/ml used at 100 μ g/ml

kanamycin	stock 20 mg/ml in H ₂ O used at 50 µg/ml
chloramphenicol	stock 30 mg/ml in ethanol, use at 150 µg/ml
tetracyclin	stock 5 mg/ml in ethanol, used at 50 µg/ml

7.3 Cell culture media and supplements

Medium for MEF

1000 ml DMEM (+Glutamax, high glucose)	Gibco BRL 41966-029
50 ml FCS	Gibco BRL
12 ml Na-Pyruvate+MEM (100 mM)	Gibco BRL 11360-039
20 µl 1-Thioglycerol	Sigma M-6145
12 ml Penicillin Streptomycin	Gibco BRL 15140-114
5 ml 200mM Glutamine	Gibco BRL
filter sterilized (0,22 µm filter)	

Medium for ES cells

1000 ml Knock-out DMEM	Gibco BRL 10829-018
120 ml FCS (ES Cell qualified)	Gibco BRL
12 ml Na-Pyruvate+MEM (100 mM)	Gibco BRL 11360-039
20 µl 1-Thioglycerol	Sigma M-6145
12 ml Penicillin Streptomycin	Gibco BRL 15140-114
1 x 10 ⁵ U/ml ESGRO™ (LIF)	Gibco BRL 13275-011
10 ml 200mM Glutamine	Gibco BRL
filter sterilized (0,22 µm filter)	

Gelatine solution for coating plates

1,5 g gelatine (Type A from porcine skin) Sigma G-1890
dissolved in 1000 ml PBS or 0,9% NaCl saline, autoclaved

Trypsin solution

10 ml Trypsin (10x) in 100 ml PBS (sterile) Gibco BRL

G418 Stock-solution

5 g G418 sulfate Gibco BRL 11811-031
in 37 ml ES cell medium and 0.4 ml 10M NaOH, 300µg/ml active concentration

Freezing medium

90% FCS
10% DMSO

7.4 Vectors

vector	Insert	Constructor, Reference	Application
pCR4-TOPO (4 kb)	none	Invitrogen	Cloning of PCR fragments with TA additions
pDZ18 pBSL-flneo-DT4 (6.6 kb)	1.5 kb flox-neo Bsp120I-XbaI fragment pGI2neo(m)+ into NotI-XbaI linearized pBSL-DT4	D. Zimmer, BII	Backbone of the KRC targeting construct
pDZ19 pBSL-flneo-DT4tox (6.6 kb)	1.5 kb flox-neo Bsp120I-XbaI fragment into NotI-XbaI linearized pBSL-DT4tox	D. Zimmer, BII	Backbone of the KRC targeting construct, attenuated DTA cassette
pDZ18-KRC-L/R (14.5 kb)	1 kb fragment of amplified KRC genomic DNA (primer 665/664) into the NotI site and the 7kb KRC fragment of (primer 833/832) into the Ascl site of pDZ18 pBSL-flneo-DT4 .	E. Harfst, this thesis	KRC targeting construct
pDZ19-KRC-L/R (14.5 kb)	1 kb fragment of amplified KRC genomic DNA (primer 665/664) into the NotI site and the 7kb KRC fragment (primer 833/832) into the Ascl site of pDZ19 pBSL-flneo-DT4 .	E. Harfst, this thesis	KRC targeting construct, attenuated DTA cassette

7.5 Primers

Primer	Sequence (5'-3')	Application
664 KRC 5' left	gcgccgcccggactagggatgacaggccatgg	Cloning of the 5' arm of the KRC targeting construct, + NotI site
665 KRC right 3'	gcgccgctgcagattgacatatatacttgctg	Cloning of the 5' arm of the KRC targeting construct, + NotI site, left arm southern probe
689 + 856 int-neo	ggatcgcgctccccgattcgc	Internal neo primer used for targeting screening PCR
859 pDZ18/19-L-3'	ccgagctcgaattcgagctctcccatatggctg	Internal targeting construct primer used for targeting screening PCR
718 moKRcf	catggatcctgaccaaagcatcaagggcacc	Inverted PCR for cloning of flanking genomic sequences, exon II
719 moKRcr	ggttggccagtgtgtgtggtagcccaag	Inverted PCR for cloning of flanking genomic sequences, exon II
722 moKRcnestf	ccccaaactccctgagtagcatctgaagtc	Inverted PCR for cloning of flanking genomic sequences, exon II
723 moKRcnestr	atggagctgctgcgatccagtgtgggaag	Inverted PCR for cloning of flanking genomic sequences, exon II
726 moKRC SOE f	ctcttctcttgcaacagctcttgctcag	Inverted PCR for cloning of flanking genomic sequences, exon II
727 moKRC SOE r	ctgaggcaagagctgttgcaaggagaagag	Inverted PCR for cloning of flanking genomic sequences, exon II
740 mKSf	acatatctccctcggccgctcgcaca	Inverted PCR for cloning of flanking genomic sequences, exon II
741 mKSr	atcaaaggagtagctaccacggaaggtgtg	Inverted PCR for cloning of flanking genomic sequences, exon II
744 mKMf	cacaccttcggtgtagctactccttgat	Inverted PCR for cloning of flanking genomic sequences, exon II
745 mKMr	tgtgcgagccgagccgagggagatgtg	Inverted PCR for cloning of flanking genomic sequences, exon II
786 KRC-exon3-5	ctttcaatctgacctgagaacacc	Cloning of the 3' targeting arm and inverted PCR
787 krc-exon3-3	gggtgtagaaggtctccacacagg	Cloning of the 3' targeting arm and inverted PCR
788 krc-exon2-3	cctgcctcaggatcgagctgtgg	Cloning of the 3' targeting arm and inverted PCR
789 krc-exon2-5	cttgtctcagatgtatccgacc	Cloning of the 3' targeting arm and inverted PCR
790 KRC-exon3-5'	gggtcaagatcttgaaggagg	Cloning of the 3' targeting arm and inverted PCR, right arm southern probe-> left end
791 KRC-5'introninside	catggacaccgaccagccctctcc	Cloning of the 3' targeting arm and inverted PCR
792 KRC-5'intronoutside	cttggtacagtggcttccatgcc	Cloning of the 3' targeting arm and inverted PCR
793 KRC-3'intronoutside	gcagtgagctcccaatgacaacc	Cloning of the 3' targeting arm and inverted PCR
794 KRC-3'introninside	atgactatcatggcaggagcatgg	Cloning of the 3' targeting arm and inverted PCR
803 KRC-exon-3-3'	aagtacatctgaatccaggtgcccc	Cloning of the 3' targeting arm and inverted PCR, right arm southern probe-> left end
806 jfk43e05.g1	cccaggagcttctctatgccagcc	Cloning of the 3' targeting arm and inverted PCR, right arm southern probe-> middle
807 KRC-3'intronoutside2	ttggaggagatccatgtgtgtgg	Cloning of the 3' targeting arm and inverted PCR
808 KRC-3'introninside2	ctactgtcctcagcaccatgcctgcc	Cloning of the 3' targeting arm and inverted PCR
824 G10P604282	ggcctaactggagggtagg	Cloning of the 3' targeting arm and inverted PCR
825 jmf46f06	tagtggtagcaccgagccc	Cloning of the 3' targeting arm and inverted PCR
826 G11P60253FH6	atccctgcatcctaccctcc	Cloning of the 3' targeting arm and inverted PCR, right arm southern probe-> middle

Materials and Methods

Primer	Sequence (5'-3')	Application
827 ml2C-a1623h08.p1c3'	tgcaagctgggaagcaatggcaagg	Cloning of the 3' targeting arm and inverted PCR
828 G10P608000FF7-2	atgttgtaggagcgggtgtggcg	Cloning of the 3' targeting arm and inverted PCR
829 mleC-a1623h08.p1c	ttccttctaccagttccactcc	Cloning of the 3' targeting arm and inverted PCR
830 ml2C-a3348a11.q1c	ttgcttcaggaagatgagcgggg	Cloning of the 3' targeting arm and inverted PCR
831 G10P627493RH7	tgcttatgccgtgggtgagcagg	Cloning of the 3' targeting arm and inverted PCR
832 790-Ascl krc	ttggcgcgcgggtcaagatcttgaaggagg	Primer used for cloning of the 3' arm of the KRC targeting construct, + Ascl site
833 830-Ascl krc	ttggcgcgccttctcaggaagatgagcgggg	Primer used for cloning of the 3' arm of the KRC targeting construct, + Ascl site
853 pDZ18/19-KRC-1kb	gcgggatcactagtgccg	Inverted PCR for cloning of flanking genomic sequences, vector specific
854 pDZ-18/19-7kb	gatatcaagcttatcgatacc	Inverted PCR for cloning of flanking genomic sequences, vector specific
855 1,1-KRC-left5'new -NotI	ccgtgatttctcctctgaggtgctc	5' upstream genomic primer used for targeting screening PCR, left arm southern probe
857 1,1-KRC-left5'-2	cagaattcaagggcagaagagg	5' upstream genomic primer used for targeting screening PCR
858 int-neo-2	ggcgaatgggctgaccgttcc	Internal targeting construct primer used for targeting screening PCR
859 pDZ18/19-L-3'	ccgagctcgaattcgagcttcccatggctg	Inverted PCR for cloning of flanking genomic sequences, vector specific
860 KRC-1,1-5'-3	ccgtgatttctcctctgaggtgctattctcc	Inverted PCR for cloning of flanking genomic sequences, vector specific
861 KRC-1,1-5'-5	caatacagaattcaagggcagaagagg	Inverted PCR for cloning of flanking genomic sequences, vector specific
862 KRC-1,1-5'-4 862	cccagcatccattgtggcatctctcc	Inverted PCR for cloning of flanking genomic sequences, vector specific
863 KRC-II-5'-3	gtggagcatcgggtgtagtagtggtg	5' upstream genomic primer used for targeting screening PCR
864 KRC-II-5'-2	gggtgaggcatcctgtttgaatgtctctg	5' upstream genomic primer used for targeting screening PCR
865 KRC-II-5'-1	ctgtggacagcctcagtaaatcctttcc	5' upstream genomic primer used for targeting screening PCR
866 KRC-7kb-3'	ccctgaattccccttaagagatagcc	Inverted PCR for cloning of flanking genomic sequences, right targeting arm
867 KRC-7kb-5' 2	cggtgttccagaagtcgataccagctcg	Inverted PCR for cloning of flanking genomic sequences, right targeting arm
868 pDZ18191kb5 853	gccgcgggatcactagtgccg	Inverted PCR for cloning of flanking genomic sequences, vector specific
869 pDZ18/19asc5'	gaattcgatatcaagcttatcgatacc	Inverted PCR for cloning of flanking genomic sequences, vector specific
870 pDZ18/19-Asc-5'-3	tattgaatgatcggaattcctcagcttagg	Inverted PCR for cloning of flanking genomic sequences, vector specific
871 pDZ1819Asc5'-2	atatcaagcttatcgataccgtcgacc	Inverted PCR for cloning of flanking genomic sequences, vector specific
899 Krc-exon2-rev1	ggctggcgttttagcatcc	Inverted PCR for cloning of flanking genomic sequences, exon II
900 KRC-exon2-f1	gaagagccacctgcctttggcagcc	Inverted PCR for cloning of flanking genomic sequences, exon II
901 KRC-exon2-r2	agctggctgggtgtagcacagtagg	Inverted PCR for cloning of flanking genomic sequences, exon II
902 KRC-exon2-r3	catattccttcaagcttctgagcc	Inverted PCR for cloning of flanking genomic sequences, exon II
903 KRC-exon2-f2	gcctgacacagagcctgagccg	Inverted PCR for cloning of flanking genomic sequences, exon II
910 neo-int2	ccctgatgctcttctgctcagatcatcc	Neo primer used for screening and southern blot probe

Primer	Sequence (5'-3')	Application
911 neo-int1	tcggctgctctgatgcccgcgtgttcc	Neo primer used for screening and southern blot probe
937 KRC exon II	tcctgtgctttagaggttactcttgg	Exonic KRC primer used for screening for homozygous mice/blastocysts
958 KRC-5'-gen.probe3	ggagtgcagttaagctggctaagac	Southern genomic probe 3' of left targeting arm
959 KRC-5'-gen.probe-5	gcatcctcagacacttcttactctc	Southern genomic probe 3' of left targeting arm
961 pDZ18/19outward	ccgactagtgatatcccgc	Inverted PCR for cloning of flanking genomic sequences, vector specific
962 KRC-gen.probe-R-3'	cggaggtctggaagaggatagat	Southern genomic probe 3' of right targeting arm
963 KRC-gen.probe-R-5'	agctggtatcgaacttctggaacac	Southern genomic probe 3' of right targeting arm
964 Neo-5'	ccattgaacaagatggattgc	Southern neomycin probe
965 Neo-3'	tcagaagaactcgtaagaagg	Southern neomycin probe
968 665-rev	caggcaagtatatatgtcaataactgcagcgcc	Inverted PCR for cloning of flanking genomic sequences, vector specific
983 pDZ-1,1-3'-nest	tgacggcgcctgcaggtcgacc	Inverted PCR for cloning of flanking genomic sequences, vector specific
984 pDZ-1,1-5'-nest	ctagtccggcgccgcactagtg	Inverted PCR for cloning of flanking genomic sequences, vector specific
985 pDZ18/19-3'Asc-out2	actttcatcctcttctcaatctcg	Inverted PCR for cloning of flanking genomic sequences, vector specific
986 pDZ18/19-3'Asc-out	ctattcctgtacatctggcctacgg	Inverted PCR for cloning of flanking genomic sequences, vector specific
987 961+4	gcgccgcactagtgatatcccgc	Inverted PCR for cloning of flanking genomic sequences, vector specific
E-21 RT-vector-for	cctcgagatccgaacaaacg	Genomic real time PCR quantitation detecting vector sequences
E-22 RT-KRC-WT-for	cgagggagaagcacagactct	Genomic real time PCR quantitation detecting WT KRC targeted sequences
E-23 RT-control locus -for	tgctggatgggcagatcag	Genomic real time PCR quantitation detecting vector WT exonic 5' of exon VII sequences
E-24 RT-vector-rev	gatcggcaataaaaagacagaataaa	Genomic real time PCR quantitation detecting vector sequences
E-25 RT-KRC-WT-rev	catctgtggaggacctgatg	Genomic real time PCR quantitation detecting WT KRC targeted sequences
E-26 RT-control locus -rev	gcagaggagaaccaggtaactg	Genomic real time PCR quantitation detecting vector WT exonic 5' of exon VII sequences
E-30 KRC-L-5'-2	agcatccattgtggcatctct	Inverted PCR for cloning of flanking genomic sequences, KRC intron I
E-31 KRC-L-5'-1	caatacagaattcaagggcagaag	Inverted PCR for cloning of flanking genomic sequences, KRC intron I
E-32 2int-gen5'	gtggagaagaggactggctacata	Inverted PCR for cloning of flanking genomic sequences, KRC intron I
E-33 KRC-vector-L3'	gtctgaagaggagttacgtccag	Inverted PCR for cloning of flanking genomic sequences, vector specific
E-34 RT-Rarm-f	cacttcccgtggtctgaa	Genomic real time PCR quantitation detecting 5' targeting arm sequences
E-35 RT-Rarm-r	gtgggcaaggcagagacagt	Genomic real time PCR quantitation detecting 5' targeting arm sequences
E-36 KRC-L-3'-gen	ctgtgtgtgagcgaatgtgtt	Inverted PCR for cloning of flanking genomic sequences, KRC exon II
GABAR1-E7-f	tgccctggaggactttaac	Genomic real time PCR quantitation, GABA-Receptor 1 control locus, gift of Samuel Barbieri
GABAR1-E7-r	ttcatggcccggtagatttg	Genomic real time PCR quantitation, GABA-Receptor 1 control locus, gift of Samuel Barbieri

7.6 Antibodies

7.6.1 Antibodies for FACS Analysis

Commercial antibodies were diluted 1:200 final dilution for FACS staining.

Antigen	Clone		
α -mouse IL7-R (CD127)	(A7R34)	PE	eBioscience
α -mouse CD21 (CR2/CR1)	(7G6)	FITC	PharMingen
α -mouse CD23 (Fc ϵ RII)	(B3B4)	FITC/PE	PharMingen
α -mouse CD9	(KMC8)	Biotin	PharMingen
α -mouse CD1d (CD1.1)	(1B1)	Biotin	PharMingen
α -mouse CD5 (Ly.1)	(53-7.3)	Biotin	PharMingen
α -mouse CD4 (L3T4)	(RM4-5)	APC	PharMingen
α -mouse CD8 α (Ly-2)	(53-6.7)	PE	PharMingen
α -mouse CD3 ϵ	(142-2C11)	APC	PharMingen
α -mouse CD25 α -chain	(7D4)	FITC	PharMingen

Antibodies produced in the laboratory had been individually titrated beforehand.

α - mouse IgM	(M41)	(Leptin, 1985)
α - mouse CD19	(1d3)	
α - mouse IgD	(1.19)	
α - mouse c-kit (CD117)	(ACK4)	(Ogawa et al., 1991)
α - mouse 493 (C1qRp, AA4.1)		(Rolink et al., 1998)

Secondary FACS reagents

Streptavidin-PE-Cy7	Dil: 1:400	PharMingen
Streptavidin-APC	Dil: 1:200	Becton Dickinson
Streptavidin-PE	Dil: 1:1000	Southern Biotech

7.6.2 Antibodies for ELISA

		Dilution
Goat α -mouse IgG	AP conjugate	1:1000 Southern Biotech
Goat α -mouse IgM	AP conjugate	1:1000 Southern Biotech
Goat α -mouse IgG1	AP conjugate	1:1000 Southern Biotech
Goat α -mouse IgG2a	AP conjugate	1:1000 Southern Biotech
Goat α -mouse IgG2b	AP conjugate	1:1000 Southern Biotech
Goat α -mouse IgG3 (R40-82)	AP conjugate	1:1000 PharMingen

7.6.3 Antibodies for Histology

		Dilution	
Biotinylated Peanut agglutinin		1:200	Vector Laboratories
T24 (α -Thy1.1)	FITC	1:50	produced in the laboratory
Moma-1	bio	1:50	produced in the laboratory
Ly5.1	bio or FITC	1:50	produced in the laboratory
Ly5.2	bio or FITC	1:50	produced in the laboratory

M41 (α -IgM)	APC	1:50	produced in the laboratory
Streptavidin RPE		1:200	Southern Biotech
Neutralite Avidin-TXRD		1:200	Southern Biotech

7.7 Molecular biology methods

7.7.1 Agarose gel electrophoresis of DNA fragments

DNA was separated for analytical or preparative purposes by gel electrophoresis using 0.75% (w/v) agarose gels containing already 0.1 μ g/ml ethidium bromide in 1 x TAE. 6x sample buffer was added to each sample. Electrophoresis was performed at 3-5 V/cm.

7.7.2 Preparation of electro-competent *E. coli*

1 l of LB medium was inoculated with 10 ml of fresh overnight culture of bacteria. Bacteria were grown at 37°C shaking to an OD₆₀₀ of 0.7-0.9. The culture was then chilled on ice for half an hour and eventually centrifuged at 1500 g and 4°C for 15 minutes. The pellet was then resuspended in 1 l of ice-cold 0.5 mM HEPES (pH 7.0) and again centrifuged at 1500 g and 4°C for 15 minutes. Cells were resuspended in 500 ml ice-cold 0.5 mM HEPES (pH 7.0) and pelleted again by centrifugation. Next the bacteria were resuspended in 20 ml ice-cold 10% glycerol, again centrifuged and resuspended in 2 ml ice-cold 10% glycerol. Bacteria were fractioned in 400 μ l aliquots, frozen on dry ice and stored at -70°C.

7.7.3 Transformation of electro-competent *E. coli*

Electro-competent *E. coli* were thawed on ice and 40-50 μ l of bacterial suspension were transferred into a prechilled 0.1 cm gap Gene Pulser cuvette (Bio-Rad). 1 μ l DNA solution was added. The samples were pulsed with 1,6 kV, 25 μ F and 200 Ω . After pulsing bacteria were immediately transferred into 1 ml of LB medium and incubated for around 1 hour at 37°C. Afterwards bacteria were spun down (7000 g, 1 min), resuspended in 70 μ l of LB medium and plated onto selecting agar plates. After overnight growth at 37°C, colonies were expanded in LB with added corresponding antibiotic. On these mini-preps were performed and the isolated DNA was analyzed for the correct product by restriction digest.

7.7.4 Preparation of plasmid DNA from *E. coli* cultures

Plasmid DNA was prepared with QIAGEN Maxi-prep and Mini-prep Kits according to the manufacturer's protocols and dissolved in TE.

7.7.5 Restriction enzyme digestion of DNA

Restriction enzyme digest was carried out in either 10 μ l (for analytical purposes) or in 20-50 μ l volume (preparative digests) at conditions recommended by the manufacturer (NEB-Biolabs) with the appropriate enzyme buffer. Preparative digests were performed for at least 3 hours or ON, analytical digests for about 1 hour.

7.7.6 Purification of DNA from agarose gels

Agarose gels were examined under UV light (366 nm) and the bands of interest excised as fast as possible to minimize exposure to UV light. Purification was then performed with the QIAquick Gel Extraction Kit (QIAGEN) according to the manufacturer's protocol.

7.7.7 Phosphatase treatment of DNA

To prevent self-religation of vectors, after restriction enzyme digest, plasmids were treated with 1 U of calf intestine alkaline phosphatase for additional 30 minutes at 37°C. The alkaline phosphatase which removes 5' phosphates was then inactivated by heating the reaction mix to 75°C for 10 minutes. To remove the alkaline phosphatase gel electrophoresis was performed and the dephosphorylated vector was then gelpurified.

7.7.8 Ligation of DNA fragments into vectors

- A) Ligations of restriction enzyme fragments with cohesive ends were performed at a molar ratio between vector and insert of 1:2-4 in a volume of 20 μ l using 1 μ l of NEB T4 DNA ligase (400 U). The mix was either incubated 20 minutes at RT or ON at 16°C. 1 μ l of the ligation reaction was then transformed into electro-competent bacteria.
- B) PCR fragments were directly cloned into the pCR-Vector or pCR-Blunt-vector (TA Cloning Kit or Zero Blunt PCR Cloning Kit ,Invitrogen) according to the manufacturer's protocol.

7.7.9 DNA Ethanol Precipitation

Plasmid and genomic DNA was precipitated by adding 1/10 volume of 3 M sodium acetate (pH 4.8) and 2 volumes of 100% ethanol to the solution. The mixed DNA solution was then incubated for 20 minutes at -20°C followed by 15 minutes centrifugation (21 000 g, 4°C). The pelleted DNA was then washed with ice-cold 70% ethanol and air dried. DNA was dissolved either in TE or 10 mM Tris (pH 8.0).

7.7.10 DNA phenol-choloroform Extraction

To remove protein and other impurities of DNA solution a phenol-chloroform extraction was performed. For this 1 volume pure phenol (TE saturated) was added, the sample was shaken and spun for 10 minutes at RT and 21'000 g. The supernatant was transferred into a new tube and extracted with 1 volume of a 1:1 mixture of phenol and chloroform followed by a chloroform extraction. To precipitate the DNA 1 volume isopropanol was added and 1/10 volume of 3 M sodium acetate. The mixture was let to precipitate at -20°C for 20 minutes. DNA was pelleted by a centrifugation for 20 minutes at 21'000g and 4°C. The pellet was air dried and redissolved in an appropriate volume of TE.

7.7.11 Polymerase chain reaction

The PCR reactions were mixed on ice in 0.2 ml thermo PCR tubes. The set-up was the following:

1-5 μ l template DNA
 6 μ l 5x S PCR buffer
 500 μ M forward primer
 500 μ M reverse primer
 200 μ M each dNTP
 0.2 μ l Taq-polymerase (0.25 U) (Roche Diagnostics)

The PCR reaction was performed either in a T3 thermocycler (Biometra) or a Robocycler 96 (Stratagene) with the following standard protocol:

94.5°C	2 min	initial denaturation	1 cycle
94.5°C	30 sec		
x°C	30 sec		
72°C	60 sec / kb of expected product length		30-40 cycles
72°C	5 min (or 1 1/2 x time of step 4)		1 cycle
4°C	infinite		

Annealing temperature was calculated based on the primer sequence by adding up A and T as 2°C and counting G and C as 4°C. The PCR product was analyzed after completed PCR reaction by gel electrophoresis and, if necessary, further processed i.e. purified and/or digested.

7.7.12 Sequencing of plasmid DNA

Sequencing of plasmid DNA was performed by capillary electrophoresis (ABI PRISM, Genetic Analyzer 310) using fluorescent terminator dideoxynucleotides supplied in a ready-to-use solution (Big Dye, Perkin-Elmer). The set-up was the following:

up to 6 μ l mini-prep DNA (1-2 μ g)
 1 μ l primer (3.2 pmol/ μ l)
 4 μ l mix
 add up to 20 μ l with H₂O

The reaction was performed with the following standard program:

96°C	30 sec	
50°C	15 sec	
60°C	4 min	25 cycles
4°C	infinite	

The samples were ethanol precipitated by adding 80 μ l of 75% ethanol, centrifuged at maximum speed for 20 minutes, washed once with 70% ice-cold ethanol, air dried and resuspended in 40 μ l H₂O. Sequencing was performed on the Genetic Analyzer 310 (ABI PRISM) with a usual injection time of 3-4 seconds. Sequence analysis was performed using the ABI PRISM Autoassembler software (version 1.4.0).

7.7.13 Quantitative Real-Time PCR Assay

7.7.13.1 PCR reaction setup for quantitative real-time PCR assay

For reaction setup the Platinum® Quantitative PCR SuperMix-UDG universal PCR master mix (Invitrogen) was used. This master mix was a 2x concentrated premix of all necessary components, except primers, probe and template. To 12.5 μ l master mix 5 μ l genomic DNA (6-12 ng total RNA), 300 mM forward and reverse primer and water were added to a final volume of 25 μ l. Reactions were transferred to a MicroAmp® optical 96-well plate and covered with MicroAmp® optical caps (both from Perkin Elmer Applied Biosystems). The real-time PCR was performed in an ABIPRISM™ 7000 Sequence Detector (Perkin Elmer Applied Biosystems). The cycling conditions were 2 minutes 50°C, 10 minutes 95°C and 45 cycles of 15 seconds 95°C denaturation, 1 minute 60°C combined annealing and primer extension. Data were evaluated with the SDS 1.6.3 software (Perkin Elmer Applied Biosystems).

7.7.13.2 Primers and probes for real-time quantitative PCR

Primers and probe sets for the genes of interest were designed with help of the Primer Express 1.0 software (Perkin Elmer Applied Biosystems) with the standard settings. Primers have an annealing temperature of 58 to 60°C. The amplicons size should be in the range of 50 to 200 bp to give consistent results. Primers were synthesized by QIAGEN (Germany). Following primers were used: E-34 RT-Rarm-f, E-35 RT-Rarm-r, GABAR1-E7-f, GABAR1-E7-r, E-21 RT-vector-for, E-24 RT-vector-rev, E-22 RT-KRC-WT-for, RT-KRC-WT-rev, E-23 RT-control locus –for and E-25 E-26 RT-control locus–rev, see section primers.

7.7.13.3 Interpretation of real-time PCR data

The software (SDS 1.6.3) included in the ABIPRISM™ 7000 Sequence Detector (Perkin Elmer Applied Biosystems, Rotkreuz, Switzerland) analyses the emission data by first calculating the contribution of each component dye to the experimental spectrum. The reporter signal is then normalized with the signal of the passive reference dye, i.e. ROX (6-carboxy-X-rhodamine) which is included in the buffer but does not participate in the reaction. This normalization is necessary to correct for fluorescent fluctuations due to changes in concentration or volume. Normalization is accomplished by dividing the emission intensity of the reporter dye by the emission intensity of the passive reference to obtain a ratio defined as normalized reporter (R_n) for a given reaction tube. To reliably indicate the magnitude of the signal generated by the given set of PCR conditions, the SDS software calculates ΔR_n using the equation $\Delta R_n = (R_n^+) - (R_n^-)$. Where R_n^+ equals the ratio of reporter and passive reference at any given time during a reaction, and R_n^- equals the mean of the reporter and passive reference ratio of cycles 3 to 15, resulting in a baseline. The threshold cycle value (C_T) is the fractional cycle number at which the reporter fluorescence passes a fixed

threshold. This fluorescence threshold was set to the same value for all samples of the same gene. It was set manually in the exponential phase of the PCR amplification.

7.7.13.4 Relative quantitation with the comparative method

The gene of interest and an internal standard were assessed in separate tubes and relatively quantitated by the comparative method. Amplification efficiencies were used to normalize the assessed quantities (Liu and Saint, 2002).

Three ΔR_n fluorescence thresholds were set manually in the exponential phase of the amplification reaction at the beginning, the middle and the end. The threshold cycle value (C_T) is the fractional cycle number at which the reporter fluorescence passes the fixed ΔR_n threshold. Efficiency of amplification was then calculated with the following formula:

$$efficiency = \left(\left(\frac{C_{tupper}}{C_{tlower}} \right)^{\frac{1}{C_{valueupper} - C_{valuelower}}} \right) - 1$$

The corrected value was then calculated with the following equation:

$$\text{Corrected Value} = \frac{C_{t\text{sample}}}{C_{t\text{control}}} \frac{(1 + \text{mean of efficiencies})^{C_{t\text{valuecontrol}}}}{(1 + \text{efficiency of sample})^{C_{t\text{value sample}}}}$$

The ratio of the corrected values was used to relatively quantitate the amount of cDNA in the different samples.

7.7.14 Preparation of genomic DNA of mouse tails

A piece of 0.2-0.8 cm of mouse tail was cut and incubated ON at 56°C in mouse tail lysis buffer. After lysis 300 μl of saturated sodium chloride solution was added and the mixture was shaken for 5 minutes at RT followed by a 10 minutes centrifugation at 18'000 g and RT. 5 μl of the lysate supernatant were diluted in 150 μl H₂O and 2 μl of this used as template for typing PCRs. 800 μl of the supernatant were transferred into a fresh tube and mixed with 500 μl isopropanol. The tubes were then centrifuged 5 minutes at 18'000 g, the DNA pellet was washed with 70% ethanol (was left at -20°C for some time with 70% ethanol), dried and resuspended for at least 1 hour at 56°C in 70 μl TE. A 25 μl (10-15 μg DNA) aliquot was taken for a southern blot experiment.

7.7.15 Extraction of ES cell genomic DNA

After trypsinization ES cells of 1 24-well were transferred into 1 ml medium, washed once with PBS, resuspended in 400 μl proteinase K solution and incubated ON at 55°C shaking in a thermoblock. The next day 200 μl phenol and 200 μl chloroform were added and the tubes were shaken and centrifuged 6 minutes at 21'000 g at RT. The supernatant was transferred into a new tube and 400 μl of chloroform were added. The tubes were shaken and again centrifuged at 21'000 g at RT. The supernatant was transferred into a fresh tube and the DNA was precipitated at -20°C

for 20 minutes after addition of 400 μ l of isopropanol and 1 μ l glycogen (20 mg/ml). Eventually tubes were spun for 20 minutes at maximum speed, washed once with ice-cold 70% ethanol, air dried and resuspended in 50 μ l TE for 1 hour at 55°C. Of this DNA solution 2 μ l were used as template for a 30 μ l screening PCR reaction. ES cells were screened first in pools of 8-10 ES cell clones and of the positive pool(s) single clones were then analyzed.

7.7.16 Southern blot analysis

7.7.16.1 Digestion and gel electrophoresis of genomic DNA

10-15 μ g of genomic DNA were digested ON in a 100 μ l digest with the corresponding enzyme buffer, 50 U restriction enzyme and 100 μ g/ml BSA. Digest efficiency was assessed the next day by gel electrophoresis of 3 μ l of digest on a 0.7% agarose gel. The digests were then ethanol precipitated and resuspended in 20 μ l of TE. The complete genomic DNA digests were loaded into one lane of a 0.7% agarose gel. Electrophoresis was performed ON with 1x TAE (without ethidium bromide) and at very low voltage (18-20 V). The gel was stained 20 minutes with 0.5 μ g/ml ethidium bromide and photographed with a ruler as reference.

7.7.16.2 Alkaline Blotting

The agarose gel was agitated in 0.25 N HCl for approximately 10 minutes. Then the DNA was denatured by soaking the gel in 0.4 N NaOH for 30 minutes. Meanwhile the nylon membrane (GeneScreen Plus, PerkinElmer Life Sciences) was cut to the exactly the same size as the gel and pre-wet in distilled water for a few seconds followed by an equilibration in 0.4 N NaOH for 10-15 minutes. Eventually a capillary blot was set up using 0.4 N NaOH as the transfer solution being careful to remove all bubbles between the different layers. Blotting was performed for 3 hours to ON. After transfer the membrane was washed in excess 2 x SSC for 1-2 minutes and the DNA was fixed by UV crosslinking onto the damp membrane (120 mJ, UV Stratalinker 2400, Stratagene).

7.7.16.3 Labeling of a southern blot probe

The 0.5-1.2 kb DNA probe which was mostly PCR amplified was labeled with the Random Primers DNA Labeling System (Invitrogen) according to the manufacturer's manual with [α -³²P]dATP as labeled nucleotide. Before hybridization the probe was separated from unincorporated nucleotides with MicroSpin S-300 or S-200 HR Columns (Pharmacia Biotech).

7.7.16.4 Hybridization and washing of the blot

The blot was prehybridized for 2 hours at 65°C with 30 ml of prewarmed hybridization solution. Immediately before hybridization the labeled probe was

denatured 5 minutes at 95°C, chilled on ice, mixed with 20 ml prewarmed hybridization solution and poured onto the prehybridized membrane. Hybridization was performed ON at 65°C. Blots were washed with 100-200 ml of prewarmed washing solution 2 times for 20 minutes at 65°C. After washing the membrane twice in 2 x SSC it was wrapped in cling film and exposed either to phosphor imaging screens (3 hours to ON) and scanned with Phospho-Imager STORM (Molecular Dynamics) or exposed to BIOMAX MS films (Kodak) 1-2 days at -70°C using an intensifying screen.

7.7.16.5 Stripping of blots

The membrane was shaken in 0.2 M NaOH for 15 minutes at RT. Then the blot was neutralized 2 times 15 minutes in a 25 mM NaHPO₄ pH 6.8 and 1 mM EDTA solution. Eventually the filter was newly hybridized or air dried.

7.7.17 Typing of single blastocysts

3.5 dpc blastocysts were taken, transferred individually into 30 µl of blastocyst digestion buffer and incubated for 1 hour at 55°C. Eventually the samples were heated 10 minutes to 95°C. 2 µl of the supernatant were taken as template for a 30 µl nested PCR reaction.

First and nested PCR followed the standard protocol with 40 cycles each, 1 minute 45 seconds elongation time and 62°C annealing temperature. For the nested PCR 2 µl of the first PCR were used as template. The WT locus was detected by a PCR with the genomic primers 864 + 1008 for the first PCR and 865 + 937 for the second. The integration of the targeting construct was detected by a PCR with the genomic primer 864 and the construct specific primer 856 in the first round and the genomic primer 865 and construct primer 859.

7.7.18 Identifying genomic integration sites by Inverse PCR

The strategy was to obtain fragments of DNA including part of the integrated construct as well as flanking genomic sequence. Genomic DNA was digested with enzymes cutting in and outside of the integrated vector. The fragments were religated and eventually a PCR with construct specific primers was performed directed over the included unknown genomic region amplifying thereby the genomic flanking sequences.

1 µg genomic DNA was digested separately with different restriction enzymes cutting inside the integrated construct (most possibly near to the construct ends). The digested DNA was purified using QIAquick PCR purification Kit (QIAGEN) and resuspended in 30 µl 10 mM Tris pH 8.0. Ligation of the DNA fragments was performed with the Rapid DNA Ligation Kit (Roche) according to the manufacturer's manual using once 66 ng of digested DNA in a 20 µl ligation or 766 ng DNA in a 60 µl volume. After 30 minutes ligation at RT the ligase was heat inactivated at 65°C for 10 minutes. Then a Touch Down PCR (meaning starting with a high annealing temperature which is lowered in each cycle to enhance specificity) was performed with 4 µl of the ligation reactions as template with the following program:

94°C	2 min	initial denaturation	1 cycle
94°C	30 sec		
72°C	30 sec	ΔT -0.5°C	
72°C	5 min		20 cycles
94°C	30 sec		
62°C	30 sec		
72°C	5 min		11 cycles
72°C	10 min		1 cycle
4°C	infinite		

Then the PCR products were purified with the QIAquick PCR purification Kit (QIAGEN) and a second Touch Down PCR was performed with nested primers with a similar program as for the first one only with 20 times steps 5-7. The PCR amplifications were analyzed on an agarose gel and if distinct bands were discernable purified, cloned into the pCR-Vector with the TA Cloning Kit (Invitrogen), sequenced and the obtained sequences blasted against the mouse genome on the NCBI website.

7.7.19 ELISA

ELISAs were performed in 96-well flat-bottom Maxisorp immuno-plates (NUNC). Therefore the plates were coated with the corresponding antigen e.g. NIP-BSA at a concentration of 10 µg/ml in 50 µl PBS /well ON at 4°C. The plates were washed 2 times with tap water with 0.05% Tween and then 100 µl of ELISA buffer were added to each well. A masterplate with usually a 1:30 dilution in ELISA buffer of all sera to be analyzed was pipetted. 50 µl of these dilutions were then transferred into row A of the prepared antigen coated plates and serially diluted 1:3 till row H. The plates were incubated ON at 4°C and washed the next day 5 times with tap water (+Tween). Then 50 µl of a 1:1000 dilution in ELISA buffer of the revealing antibody e.g. anti-IgM or anti IgG coupled to the alkaline phosphatase enzyme were given into each well. The plates were incubated 2 hours at 4°C and then washed again 5 times. Then 50 µl of the substrate solution (1 mg/ml of 4-Nitrophenylphosphate in ELISA substrate buffer) were added and the plates were incubated at RT for about 15 minutes. The reaction was stopped by adding 25 µl of 2.5 M NaOH and the plates were measured at 405 nm in a THERMO_{max} microplate reader (Molecular Devices).

7.8 Cellular techniques

7.8.1 Lysis of red blood cells

The cell suspension containing erythrocytes was centrifuged 5 minutes at 4°C and 250 g and 4°C. Cells were resuspended in 1-2 ml of ACK buffer, let stand for 1-2 minutes at RT. Lysis reaction was stopped by adding 10 ml FACS buffer. The cells were centrifuged again and then resuspended in medium.

7.8.2 Surface staining of cells for FACS analysis

For FACS staining normally cell suspensions of $20-10 \times 10^6$ cells/ml were prepared. The antibodies used were either directly labeled with fluorescent dyes like e.g. FITC or the antibodies were biotinylated and revealed by a second step with a fluorescently labeled streptavidin reagent. The appropriate dilutions for the antibodies had been titrated beforehand. Commercial antibodies were mostly used at a final dilution of 1:200 in FACS buffer.

For staining 50 μ l of cell suspensions were mixed together with 150 μ l of antibody dilution and stained in U-bottom 96-well plates. The cell suspensions were protected from light covered and incubated for at least 30 minutes on ice. Eventually 100 μ l of FACS buffer were added to each well, the plates were spun for 5 minutes at 250 g and 4°C, checked for cell pellets and the supernatant was flicked off. Cells were resuspended in the wells by vortexing the 96-well plate. Either the cells were then directly resuspended in 150 μ l of FACS buffer and analyzed or staining procedure was repeated with the second step reagent for another 15 minutes on ice and the samples were then analyzed. If no PE-Cy7 was used as fluorescent dye for staining the cells they were resuspended in FACS buffer containing 10 μ g/ml propidium iodide to discriminate between living and dead cells. Negative (no staining or only secondary reagent) and single stained compensation controls were always included. FACS analysis was carried out on a FACSCalibur (Becton Dickinson) and analyzed with the CellQuest Pro v4.0.1 software (Becton Dickinson). Cells were gated on the lymphoid FSC/SSC gate and, if included, on living cells excluding PI.

7.8.3 Intracellular anti-BrdU staining

Incorporated BrdU was detected by intracellular staining with the BrdU Flow Kit (BD Biosciences). For the intracellular staining at least 10^6 cells, better $2-3 \times 10^6$, were stained for the surface antigens as usual (including streptavidin combinations). All single stainings for compensation were performed. Basically the manufacturer's protocol was followed.

Surface stained cell pellets in tubes (no propidium iodide added) were centrifuged and resuspended in 100 μ l Cytotfix/Cytoperm and incubated for 20 minutes on ice. 1 ml of Permash buffer was added and the cells were spun down, resuspended in 100 μ l Cytoperm Plus and incubated 10 minutes on ice. Again 1 ml of Permash was added, the cells were centrifuged, resuspended in 100 μ l in the kit provided DNase solution (alternatively DNase I 2000 U/ml in PBS) and incubated 1 hour at 37°C. After this 1 ml Permash was added, cells were centrifuged, resuspended in 50 μ l 1:100 dilution of the anti-BrdU antibody and incubated for 20 minutes at RT. Cells were then again washed with 1 ml Permash, centrifuged, resuspended and analyzed on a

FACSCalibur (Becton Dickinson) with the CellQuest Pro v4.0.1 software (Becton Dickinson).

7.8.4 Staining of sections for fluorescence microscopy

The 5 μm organ sections were fixed 10 minutes in acetone and then stored at -20°C . Before staining the slides were allowed to thaw for 10 min at RT. Then a hydrophobic ring was drawn around the sections with a Dako Pen (DAKO) to minimize the need of antibody solution. For staining the sections were covered with antibody solution and incubated for 30 minutes at RT in the dark. Antibodies were used at a 1:50 dilution in FACS buffer, only biotinylated peanut agglutinin was diluted 1:200. After staining with the first antibody, slides were shortly rinsed in PBS and then washed by shaking another 15 minutes in PBS. For the second step sections were covered with Neutralite Avidin-TXRD (1:200) for 15 minutes at RT. Slides were then washed as described above, 1-2 drops of a 1:1 mixture of PBS and glycerin were given onto the slide which was then covered with a 24 x 45 mm cover glass (Meditate).

7.9 Mouse work

7.9.1 Thymus dependent and independent Immunization

5 week old $\lambda 5\text{T}/\lambda 5\text{T}$ and 11 week old C57BL/6 mice were injected either s.c. with 50 μg NIP-Ovalbumin with Freund's complete adjuvant mixed 1:1 (TD) or i.v. with 100 μg NIP-Ficoll in PBS (TI). For the secondary TD immune response mice received a second NIP-Ovalbumin injection after 4 month. Sera were obtained from tail bleeding and kept at -20°C until they were used. Total and hapten-specific Ig levels were determined by ELISA.

7.9.2 BrdU labeling

Mice received an initial intraperitoneal injection of 1mg BrdU dissolved in PBS and were thereafter fed with drinking water containing 1 mg/ml BrdU for different periods of time. The BrdU-containing drinking water was light protected and was changed every 4 days. Cells were then prepared from different lymphoid organs and were analyzed with the BrdU Flow Kit (BD Biosciences) as described in the section „Intracellular anti-BrdU staining“.

7.9.3 Mixed bone marrow chimeras

Donor bone marrow cells were harvested from 5 $\text{Ly}5.2^{+}$ $\lambda 5\text{T}/\lambda 5\text{T}$ and 5 $\text{Ly}5.1^{+}$ C57BL/6 mice. Cells were spun 10 minutes at 10'000 rpm and red blood cell lysis was performed. Cells were resuspended in 3 ml PBS with 2% FCS (without sodium azide) and stained with $\alpha\text{-CD}3\epsilon\text{-PE}$ (1:200) for 30 minutes. Eventually cells were washed with PBS/2% FCS, shortly spun (only till 600 rpm) and then filtered through a silk mesh. $\text{CD}3\epsilon^{-}$ cells were conservatively sorted on a FACS Aria (Becton Dickinson). Subsequently cells were resuspended in 1 ml serum free DMEM, counted and diluted to a concentration of $2 \times 10^6/\text{ml}$. Four hours after completion of sublethal irradiation (450 rad) the male C57BL/6 $\text{Rag}2^{-/-}$ recipient mice were injected through the tail vein with 1×10^6 sorted donor bone marrow cells either only $\text{Ly}5.2^{+}$ $\lambda 5\text{T}/\lambda 5\text{T}$ or $\text{Ly}5.1^{+}$

C57BL/6 cells or a 1:1 mixture of both types. Approximately 4 weeks later different organs of the mice were analyzed for lymphoid engraftment and chimerism by flow cytometric analysis.

7.10 Cell culture methods

7.10.1 Determination of cell numbers

A 10 μ l aliquot of a cell suspension was diluted with 90 μ l trypan blue solution (0.4% w/v) and cells were counted with a Neubauer counting chamber (0.1 mm depth). The number of living cells (excluding the dye) in 16 small squares multiplied with 10^4 gave the cell density of cells/ml.

7.10.2 Freezing and thawing of cells

Logarithmically growing cells were frozen by pelleting them by centrifugation with 250 g at 4°C and resuspending them in freezing medium. Then they were transferred into Cryotubes and placed ON at -70°C. For long-term storage they were transferred into the liquid nitrogen tank.

Frozen cells were quickly thawed in a 37°C waterbath, immediately diluted 1:10 in the appropriate medium, centrifuged at 250 g and the cell pellet was then resuspended in fresh medium and cultured with the appropriate conditions.

7.10.3 ES cell culture, transfection and selection

Gelatinizing of plates

Tissue culture dishes (\varnothing 10 cm) were gelatinized by incubating them with 8 ml 0,15% gelatine-saline solution for around 15 minutes at RT.

MEF culture

1 vial mouse embryonic fibroblasts (MEF or feeder cells) was thawed in a 37°C waterbath and resuspended in 60 ml MEF medium. The gelatine solution of the plates was aspirated and 10 ml of MEF suspension was plated on each gelatinized plate. Feeder cells were incubated for around 3 days at 37°C and 10%CO₂.

Trypsinization and replating of MEF

Medium was aspirated of the feeder cells and the plates were rinsed once with PBS followed by a trypsinization of 5 minutes with 2 ml 1x trypsin solution. Trypsinization was stopped by adding 8 ml of medium and the cells were harvested by pipetting the medium 6 to 7 times over the plate. Cells were collected, diluted according to the passage and plated in 10 ml medium on new gelatinized plates. For the second passage MEF were expanded from 6 to 26 plates and for the third passage cells could further be expanded 3 times. After 3 passages feeder cells were not split anymore but could be replated on different tissue culture dishes.

Freezing of MEF

MEF of 4 plates were harvested by trypsinization and frozen into 1 freezing vial with 1 ml freezing medium. The vials were first transferred to -70°C ON and stored for longterm in the liquid nitrogen tank.

Culture of ES cells

1-2 MEF plates were irradiated for 45 with 94 rad/min. 1 ES cell vial was thawed in a 37°C waterbath and resuspended in 10 ml ES cell medium, spun down (1200 rpm, 5 minutes) and resuspended in 10-20 ml fresh ES cell medium. The medium of the feeder cell plates was removed and ES cells were plated on 1-2 irradiated feeder cell plates. Cells were incubated at 37°C and 10% CO_2 changing medium every day.

Expansion of ES cells

Plates were washed once with PBS and trypsinized with 2 ml 1x trypsin solution for up to 5 minutes. 8 ml of ES cell medium was added, cells were harvested and resuspended. The cell suspension was transferred into a 15 ml tube and allowed to settle for 10-15 minutes. The upper 8 ml of the ES cell suspension were used for further expansion. 1 ml of the ES cell suspension was plated on 1 irradiated feeder cell plate with fresh ES cell medium.

Freezing of ES cells

ES cells were harvested (as described above), the upper 8ml of cell suspension was centrifuged for 8 minutes at 1200 rpm and cells were resuspended in freezing medium (2-4 vials per plate). The tubes were transferred overnight to -70°C and for long-term storage into the liquid nitrogen tank.

Transfection and selection of ES cells

ES cells were harvested from 5-6 plates (as described above), the upper cell suspension was spun and resuspended in 20- 30 ml serum-free medium. Cells were counted and split into $1-2 \times 10^7$ cell fractions and again spun down. The fractions were then resuspended in 800 μl serum-free medium with 40 μg of linearized vector DNA (ON linearized vector, phenol chloroform extracted, ethanol-acetate precipitated, washed with 100% ethanol, resuspended in 50 μl sterile TE and filter sterilized through a mini-0.2 μm filter). The cell suspensions were then transferred into a 0.4 cm gap cuvette. Cells were pulsed with 0.22 kV and 960 μF . As selection control served a pulsed sample without DNA. Cells were directly resuspended after the pulse in ES medium and plate selection control sample on to 2 feeder plates and transfected cell sample on 4 plates of irradiated feeder cells.

One day after transfection selection was started with 300 $\mu\text{g/ml}$ G418. Medium was changed every day. 8-10 days after transfection, individual ES cell colonies were distinguishable which were then eventually picked.

Picking ES cell colonies

Medium on the ES cell plates was exchanged for PBS and the colonies were picked with a gilson pipette set on a volume of 50 μ l. The aspirated colonies were transferred individually into 50 μ l 1xtrypsin/EDTA solution in a 96-well plate and resuspended by pipetting. The cells suspension was halved and each part was plated onto an irradiated 96-well feeder plates with 150 μ l of ES cell medium with 300 μ g/ml G418.

Expansion of ES cell colonies

ES cells were always plated onto new feeder plates before the colonies touched each other or the colonies were growing to big. Wells were rinsed once with PBS and then trypsinized with a small volume of 1xtrypsin/EDTA solution (for e.g. 50 μ l for a 96-well) for around 10 minutes at 37°C. After resuspension with a pipette, the cell suspension was either transferred into a new well with irradiated feeder cells, frozen with at least 10 x volume of freezing medium or washed once with PBS and processed further for extraction of DNA.

7.11 Computational methods

7.11.1 *In silico* genome walking

To obtain the unknown downstream intronic sequence of exon III of the *KRC* gene we took advantage of the ongoing sequencing project of the mouse genome. Different organizations like the Sanger Institute provided an open accessible archive of not yet assembled DNA sequencing reads coming from the whole genome shotgun projects. So the known sequence of exon III was used as a starting point to search it against the Ensembl trace repository (<http://trace.ensembl.org/>) with the SSAHA program (Sequence Search and Alignment by Hashing Algorithm). The retrieved matching sequences were then assembled using the Lasergene (DNASTAR) program resulting in a larger contiguous consensus sequence also referred to as contig. Eventually the most 3' located sequences were again searched against the Ensembl trace repository, integrated into the contig and the latter that way extended. This was repeated until no matching sequences could be found anymore. In this case one took advantage of the fact that part of the sequence traces were marked as corresponding to the same genomic fragment (normally 2–4 kb) just representing the two different ends. Therefore one took sequence pairs with one sequence lying in the already assembled contig and took the other corresponding one as starting point for a new contig. Primers were then designed based on the gained unctiguos sequence information with which the accuracy of the assembled sequences could be verified.

7.12 References

- Leptin, M. (1985). Monoclonal antibodies specific for murine IgM. II. Activation of B lymphocytes by monoclonal antibodies specific for the four constant domains of IgM. *Eur J Immunol* 15, 131-137.
- Liu, W., and Saint, D. A. (2002). A new quantitative method of real time reverse transcription polymerase chain reaction assay based on simulation of polymerase chain reaction kinetics. *Anal Biochem* 302, 52-59.

- Ogawa, M., Matsuzaki, Y., Nishikawa, S., Hayashi, S., Kunisada, T., Sudo, T., Kina, T., and Nakauchi, H. (1991). Expression and function of c-kit in hemopoietic progenitor cells. *J Exp Med* 174, 63-71.
- Rolink, A. G., Andersson, J., and Melchers, F. (1998). Characterization of immature B cells by a novel monoclonal antibody, by turnover and by mitogen reactivity. *Eur J Immunol* 28, 3738-3748.

9 Acknowledgements

I would like to thank Ulf Grawunder for accepting me as a Ph.D. student and giving me the opportunity to work in his laboratory. A journey starting with the exciting time at the BII, then leading to the University in Ulm and finally to the Pharmacenter of the University of Basel. I am grateful for his faith and support.

I especially want to thank Ton Rolink for the substantial support during my time at the Pharmacenter and granting me the opportunity to do the analysis of the $\lambda 5$ deficient mice.

I would also like to express my gratitude to Rod Ceredig and Jan Andersson for giving me a helping hand with the *in vivo* experiments and for their critical reading of this thesis.

I also would like to thank Ed Palmer for the excellent atmosphere in the lab at the BII and being a coreferent for my thesis.

As well, I want to thank Hans-Reimer Rodewald for his support during and after my time at the University of Ulm. In the same line I want to thank Hans-Joerg Fehling for his advice and support with the knockout project. I am particularly grateful to Carmen Blum for her help in generating and maintaining the knockout mice in Ulm. Many thanks to Claudia Waskow for her help in the lab and our common home in Ulm, Thorsten Feyerabend for his advice with the ES cell work, Hervé Luche for his helpfulness and enduring my french exercises, and to all the other at the laboratory in Ulm who made this work possible.

Technical assistance is an important part of any project, and I would like to thank all those helpful and accomodating individuals who saved me countless hours of work. In particular, I want to express my gratitude to Hannie for preparing tissue sections and teaching me the procedure, Ernst for taking care of the mice, Daniela, Annette and Manuela of the TMCF for helping to transfer the mice to Basel, showing me how to take blastocysts and to find the way to the infundibulum and finally to Markus Ruegg for allowing me to use the fluorescent microscope

Thanks also to Steffen, as the man behind me, for his help in the lab and to Lukas our lab troubleshooter as well as all the others I had the pleasure to work with for being helpful and making the lab atmosphere pleasant and productive.

I also want to thank all my fellow students at the BII, in Ulm and Basel for the great time we had together and the support during the final time.

Special thanks also to Didi, for his incredible patience, his support in and outside of the lab and the intensive discussions. We are all looking forward to your seminar.

Finally, I want to thank my parents who always supported me and believed in me, *muchísimas gracias*.

This work was supported by F. Hoffmann-LaRoche, Basel, Switzerland.

Advanced Immunology

Prof. Dr. A. Rolink
Prof. Dr. E. Palmer
Prof. Dr. J. Andersson
Prof. Dr. G. De Libero

Molecular Virology

Prof. Dr. K. Ballmer-Hofer
Prof. Dr. T. Hohn

Biochemistry, Cell biology and Immunology

Prof. Dr. J. Pieters

*Grundlagen der Immunologie
(Ulm, D)*

Prof. Dr. Hans-Reimer Rodewald
Prof. Dr. Hans-Jörg Fehling